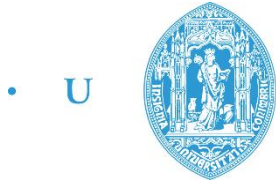Fábio Pedro Reis

DEVELOPMENT OF AMPHIPHILIC BLOCK
COPOLYMERS FOR GENE DELIVERY APPLICATIONS

Dissertation presented to the Faculty of Sciences and Technology of the University of Coimbra to obtain a Master's
degree in Biomedical Engineering

September 2016

· U C ·

UNIVERSIDADE DE COIMBRA

Fábio Pedro Reis

Development of amphiphilic block copolymers for gene delivery applications

Dissertation presented to the Faculty of Sciences and Technology to obtain a Master's degree in Biomedical Engineering

Supervisors:

Prof. Dr. Jorge Coelho

Dr.ª Joana Góis

Coimbra, 2016

· U   C ·

UNIVERSIDADE DE COIMBRA

This work was developed in collaboration with:

Fábio was born in Leiria, Portugal in 1993. He has a strong passion for the Healthcare Industry, focused on technology development. For this reason, he decided to take the MSc Biomedical Engineering, in the University of Coimbra. During the college years, Fábio participated in several projects and associations, such as in the Students Association at Physics Department as Developer of External Relations, and also in a summer internship at Innovnano.

What he finds most motivating about the field of bioengineering and health sciences is the required synergy of people with different areas of expertise. Breakthroughs in health sciences often require contributions from physiologists, engineers and physicians. His career aspirations are the development of biocompatible prostheses, medical devices (ranging from clinical equipment to micro-implants), regenerative tissue growth and pharmaceutical drugs, towards the improvement of the human condition.

Acknowledgements

This project is collaboration in the truest sense, and could not exist without the support and input of more people than I can name on one written page. I would like to thank the following people who played an important role in the process.

First of all, I would like to thank my supervisor, Prof. Dr. Jorge Coelho who granted me leave to embark on this project, for allowing me to join his team, for his expertise, advice, good ideas and most of all for his kindness.

I also would like to specially thank my co-supervior, Dr.ª Joana Góis, for her patience. Throughout my thesis-writing period, she provided good teaching, good company, lots of good ideas and steady support in the most difficult times.

I thank all the members of the Polymer Research Group, for all the friendship, for offering their suggestions and for making my days more cheerful. I really enjoyed the stimulating and fun environment that you provided. I am particularly grateful to Pedro Santos, Joana Mendes, João Costa and Patrícia Mendonça. Thank you for putting up with all my questions and doubts, and for all your help and friendly advice.

Thanks to Professor Fani Sousa (The Health Sciences Research Centre of the University of Beira Interior) for her helpful scientific studies to evaluate cytotoxicity and gene complexation of several block copolymers.

Importantly, thanks to my friends who listened to my frustrations and gave me precious advice, and to those with whom I shared so many fun moments. André Pedrosa, Alexandre Sayal, João Marques, Rute Marto, Raquel Monteiro, Carolina Travassos, Sara Oliveira, … thanks for your help, encouragement and care through difficult times. Life is so much easier if people like you are around!

The time I spent in Coimbra was both extremely intense and fruitful, and I feel profoundly privileged for having enjoyed this experience. Thank you for your kindness and support.

Last, but not the least, I would like to thank my family for their unconditional love and for teaching me how to dream. Special thanks go to my parents, for being most inspiring and brilliant teachers in life. They have always put education as a first priority in my life, and raised me to set high goals for myself.

Thanks also for my late grandfather who motivated me to become a good man in life and accomplish big and for my sister for providing inspiration to do hard work. They taught me to value honesty, courage, and humility above all other virtues. Their presence at my side is a source of inspiration.

I do genuinely appeal to the graciousness of those whom I have failed to name above to magnanimously forgive the oversight and continue to maintain the interaction.

Resumo

A terapia genética tem tido um crescente interesse devido às suas potencialidades no tratamento de doenças, como o cancro, infeções e até mesmo doenças genéticas. Para que a terapia genética seja bem sucedida, um dos fatores mais importantes é o desenvolvimento de sistemas adequados para a libertação controlada de material genético. Têm vindo a ser desenvolvidos vários métodos de transferência de genes por vetores não virais de modo a superar os problemas de segurança associados aos vetores virais. Os vetores não virais têm diversas vantagens quer na segurança, quer na prevenção da potencial imunogenicidade e toxicidade, permitindo a administração de repetidas doses, e a facilidade no estabelecimento de boas práticas de fabrico.[1] Neste sentido, têm sido amplamente utilizados copolímeros de bloco anfifílicos (ABCs) em aplicações farmacêuticas, como é o caso das tecnologias de libertação controlada em terapia genética. Os ABCs têm sido extensivamente utilizados devido à sua composição química única, a qual é caracterizada por segmentos hidrofílicos e hidrofóbicos que, em solução aquosa são capazes de se auto-agregar em diferentes morfologias.[2] As diversas características presentes nos copolímeros anfifílicos torna-os adequados veículos de entrega de material genético. Devido aos recentes avanços das técnicas de polimerização radicalar por desativação reversível (RDRP) é agora possível sintetizar copolímeros de bloco com estruturas e funcionalidades específicas. Estes permitem o desenvolvimento de sistemas de libertação controlada de fármacos mediada pelo pH, biocompatíveis e de baixa citotoxicidade. A polimerização radical por transferência de átomo (ATRP) é uma das técnicas RDRP mais eficientes, versáteis e robustas. Com o intuito de reduzir a quantidade de cobre necessária para controlar as polimerizações, foram propostas novas alterações no método de ATRP, tais como a polimerização radicalar por transferência de átomo com ativador suplementar e agente redutor (SARA ATRP).[3]

Assim, o objetivo deste trabalho foi investigar novos sistemas poliméricos para entrega de material genético, compostos por copolímeros de bloco que respondem a determinados estímulos: poli(oligo(óxido de etileno) metil éter) metacrilato-bloco-poli[metacrilato de 2-(N-dimetilamino)etil] (POEOMA-*b*-PDMAEMA), poli(oligo(óxido de etileno) metil éter) metacrilato-bloco-poli(2-diisopropilamino metacrilato de etilo) (POEOMA-*b*-PDPA). Os copolímeros de bloco POEOMA-*b*-

PDMAEMA, POEOMA-*b*-PDPA, POEOMA-*b*-(PDPA-*co*-PDMAEMA) e o homopolímero PDPA foram sintetizados com diferentes pesos moleculares, por um método desenvolvido recentemente, designado SARA ATRP, que utiliza reduzidas concentrações de catalisador (cobre). Os polímeros resultantes foram caracterizados pelas técnicas de espectroscopia de ressonância magnética nuclear (NMR) e de cromatografia de exclusão molecular (SEC)

Diferentes parâmetros como pK_a, tamanho e carga superficial das partículas foram avaliados a fim de estudar o potencial destes copolímeros em aplicações biomédicas. Os copolímeros mais promissores foram enviados para o Centro de Investigação de Ciências da Saúde da Universidade da Beira Interior para avaliar as suas capacidades de complexação de genes e citotoxicicdade, obtendo resultados muito promissores.

Palavras-chave: RDRP, SARA, ATRP, copolímeros de bloco, copolímeros de bloco sensíveis ao pH, libertação controlada de genes

Abstract

Gene therapy provides great opportunities for treating diseases from genetic disorders, infections and cancer. To achieve successful gene therapy, the development of proper gene delivery systems could be one of the most important factors. Several non-viral gene transfer methods have been developed to overcome the safety problems of their viral counterpart. Polymer-based non-viral gene carriers have been used due to their merits in safety including the avoidance of potential immunogenecity and toxicity, the possibility of repeated administration, and the ease of the establishment of good manufacturing practice.[1] Amphiphilic block copolymers (ABCs) have been extensively used in pharmaceutical applications ranging from sustained-release technologies to gene delivery. The utility of ABCs for delivery of therapeutic agents results from their unique chemical composition, which is characterized by hydrophilic and hydrophobic segments that, in aqueous solution, are able to self-assemble into distinct morphologies and have been extensively used in both research and technology fields.[2] Several favourable attributes of amphiphilic copolymers have also made them suitable as drug delivery vehicles.

Due to the recent advances in reversible deactivation radical polymerization (RDRP) techniques it is now possible to synthesize block copolymers with specific structure and functionalities. These include pH-triggered drug release systems, biocompatible, and with low cytotoxicity. Atom transfer radical polymerization (ATRP) is one the most efficient, versatile and robust RDRP technique. Aiming to reduce the amount of copper required to control the polymerizations, new ATRP variations have been proposed, such as supplemental activator and reducing agent (SARA) ATRP.[3]

Thus, the aim of this work was to investigate a new polymeric-based systems for gene delivery, composed by stimuli-responsive block copolymers: poly(oligo(ethylene oxide) methyl ether) methacrylate-block-poly[2-(dimethylamino)ethyl methacrylate] (POEOMA-*b*-PDMAEMA), poly(oligo(ethylene oxide) methyl ether) methacrylate-block-poly(2-diisopropylamino ethyl methacrylate) (POEOMA-*b*-PDPA). POEOMA-*b*-PDMAEMA, POEOMA-*b*-PDPA, POEOMA-*b*-(PDPA-*co*-PDMAEMA) copolymers and PDPA homopolymers with different molecular weights, were synthetized by a recently developed SARA ATRP method that uses reduced concentrations of copper

catalyst. The ensuing polymers were characterized by nuclear magnetic resonance (NMR) spectroscopy and size exclusion chromatography (SEC) analysis.

Different solution parameters such as pK_a, particle size and surface charge were evaluated in order to study the potential of these block copolymers in biomedical applications. The most promising block copolymers synthesised were sent to the Health Sciences Research Centre of the University of Beira Interior to evaluate their cytotoxicity and gene complexation ability with very promising results.

Keywords: RDRP, SARA, ATRP, block copolymers, pH-responsive block copolymers, gene delivery.

List of acronyms

^{1}H NMR	Proton nuclear magnetic resonance
A549	Human alveolar adenocarcinoma cell line
ABC	Amphiphilic block copolymers
AGET	Activator generated by electron transfer
ARGET	Activators regenerated by electron transfer
ATRP	Atom transfer radical polymerization
bpy	2,2'-bipyridine
DDS	Drug delivery systems
DLS	Dynamic light scattering
DNA	Deoxyribonucleic acid
dNbpy	4,4'-Di-5-nonyl-2,2'-bipyridine
EBiB	Ethyl α-bromoisobutyrate
EBPA	Ethyl α-bromophenyl acetate
EE	Encapsulation efficiency
EPR	Enhanced permeability and retention
FDA	Food and drug administration
FBS	Fetal bovine serum
HMTETA	1,1,4,7,10,10-Hexamethyltriethylenetetramine
HPSEC	High performance gel permeation chromatography
ICAR	Initiators for continuous activator regeneration
IPA	Isopropanol
LC	Loading capacity
LCST	Lower critical solution temperature
Me$_6$TREN	Tris(2-dimethylaminoethyl)amine
Milli-Q	Purified water
MRI	Magnetic resonance imaging
Na$_2$S$_2$O$_4$	Sodium dithionite
NaOH	Sodium hydroxide
NMP	Nitroxide-mediated polymerization
NPs	Nanoparticles

P4VP	Poly(4-vinyl pyridine)
PAA	Poly(acrylic acid)
PBS	Phosphate-buffered saline solution
PCL	Polycaprolactone
PDI	Polydispersity index
PDMAEMA	Poly(dimethylaminoethyl methacrylate)
PDMTETA	*N,N,N',N',N''*-Pentamethyldiethylenetriamine
pDNA	Plasmid deoxyribonucleic acid
PDPA	Poly(2-(diisopropylamino)ethyl methacrylate)
PEG	Poly-(ethylene glycol)
PNIPAm	Poly(*N*-isopropylacrylamide)
POEOMA	Poli(oligo(ethylene oxide) methyl ether) methacrylate
RAFT	Reversible addition/fragmentation chain transfer
RDRP	Reversible deactivation radical polymerization
RES	Reticuloendothelial system
RNA	Ribonucleic acid
SARA	Supplemental activator and reducing agent
SEC	Size exclusion chromatography
TAE	Tris–acetate–ethylene diamine
THF	Tetrahydrofuran
TMS	Tetramethylsilane
TPMA	Tris[(2-pyridyl)methyl]amine
TREN	Tris(2-aminoethyl)amine

Nomenclature

$Đ$	Dispersity
DP	Degree of polymerization
k_{ATRP}	Equilibrium constants
k_{deact}	Deactivation rate constants
k_{act}	Activation rate constants
k_p	Propagation rate coefficient
k_t	Termination rate constants
M_n	Number average molecular weight
M_w	Weight average molecular weight
M_z	Higher average molecular weights
M	Monomer concentration at any given time
pK_a	Acid dissociation constant
R-X	Dormant initiator
R$^\bullet$	Active radical or active initiator
RR	Terminated polymer

Contents

List of Tables

List of Figures

Introduction

Chapter 1

1. Introduction

1.1. Contextualization

The expression "gene therapy" owes its origin to the term "genetic engineering" which was employed for the first time at the Sixth International Congress of Genetics held at Ithaca in 1932. Though the idea of gene therapy existed already, concrete development in this field began in late 1960s and early 1970s and gene therapy in humans was practiced in the late 1980s as a result of developments in the field of molecular biology, particularly inventions and improvements in gene delivery systems.[4]

Since the first human gene therapy trial performed in 1989 by Rosenberg and his team, in an attempt to treat advanced melanoma, more than 2300 clinical gene therapy trials were performed up to 2016. More than 64% of them were to treat cancer while 10% of them were devoted to treating monogenic genetic disorders, and only 7.6% were targeted at cardiovascular diseases (Figure 1).[4, 5]

Indications Addressed by Gene Therapy Clinical Trials

- Cancer diseases 64.4% (n=1517)
- Monogenic diseases 10% (n=235)
- Infectious diseases 7.6% (n=179)
- Cardiovascular diseases 7.5% (n=177)
- Neurological diseases 1.8% (n=43)
- Ocular diseases 1.8% (n=34)
- Inflammatory diseases 0.6% (n=14)
- Other diseases 2.3% (n=54)
- Gene marking 2.1% (n=50)
- Healthy volunteers 2.2% (n=53)

The Journal of Gene Medicine, © 2016 John Wiley and Sons Ltd   www.wiley.co.uk/genmed/clinical

Figure 1. Clinical targets for gene therapy (Journal of Gene Medicine).[6]

1.2. Gene Therapy

Gene therapy has drawn a lot of attention in the field of medicine, pharmaceutical sciences and biotechnology due to the potentials for treating chronic diseases and genetic disorders such as severe combined immunodeficiency, cystic fibrosis, Parkinson's disease, and it has also proved to be an alternative method to the traditional chemotherapy.[7] Gene therapy is a simple therapeutic method that consists on either replacing a distorted gene by a healthy one, or completing a missing gene in order to express the required protein. However, in practice this is a complex operation, due to several obstacles that must be overcome by the transgene to reach the targeted human cell-nucleus, where it should be expressed correctly.[4] This kind of therapy is an interesting substitute for the conventional protein therapy, since it can overcome the problems associated with protein administration in terms of bioavailability, systemic toxicity, *in vivo* clearance rate and manufacturing cost.[7]

The main goal of gene therapy is to insert into the targeted cell a functional gene that plays the role of the therapeutic agent in order to treat a disease or to repair a dysfunction caused by a genetic defect. At present, the ideal transfer system, called vector, should satisfy several criteria: (i) it must not trigger a strong immune response, (ii) it must be capable of transporting nucleic acids whatever their size, (iii) it must lead to the sustained and regular expression of its genetic cargo, (iv) the vector must deliver the gene to only certain types of cells, especially when the target cells are scattered throughout the body, or when they are part of a heterogeneous population, (v) it must be able to infect both dividing and non-dividing cells, (vi) it must be easy to prepare, be inexpensive and available at high concentrations commercially, and (vii) it must either remain in episomal position or integrate into a specific region of the genome, but not integrate randomly.[1, 4, 7]

1.3. Gene transfer systems

To date, human gene therapy has been limited to somatic cell alterations and there have been remarkable developments in the field. All gene therapy applications depend on the fact that the genetic material needs to be delivered across the cell membrane and ultimately to the cell nucleus. Gene transfer systems are named vectors and are classified into two types: viral and non-viral vectors. Each of the delivery systems has some advantages and disadvantages, and in the following scheme (Figure 2) there is a brief summary of all types of gene delivery systems.[8]

```
                        ┌──────────────┐
                        │ Vector Type  │
                        └──────┬───────┘
              ┌────────────────┴────────────────┐
    ┌──────────────────┐              ┌──────────────────┐
    │    Non-viral     │              │  Viral Vectors   │
    │     Vectores     │              └──────────────────┘
    └──────────────────┘
```

Non-viral Vectores:
- Naked DNA
- DNA Bombardant
- Electroporation
- Hydrodynamix
- Ultrasound
- Cationic lipids
- **Cationic polymers**
- Lipid-polymers

Viral Vectors:
- Retroviral
- Adenoviral
- Adeno-association vectors
- Herpes simplex
- Pox vírus
- Hybrid Adenoviral vector
- Lentivirous
- Herpes simplex virous
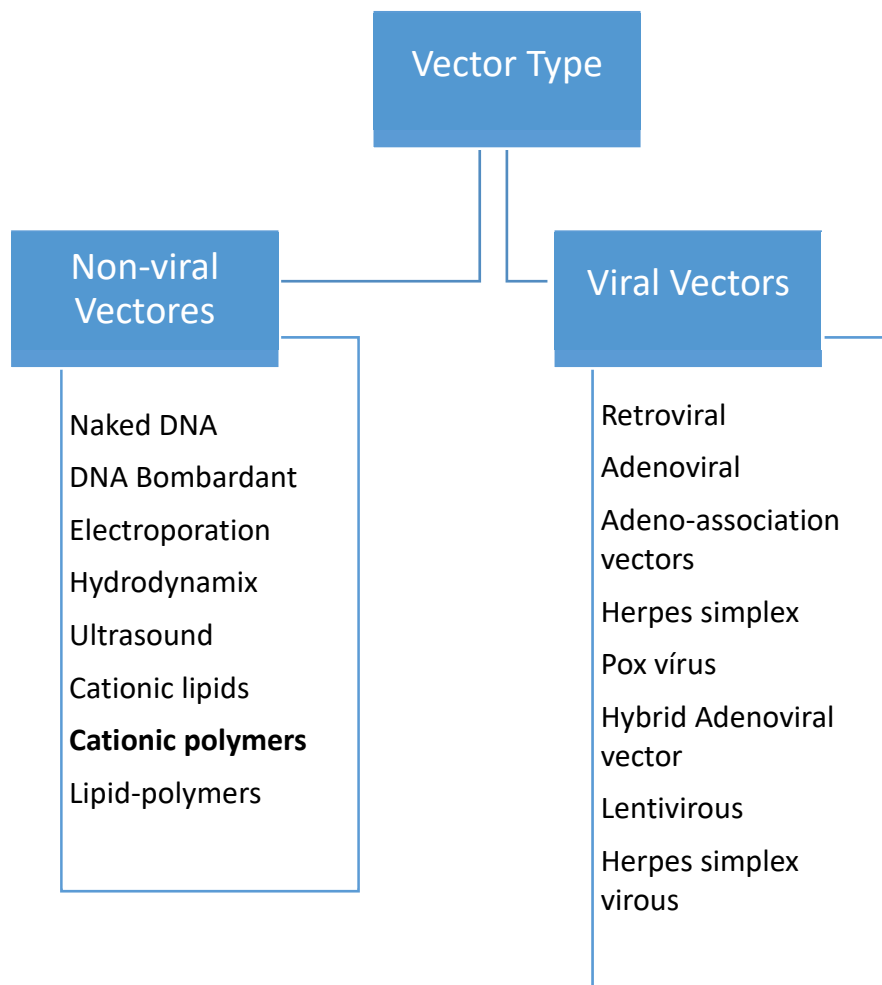
Figure 2. Summary of the main methods of gene delivery systems. Adapted from ref.[8]

Viral vectors have the advantages over non-viral vectors in terms of gene transfer efficiency. However, the non-viral vectors stand out due to their low immunogenecity, the absence of endogenous virus recombination, low production cost and reproducibility. Non-viral vectors have no limitation in DNA size for packaging and allow the vector functionalization with specific ligands for tissue- or cell-specific targeting.[8]

1.3.1.   Viral vectors

A virus is a biological entity which can penetrate into the cell nucleus of the host and exploit the cellular machinery to express its own genetic material, replicate it, and consequently spread it to the other cells. Researchers have used different viruses to deliver therapeutic genes into the cell's nucleus and exploit the virus life cycle. To use a virus as a vector to transfer a gene, it must be modified by genetic engineering. The pathogenic part of its genes is removed and replaced by the therapeutic gene. At the same time, the virus retains its non-pathogenic structures (envelope proteins, fusogenic proteins, etc.) which allow it to infect the cell. The resulting non-pathogenic virus carrying the therapeutic gene is called a viral vector.[4, 9]

To date, viral vectors are one of the most used vectors in gene therapy, due to their ability to efficiently carry the gene and ensure long-term expression. However, the risk of provoking an immune response by using viruses as delivering vectors, the high cost, the risk of toxicity, their difficulty preparation, and the limited size of the genetic materials that can be inserted into human cells, have restricted the use of viral vectors in gene therapy, and led to research safer and cheaper alternatives.[1, 4]

The most used viruses as viral vectors are retroviruses, adenoviruses, adeno-associated viruses, and simple herpes virus. Table 1 presents the main viruses used as gene transfer systems with a brief explanation of their advantages and disadvantages.[4]

Table 1. Overview of different viral vector delivery methods. Adapted from ref.[8]

Vector	Advantages	Disadvantages
Adenovirus	Very high titers (10^{12} pfu/mL) High transduction efficiency ex vivo and in vivo Transduces many cell types Transduces proliferating and nonproliferating cells Production easy at high titers	Remains episomal Transient expression Requires packaging cell line Immune-related toxicity with repeated administration Potential replication competence No targeting Limited insert size: 4–5 kb
Adeno-associated virus	Integration on human chromosome 19 (wild-type only) to establish latent infection Prolonged expression Transduction does not require cell division Small genome, no viral genes	Not well characterized No targeting Requires packaging cell line Potential insertional mutagenesis High titers (10^{10} pfu/mL) but production difficult Limited insert size: 5 kb
Herpes simplex virus	Large insert size: 40–50 kb Neuronal tropism Latency expression Efficient transduction in vivo Replicative vectors available	Cytotoxic No targeting Requires packaging cell line Transient expression, does not integrate into genome Moderate titers (10^4–10^8 pfu/mL)
Lentivirus	Transduces proliferating and nonproliferating cells Transduces hematopoietic stem cells Prolonged expression Relatively high titers (10^6–10^7 pfu/mL)	Safety concerns: from human immunodeficiency virus origin Difficult to manufacture and store Limited insert size: 8 kb Clinical experience limited
Retrovirus	Integration into cellular genome Broad cell tropism Prolonged stable expression Requires cell division for transduction Relatively high titers (10^6–10^7 pfu/mL) Larger insert size: 9–12 kb	Inefficient transduction Insertional mutagenesis Requires cell division for transfection Requires packaging cell line No targeting Potential replication competence

1.3.2.   Non-viral vectors

The drawbacks of using viral vectors as gene delivery systems, especially their severe immune response, have led scientists to find safer alternatives. Consequently, non-viral vectors have been designed for transferring DNA. Research in this field has attracted great attention as a result of their advantages in comparison to the viral vectors. Non-viral vectors are relatively safe, generally cause low immune response, and can be prepared easily, at low cost and in large quantities.[8] In addition, they can transfer different and large transgenes, and they can be stored for long periods due to their stability. However, their low transfection efficiency limits their use on a large scale.[10]

Non-viral gene delivery systems are classified into two groups (Figure 2):

- ✓ Physical vectors: these depend on a physical interaction that weakens the cell membrane to facilitate gene penetration into the nucleus. They include needle injection, electroporation, gene gun, ultrasound...[4]
- ✓ Chemical vectors: these can be prepared either by electrostatic interaction between cationic functional groups present in lipids or polymers and the anionic phosphate of DNA to form a particle called polyplexe (when the interaction occurs between the polymer and the DNA), lipoplexe (when the DNA interacts with a lipid), and encapsulation of DNA within biodegradable spherical structures that lead to micro and nanoparticles containing DNA, or by adsorption of DNA.[4]

Table 2 presents the non-viral gene delivery systems with a brief explanation of their advantages and disadvantages.[1, 7]

Table 2. Overview of different non-viral vector delivery methods. Adapted from ref.[5]

Vector	Advantages	Disadvantages
Naked plasma/Plasmid DNA- Direct delivery	Safety Simplicity	Low transfection efficiency
Gene gun	Flexibility Low cytotoxicity Good efficiency	Shallow penetration
Electroporation	Good efficiency Repeatable	Tissue damage Accessibility of electrodes to internal organ are limited
Ultrasound + micro bubble	Safety Flexibility	Low efficiency
Magnetofection	Low cytotoxicity Flexibility	Transient transfection
Inorganic molecules	Easy production Storage stability Surface functionalization	Low efficiency
Lipoplexes	Safety Low cytotoxicity	Low to medium efficiency Some results immunogenicity
Polyplexes and Dendrimers	Low immunogenicity Fair efficiency	Complement activation Low transfection Cytotoxicity

1.4.   Advanced polymeric DDS

Nanoparticle based biotechnology and its medical applications are rapidly heading to the forefront of drug delivery, diagnostic and other areas. Many important therapeutic compounds exhibit poor aqueous solubility, rendering the delivery of those agents quite challenging. The development of effective delivery systems is crucial to the success of future drugs, which may include larger and more sophisticated synthetic compounds as well as complex natural molecules.[2] Currently, several systems based on polymeric nanoparticles have been proposed as drug delivery nanocarriers. Drug delivery systems (DDS) based on stimuli-responsive polymers have been extensively investigated. Systems composed by polymeric segments that are sensitive to acidic pH have been reported as a suitable strategy for specific tumour targeting and treatment.[11] Such pH-responsive DDS take advantage of the slightly acidic extracellular pH environment of solid tumours, as well as the pH drop inside the endosome/lysosome cellular compartments, which triggers the release of its content.[11]

1.4.1.   Amphiphilic block copolymers

Amphiphilic block copolymers (ABCs) are capable of solubilizing and encapsulating genes and other hydrophobic compounds (drugs) within a hydrophobic core, and thereby enhance the bioavailability, and facilitate the drug delivery process.[12] In general, ABCs are macromolecules composed by two distinct segments, one hydrophilic and one hydrophobic. In aqueous solutions, ABCs are able to organize themselves through self-assembly, forming structures with distinct morphologies, which have been extensively used in both research and technology fields (Figure 3). In an aqueous environment, depending on solution properties, the hydrophobic blocks of the copolymer are expected to segregate into the core micelle and the hydrophilic blocks form the corona or outer shell. This shell-core micelle architecture of the polymeric micelle is essential for their utility as functional materials in pharmaceutical applications. The hydrophobic micelles core functions as a microenvironment for the incorporation of various therapeutic compounds, while the corona, or outer shell, functions as a stabilizing

interface between the hydrophobic core and the external medium.[2] As a result, polymeric micelles can be used as efficient carriers for compounds with poor solubility and/or low stability in physiological environments.[2] Although significant progress has recently been made in the field of smart polymers, the problem of their optimum delivery at physiological pH remains a challenge. Stimuli-responsive polymers exhibit a sharp change in their solution behaviour in response to external stimuli, such as <u>temperature</u>, <u>pH</u>, <u>ionic strength</u>, <u>electric field</u> and <u>chemical or biochemical agents</u>. Current approaches for the development of pH responsive micelles involve the incorporation of "ionizable" groups, including carboxylic acids, amines, and sulphonamides into the copolymer. However, the number of systems that are responsive within the physiologically pH range of 4.5-7.4 is quite limited.[9, 13]
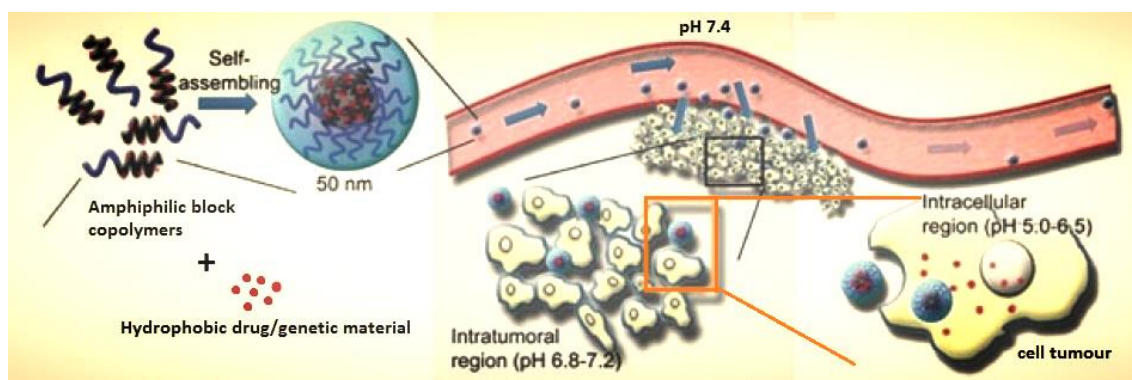
Figure 3. pH-responsive nanocarriers based on amphiphilic block copolymers and schematic representation of drug release. Adapted from ref. [4].

Due to the recent advances in reversible deactivation radical polymerization (RDRP) techniques it is now possible to design and synthesize block copolymers with specific structure and functionalities. By controlling such properties is possible to develop tailor-made systems that fulfil the required specifications for the cancer gene delivery applications. These include pH-triggered DDS, which are biocompatible, and present low cytotoxicity and targeting functionalities.[11, 14, 15]

1.4.2.   Reversible Deactivation Radical Polymerization

Chain-growth polymerization has been successfully performed for many decades through conventional free radical, anionic, or cationic polymerization. These polymerization techniques generate many important commodity polymers where their broad range of molecular weight distribution gives rise to important physical properties. While these techniques are useful for a number of applications starting from a wide variety of monomers, several applications benefit from using more precisely controlled polymers. RDRP enables the control over the polymer structure, which includes molecular weight, molecular weight distribution (dispersity), functionality, composition and architecture.[3, 16, 17] In RDRP, the occurrence of premature termination is minimized, and molecular weight increases linearly with time until all monomer is consumed or intentionally terminated. RDRP techniques have emerged over the last two decades.[18] The three most studied RDRP methods are: Atom Transfer Radical Polymerization (**ATRP**), Reversible Addition/Fragmentation Chain Transfer Polymerization (**RAFT**) and Nitroxide-mediated Polymerization (**NMP**). All of these RDRP methods involve a dynamic equilibrium between a small fraction of active polymerizing chains (propagating radicals) and a majority of dormant species.[17] They can be utilized with a broad range of vinyl monomers for a wide variety of applications. Figure 4 illustrates the trend in literature citations for the main RDRP techniques.[19]
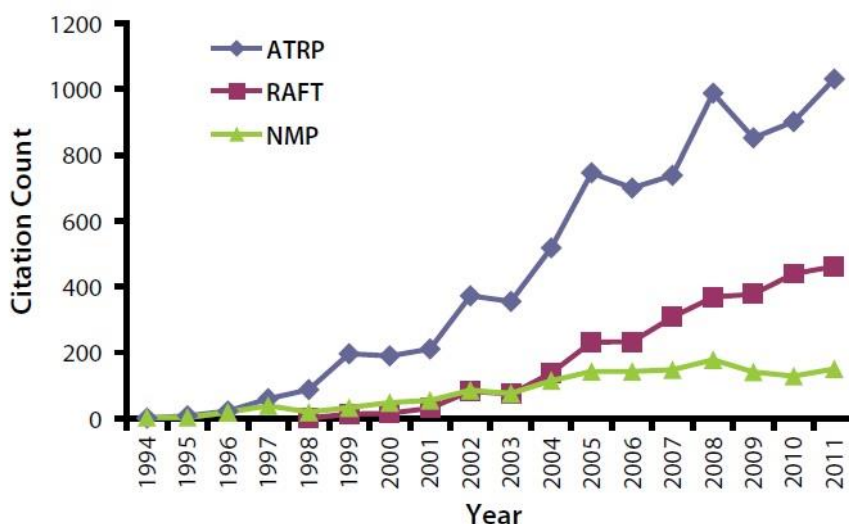
Figure 4. SciFinder search results as of 2011 for ATRP, RAFT, and NMP technologies. Adapted from [19]

All of these techniques are popular in the research community and are being explored for industrial application. ATRP has consistently held the most interest. Table 3 presents a brief summary of the advantages and limitations of the different RDRP techniques.

Table 3. Advantages and limitations of ATRP, RAFT and NMP processes. Adapted from ref. [19]

	ATRP	RAFT	NMP
Primary Benefits	• Versatile • Ability to tailor catalyst to meet specific needs	• Versatile • No use of transition metals	• No use of transition metals • Low potential for odor and discoloration
Primary Limitations	• Use of transition metals • Many variables affecting polymer characteristics	• High potencial for odor and discoloration (especially for low molecular weights)	• Least versatile

Among the RDRP techniques reported in the literature, ATRP is one of the most robust and versatile methods to polymerize a wide range of monomers under mild reaction conditions due to several intrinsic advantages, such as simplicity, high tolerance to different monomer functionalities, and the commercial availability of most compounds.[18] Moreover, ATRP has great versatility to control the molecular architecture of polymers and is an exceptionally robust method of producing block or graft copolymers.[13, 14] ATRP allows the straightforward synthesis of controlled block copolymers with potential applications in the biomedical field, including in DDS for gene delivery applications.[19]

1.4.2.1. Atom Transfer Radical Polymerization (ATRP)

The basic ATRP mechanism relies on equilibrium between the oxidation states of metal catalyst/ligand complex, which governs the activation or deactivation of the growing chain.[16, 20] In ATRP an alkyl halide is activated by a complex of a transition metal catalyst in a low oxidation state, typically Cu^I/L (L is a ligand, typically a nitrogen-based species), subsequently generating the corresponding radical and the transition metal complex in its higher oxidation state, typically $X–Cu^{II}$/L (Figure 5). The radical propagates by adding monomer units until it is deactivated to the corresponding dormant

alkyl halide by the transition metal complex in its higher oxidation state. This dynamic equilibrium between propagating radicals and dormant species ensures a low concentration of propagating radicals, and therefore suppresses the undesirable radical termination reactions, which can occur via combination or disproportionation.[16, 17, 20] In addition, the fast rate of initiation in these systems allows the simultaneous growth of most of the chains, thus contributing for a good control over the molecular weight distribution.[18]
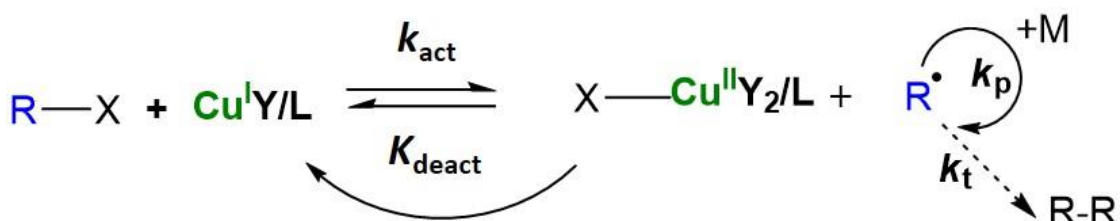
Figure 5. General mechanism of cooper catalysed ATRP. The ATRP equilibrium equation, which resides predominantly to the left/dormant side, includes dormant initiator (R-X), catalyst composed of a transition metal (Cu) with ligand (L), oxidized catalyst, active radical or active initiator (R$^{\bullet}$), and monomer (M) and terminated polymer RR The rate of reaction is marked by rate constants (k_X) where the rate of activation is k_{act}, the rate of deactivation is k_{deact}, the rate of monomer addition is k_p, and the rate of termination is k_t. The control over this equilibrium highly depends on the choice of catalyst.[17]

ATRP has demonstrated the ability to control the polymerization of a broad range of monomers. Nevertheless, some challenges still remain in the preparation of some industrially relevant monomers, such as perfluoro-olefins. Other potentially problematic functionalities include acidic monomers or initiators, such as those bearing carboxylic, sulfonic, or phosphonic acids, primary amines, as well as monomers and initiators that strongly coordinate to the metal catalyst.[20]

Several transition metals have been used in ATRP, including Cu, Ru, Fe, Ni, Mo, and Os. Copper-based catalysts are the most broadly applied and are presently superior in terms of performance, cost and environmental aspects. However, intensive research has been carried out in order to address the high toxicity of these species, which are focused on diminishing the total amount of transition metals used in an ATRP to ppm levels. Especially in biomedical applications, it is particularly important to have low levels of metal contamination in the final product in order to minimize the cytotoxic effects. Nevertheless, the complete removal of the metal from the polymer still remains a challenging task.[21] Therefore, it is of primary importance to develop and understand the

use of versatile catalyst systems that can be selected for well-controlled polymerization of a wide variety of monomers. They must be environmentally friendly i.e., use non-toxic metal(s)/solvent(s), are sustainable, employing common low cost metals, and targeting biomedical applications.[22] Catalyst activity must be modulated depending on the nature of the monomer. The activity of the selected copper complex is directly affected by the ligand. [17] Ligands also dictate the solubility of the copper complexes in solution and therefore need to be taken into account when designing an ATRP system.[20] The various ATRP techniques provide an opportunity to select a polymerization environment that is well suited to meet the application specific needs. When used in combination with the ideal catalyst for a given polymerization, well-defined polymers can be conveniently prepared.[17] Knowledge of the order of reactivity of different alkyl halides (Figure 6) is also important for the selection of appropriate initiators, especially for lower targeted DPs, but also for the efficient synthesis of block copolymers. This demonstrates the necessity of choosing an appropriate catalyst and appropriate reaction conditions for each monomer.[17, 20]
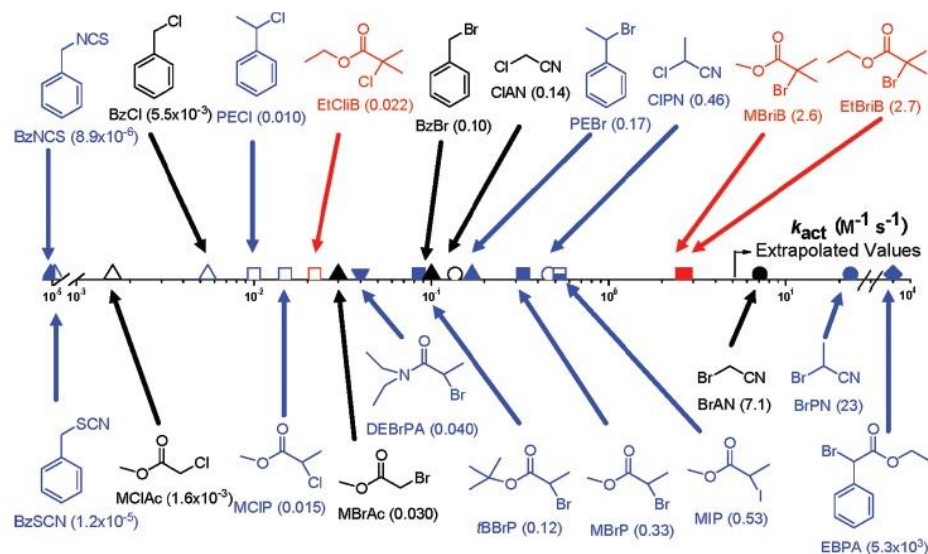
Figure 6. ATRP activation rate constants for various initiators in a system with a Cu(I)X/PMDETA catalytic complex (X = Br or Cl) in MeCN and at 35 °C. amide: ▼; benzyl: ▲; ester: □; nitrile: ○; phenyl ester: ◇. Adapted from ref. [17]

Optimizations to normal ATRP have focused on this pre-equilibrium stage and on the manipulation of the catalytic species which govern the equilibrium state.[20]

1.4.2.2. Variations of ATRP

ATRP uses transition metal complexes, usually copper-based, to mediate the fast equilibrium between dormant and active species and control the polymerization. One limitation of traditional ATRP methods is that they require catalyst concentrations greater than 1000 parts per million (ppm) to maintain an acceptable rate of polymerization. The components that are added to the reaction mixture for normal ATRP are the initiator, catalyst, and monomer. [17] The high catalyst loading leads to a significant contamination of the resulting polymer with often highly coloured and toxic transition metal complexes. The high catalyst concentrations combined with the use of organic solvents make traditional ATRP environmentally harmful. This issue is critically important not only for biomedical applications but also from the environmental standpoint. Therefore, new ATRP variations have been developed to reduce the amount of metal catalyst used in the polymerizations to less than 100 ppm, as well as to avoid the use of organic solvents.[15, 18]

- **I**nitiators for **C**ontinuous **A**ctivator **R**egeneration (**ICAR**)
- **A**ctivators **G**enerated by **E**lectron **T**ransfer (**AGET**)
- **A**ctivators **ReG**enerated by **E**lectron **T**ransfer (**ARGET**)
- **S**uplemental **A**ctivatots and **R**educing **A**gents (**SARA**)
- Reverse ATRP

These strategies (Figure 7) aim to decrease the amount of catalyst required, and to use green solvents such as water or alcohols, in order to achieve environmentally friendly reaction systems. In all cases the activator complex, namely Cu^I, is regenerated through a relatively slow reaction which compensates for termination events.[18]
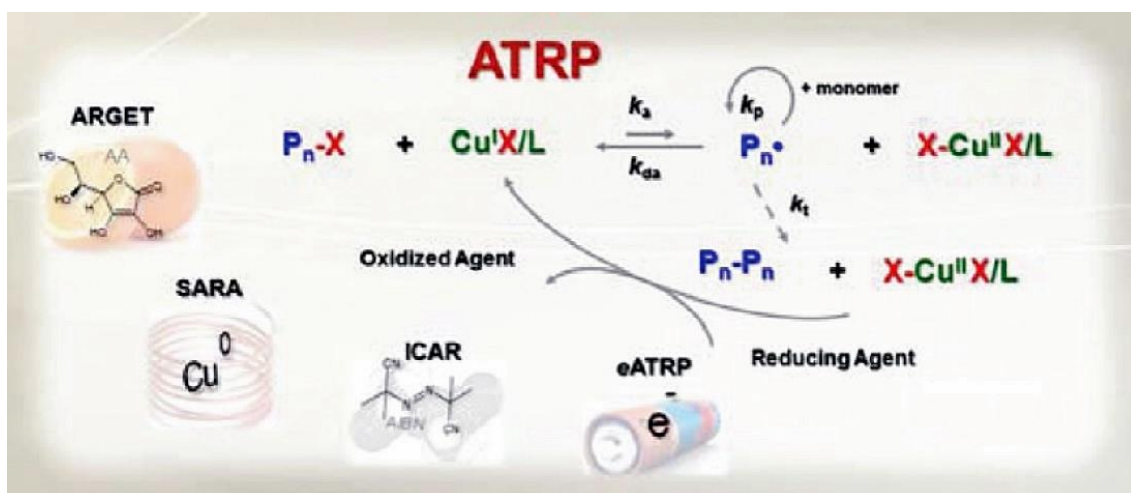
Figure 7. Different ATRP variants developed to reduce the amount of metal catalyst.[17]

Detailing the mechanisms for all of these techniques is beyond the scope of this work; however, the following table summarizes the components added to perform the different ATRP reactions.

Table 4. ATRP polymerization type and corresponding identity or concentration of popular reactants added. Adapted from ref. [19]

Polymerization	Copper(I) Catalyst Concentration (ppm)	Copper(II) Catalyst Concentration (ppm)	Popular Ligands
Normal ATRP	10,000	0-variable	All nitrogen containing ligands
ICAR	0	10	Me$_6$TREN and TPMA
AGET	0	5	Me$_6$TREN and TPMA
ARGET	0	5	Me$_6$TREN and TPMA
SARA	0	100	Me$_6$TREN and TPMA
Reverse ATRP	0	1000	Several

The relatively high levels of residual Cu by traditional ATRP are problematic for biomedical and food packaging applications where it is required to minimize or eliminate toxic components, such as heavy metals. Polymers generated by traditional ATRP contain substantial residual Cu catalyst if not properly purified. ICAR, AGET, ARGET and SARA operate at low levels of Cu during polymerization and therefore need minimal subsequent purification for catalyst removal. These new variations of ATRP are therefore useful to prepare well-defined (co)polymers for these high value applications.[23] Table 5 summarizes the advantages and limitations of the various ATRP techniques:

Table 5. Advantages and limitations for ATRP techniques. Adapted from ref. [19]

Polymerization	Benefit	Limitation
Normal ATRP	Versatile	High Cu content Unstable catalyst precursor
ICAR	Low Cu content Catalyst precursors more stable	Conventional initiator might cause side reactions
AGET	Low Cu content Catalyst precursors more stable	High Sn* content (FDA** approved)
ARGET	Low Cu content Catalyst precursors more stable	High Sn content (FDA approved)
SARA	Low Cu content Catalyst precursors more stable Uses either inorganic sulfites or zero valent transition metals to activate alkyl halides directly and to reduce excess Cu^{II} to Cu^{I} to compensate for radical termination	Without initially added Cu^{II} there is a lack of deactivator at the initial stage
Reverse ATRP	Simple Catalyst precursors more stable	Limited end group functionality Only linear Targeting MW difficult
Simultaneous reverse and normal	Catalyst precursor more stable	AIBN might cause side reactions

*Organotin compounds
**The U.S. Food and Drug Administration (FDA) examines, tests, and approves a wide range of items for medical use, including drugs and medical appliances.

1.4.2.3. Supplemental Activators and Reducing Agents (SARA) ATRP

SARA ATRP is one of the most promising ATRP variations.[3] SARA ATRP uses zero-valent transition metals (copper, iron, zinc, magnesium, etc.) or inorganic sulphites as both reducing agents and supplemental activators.[23] These compounds, activate the alkyl halides directly and reduce excess Cu(II) to Cu(I) to compensate for radical termination.[18]

Organic sulphites have recently been reported as very efficient SARA agents. Amongst the organic sulphites, sodium dithionite ($Na_2S_2O_4$) is the most efficient reducing agent that can reduce the Cu(II) species to Cu(I).[24] The use of reduced amounts of copper catalyst and the biocompatibility of the reducing agents is particularly attractive for the preparation of polymers for biomedical applications as the low toxicity negates the need for exhaustive purification steps.[20] Apart from the low amount of catalyst used in SARA ATRP, this method is also very useful for the preparation of biomaterials, since the polymerization can be conducted using environmentally friendly solvents/solvent mixtures at room temperature.[15, 20, 23]

1.4.3. Stimuli-responsive polymers

The concept of stimuli-responsive drug delivery has been studied for over three decades for delivery of therapeutic agents. The design and synthesis of stimuli-responsive systems that recognize their microenvironment and react in a dynamic way, mimicking the responsiveness of living organisms is a very attractive strategy for the development of advanced DDS. However, this approach is rather complex. It requires the use of biocompatible materials that are able to undergo reversible changes in their physicochemical properties as a result of an external stimuli.[25]

Stimuli-responsive polymers can be designed to be responsive to a specific stimulus, thus that the cargo is only released or activated when desired (Figure 8). Smart nanocarriers that respond to externally applied stimuli usually involve application of physical energy. This physical energy can be applied from outside the body and can cause

cargo release, activate the nanostructure to be cytotoxic, or both. The stimuli covered include **light** of various wavelengths (ultraviolet, visible or infrared), **temperature** (increased or decreased), **magnetic fields** (used to externally manipulate nanostructures and to activate them), **ultrasound**, and **electrical** and **mechanical forces**.[26] The most studied synthetic responsive polymer is poly(N-isopropylacrylamide) (PNIPAm), which undergoes a sharp coil–globule transition in water at 32 °C, changing from a hydrophilic state below this temperature to a hydrophobic state above it.[27]
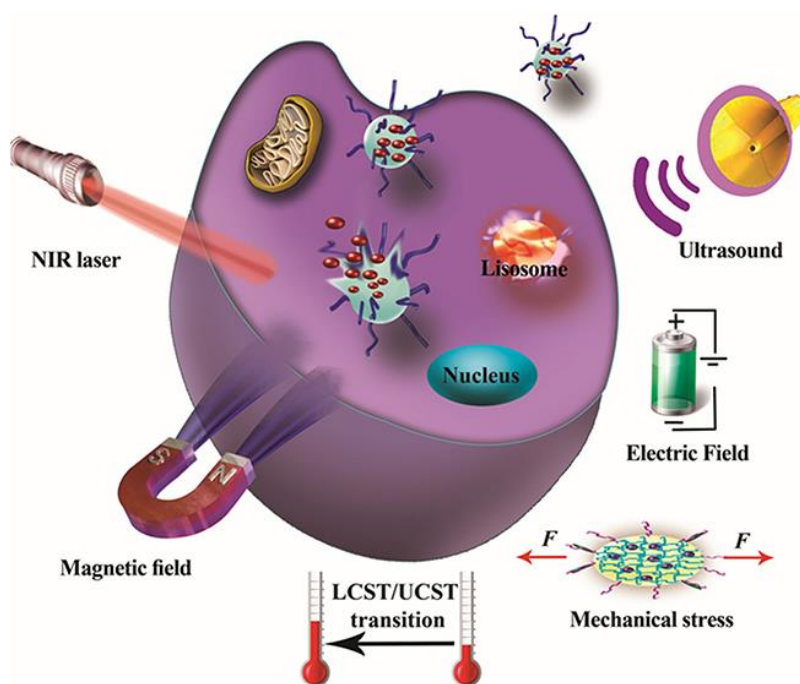
Figure 8. Different externally applied stimuli that influence different stimuli-responsive polymers.[26]

ATRP reactions should create living polymer chains, i.e. with preserved active chain-end functionalities. Since the radical termination is minimized, all the chains retain their active centers even after the consumption of the monomers. This provides the opportunity for the subsequent incorporation of an additional monomer. This unique feature enables the preparation of macroinitiators and block copolymers with different architectures. The possibility of synthesizing tailor made polymers with controlled composition, architecture, molecular weight (M_w) and active chain-end functionalities by radical reactions has opened a myriad of opportunities for macromolecular engineering.[18] Various examples of gradient, block and graft copolymers have been

created (Figure 9 a), as well as polymers with more complex architectures, including stars, comb-shaped brushes, and hyper-branched polymers (Figure 9 b).[9, 28] SARA ATRP systems provides a good opportunity to control and manipulate the polymers composition, topology and functionality at molecular level (Figure 9).[17, 29]

a) Composition
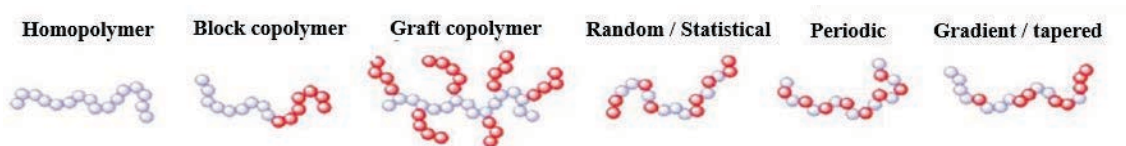
b) Topology
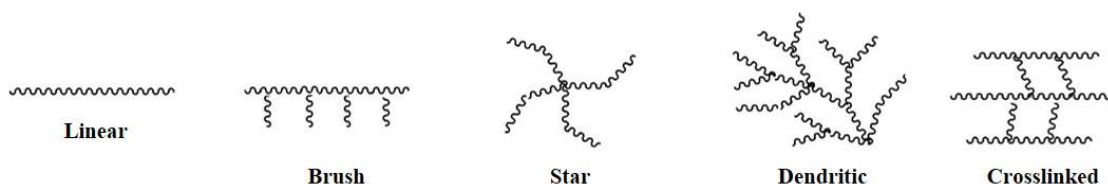
c) Functionality
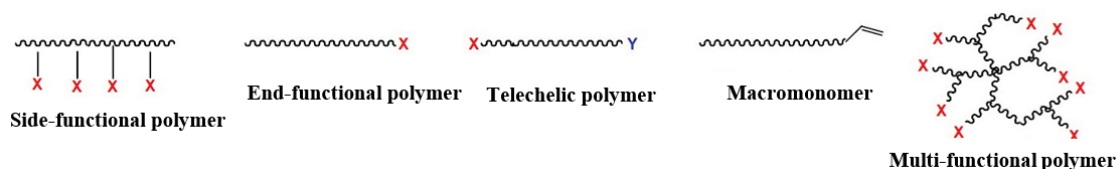
Figure 9. Main precision controls provided by ATRP, including (a) composition, (b) topology or (c) functionality. Adapted from ref. [17, 29]

In stimuli-responsive block copolymers for drug delivery applications, one of the blocks is permanently hydrophilic while the hydrophilic/hydrophobic character of the second block varies in response to an external stimulus which is usually a change in **temperature**, **pH**, **light** or **glucose concentration**.[9, 28] The evolution of RDRP methods has prompted the synthesis of a wide variety of stimuli-responsive block copolymers with controlled block lengths.[17, 30]

A common approach toward the use of stimuli-responsive materials in micellar systems is the incorporation of one (or more) stimuli-responsive core blocks and one

purely hydrophilic stabilizer block, usually poly(ethylene glycol) (PEG). In the presence of the external stimuli, the sensitive block undergoes a conformational change, promoting the self-assembly of the block copolymers into micelle-like structures with a hydrophobic core and a hydrophilic corona (Figure 10). These structures can sequester hydrophobic molecules, which can be released later, in response to changes in the surrounding environment. This stimuli-induced change in nanoparticle structure triggers the release of the previously encapsulated compounds such as drugs, genes or imaging agents.[20, 30]

Unimers

Stimulus

Miceles
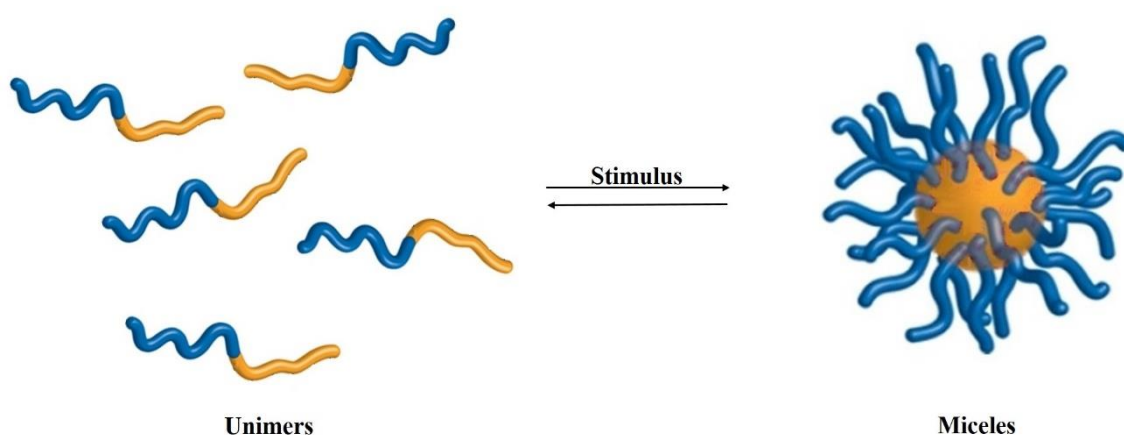
Figure 10. Reversible micellization in response to an external stimulus.

For example, based on the Wu results[31], a succinic anhydride (SA)-modified poly(2-diisopropylaminoethyl methacrylate)-block-poly(2-aminoethyl methacrylate hydrochloride) drug-loaded (PDPA-*b*-PAMA/SA@DOX•HCl) exhibited obvious aggregation through electric interaction between the positive charge of the protonated PDPA block and the negative charge of the PAMA/SA block at tumour sites under slightly acidic condition. Moreover, the drug-loaded nanocarriers exhibited accelerated drug release profiles in response to the acidic condition due to the electric repulsion between the protonated PDPA block and positive DOX•HCl. Cytotoxicity assay results demonstrated that the pH-sensitive block copolymer did not demonstrate obvious cytotoxicity. Thus, these results suggest that PDPA-*b*-PAMA/SA provides a feasible platform for efficient tumour-targeted therapy.[31]

Most stimuli-responsive block copolymers have been synthesized by ATRP, due to its versatility in terms of monomer selection and the mild reaction conditions that this technique offers.[30] Some frequently used monomers for generating stimuli-responsive polymers are shown in Figure 11.[20]
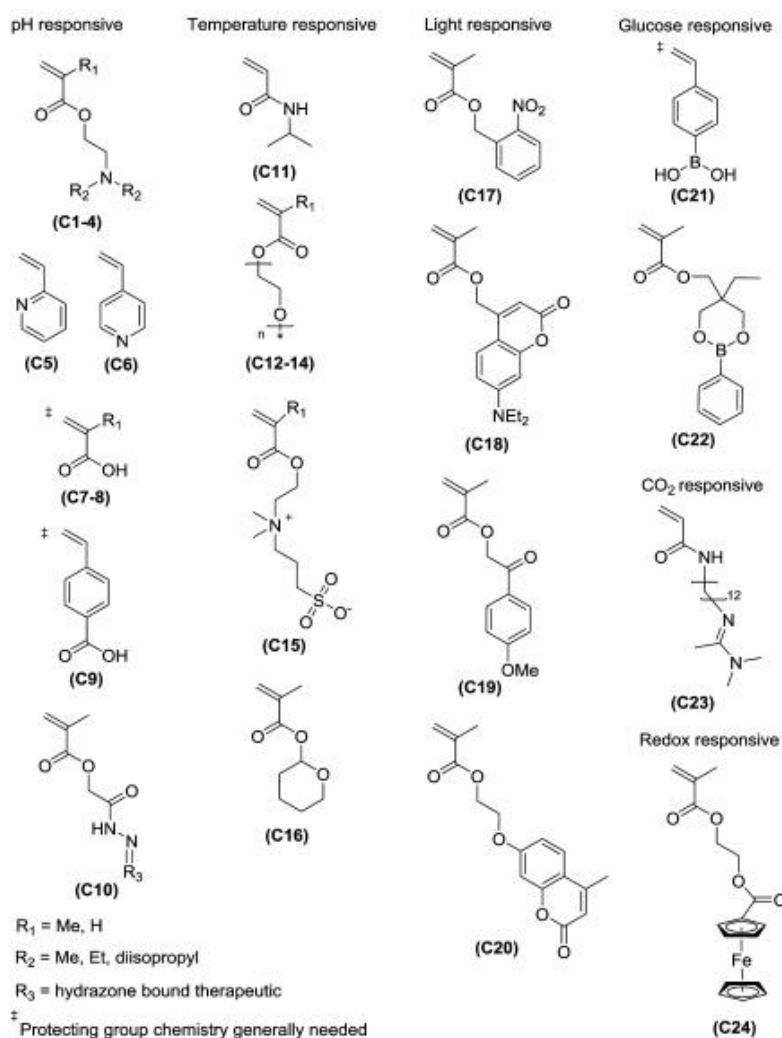
Figure 11. Common examples of stimuli-responsive monomers that can be polymerized by copper-mediated living radical polymerization. pHresponsive monomers: (C1) DMAEMA = 2-(dimethylamino)ethyl methacrylate, (C2) DMAEA = 2-(dimethylamino)ethyl acrylate, (C3) DEAEMA = 2-(diethylamino)ethyl methacrylate, (C4) DPA = 2-(diisopropylamino)ethyl methacrylate, (C5) 2VP = 2-vinylpyridine, (C6) 4VP = 4- vinylpyridine, (C7) MAA = methacrylic acid, (C8) AA = acrylic acid, (C9) VBzA = 4-vinylbenzoic acid, (C10) MEMA-Hyd = 2-hydrazinyl-2-oxoethyl methacrylate (hydrazide precursor); temperature-responsive monomers: (C11) NIPAAm = N-isopropylacrylamide, (C12) OEGMA = oligo(ethylene glycol) methyl ether methacrylate, (C13) OEGA = oligo(ethylene glycol) methyl ether acrylate, (C14) MEO2MA = OEGMA where n = 2, (C15) MEDSA = [2-(Methacryloyloxy)ethyl]dimethyl-(3-sulfopropyl)ammonium hydroxide, (C16) THPMA = tetrahydropyranyl methacrylate; light-responsive monomers: (C17) NBMA = ortho-nitrobenzyl methacrylate, (C18) DEACouMA = (7-(diethylamino)-2-oxo-2Hchromen-4-yl)methyl methacrylate, 7-(diethylamino)coumarin-based methacrylate, (C19) PMPMA = p-methoxyphenacyl methacrylate, (C20) CouHEMA = 2-((4-methyl-2-oxo-2H-chromen-7-yl)oxy)ethyl methacrylate; glucose-responsive monomers: (C21) 4VPBA = (4-vinylphenyl)- boronic acid, (C22) pBDEMA = (5-ethyl-2-phenyl-1,3,2-dioxaborinan-5-yl)methyl methacrylate; CO2-responsive monomers: (C23) ADAm = (Namidino)dodecyl acrylamide; and redox-sensitive monomer: (C24) MAEFc = 2-(methacryloyloxy) ethyl ferrocene-carboxylate.[20]

Taking into account all these factors DPA and DMAEMA, which are stimuli-responsive monomers with a pH transition near physiological values, were chosen for the synthesis of the copolymers in this work.

1.4.3.1. PDPA

Poly(2-(diisopropylamino)ethyl methacrylate) (PDPA) is a tertiary amine methacrylate with a hydrophilic/hydrophobic transition at pH around 6.2, typically used in biomedical applications. PDPA-based copolymers have been widely used in the preparation of smart nanostructures for the controlled release of small molecules, complexation and delivery of genetic material, specific targeting, or magnetic resonance imaging (MRI) contrast agents.[18] Usually, the PDPA segment is linked to a permanently hydrophilic block such as PEG.[32] In solution, for pH above the pKₐ of PDPA, these block copolymers undergo a self-assembly into micellar structures. The PDPA segment is located at micellar core which can encapsulate hydrophobic anticancer drugs. This block undergoes a sharp hydrophobic/hydrophilic pH-induced transition within a pH range that is particularly attractive for tumour-targeting drug delivery, because tumour tissue have lower pH (5.7–7.8) and higher temperature than that of normal tissues.[33]

Several studies have been reported using DPA-based copolymers. The first reported ATRP of DPA was carried out in methanol with a Cu(I)Br/2,20-bipyridine (bpy) complex using a water soluble poly(2-methacryloyloxyethyl phosphorylcholine) macroinitiator.[24] Several DPA based copolymers have been synthesized using the same approach with slight variations in the solvent used and the copper based catalytic complexes.[24] However, the abovementioned systems required a considerable amount of copper catalyst to control the polymerization and to afford polymers of low dispersity. Concerning the potential of PDPA-based polymeric structures for biomedical applications, herein we propose the SARA ATRP of DPA using a more biocompatible and eco-friendly catalyst system that involves the use of only trace amounts of copper catalyst.[24]

1.4.3.2. PDMAEMA

Block copolymers with poly(dimethylaminoethyl methacrylate) PDMAEMA segments are of interest for gene delivery applications, due to their higher transfection efficiency and lower cytotoxicity.[22] PDMAEMA is nontoxic in its nonquaternized form and water-soluble in its protonated form; it can be absorbed by endocytosis and can be used as a non-viral gene vector.[30, 34]

Contrarily to PDPA, PDMAEMA is a pH and temperature-sensitive polymer with a pK_a around 7.4, and a lower critical solution temperature (LCST) between 32 and 46 °C, depending on the molecular weight and solution pH. Above the LCST PDMAEMA becomes hydrophobic, and bellow becomes hydrophilic.[30, 34]

In 1998, several studies have been published concerning the ATRP synthesis of PDMAEMA.[35-37] Most of them were carried under mild reaction conditions, *i.e.,* in polar media and ambient temperature. However, the use of high amounts of copper catalyst to afford controlled polymers is an issue for the synthesis of polymers to be applied in the biomedical field. Some authors reported the synthesis of PDMAEMA block copolymers using macroinitiators of biomedical relevance, such as hydrophilic and biocompatible cholesterol and PEG due to the compatibility of PEG with biological systems.[22, 37]

Lin et al. [36] developed an acid-labile block copolymer consisting of (PEG-a-PDMAEMA) connected through a cyclic ortho ester linkage synthesized by ATRP of DMAEMA using a PEG macroinitiator with an acid-cleavable end group. PEG-a-PDMAEMA condensed with plasmid DNA formed polyplex nanoparticles with an acid-triggered reversible PEG shield. At pH 7.4, polyplexes generated from PEG-a-PDMAEMA exhibited smaller particle size, lower surface charge, reduced interaction with erythrocytes, and lower cytotoxicity. In vitro transfection efficiency of the acid-labile copolymer greatly increased.[36]

Aim of the Project

Chapter 2

2. Aim of the Project

For many years the molecular weight, or chain length, of polymers has been shown to have significant impact on gene delivery.[11] The relationship between polymer molecular weight and transfection efficiency has been studied in many polymers. The length of the amphiphilic block exerted significant influence on how the polymer carrier interacted with genes.[38] In general, increasing molecular weight will increase gene expression. However, some discrepancies exist and a fundamental understanding of the influence of linear polycation chain length on the gene transfer process remains elusive. Controlled polymerization techniques such as ATRP make it possible to prepare amphiphilic polymers with defined chain length in a facile way.[11, 38]

Considering the relevance of DMAEMA and DPA for biomedical applications, a new polymeric-based systems for gene delivery were investigated, composed by stimuli-responsive block copolymers: POEOMA-*b*-PDPA and POEOMA-*b*-PDMAEMA.

POEOMA is the permanent hydrophilic segment. It is nontoxic to cells and biocompatible.[39, 40] **PDPA** and **PDMAEMA** are pH-responsive polymers with potential applications into the biomedical field that undergoes hydrophilic/hydrophobic pH-induced transition within a physiologically relevant pH window (Figure 12). In the case of PDMAEMA, the polymer is also thermo-responsive.
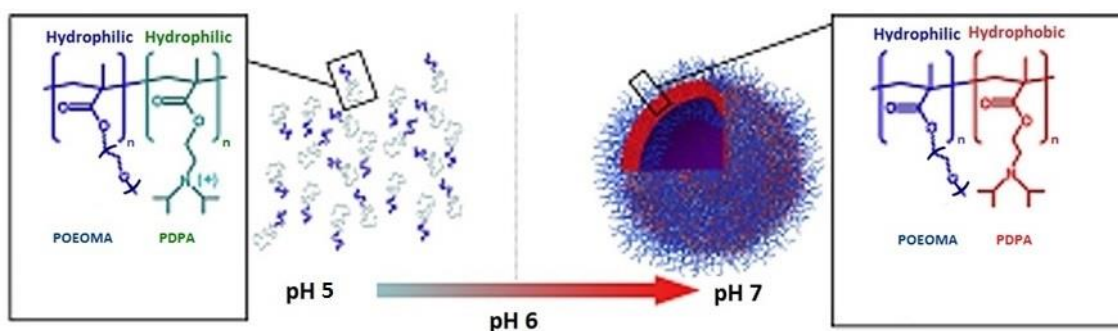
Figure 12. Chemical structure of the POEOMA-*b*-PDPA block copolymer in solution. Below the PDPA pK$_a$ the tertiary amine groups are protonated and the block copolymer is soluble. Above pH 6 the PDPA tertiary amine groups become deprotonated and induces the self-assembly. Adapted from ref.[2].

The main objective of this work is the synthesis of well-defined stimuli-responsive block copolymers, with different compositions and distinct degree of polymerization (DP) for target biomedical applications using a more eco-friendly catalytic ATRP system (Figure 13). The SARA ATRP mediated by $Na_2S_2O_4$ was chosen as the synthesis method and several reaction parameters were evaluated in order to obtain well-defined (co)polymers using reduced concentrations of copper catalyst. A library of copolymers of PDPA and PDMAEMA was synthesised and fully characterized by gel permeation chromatography and ^{1}H nuclear magnetic resonance. The solution properties of these copolymers were studied, such as **pH transition** as well as the properties of the resultant self-assembly structures (**size** and **surface charge)** and related to the block copolymer **molecular composition. The relationship between the polymeric structure and the solution properties was established.** At the end, the resultant block copolymers was evaluated for gene delivery.
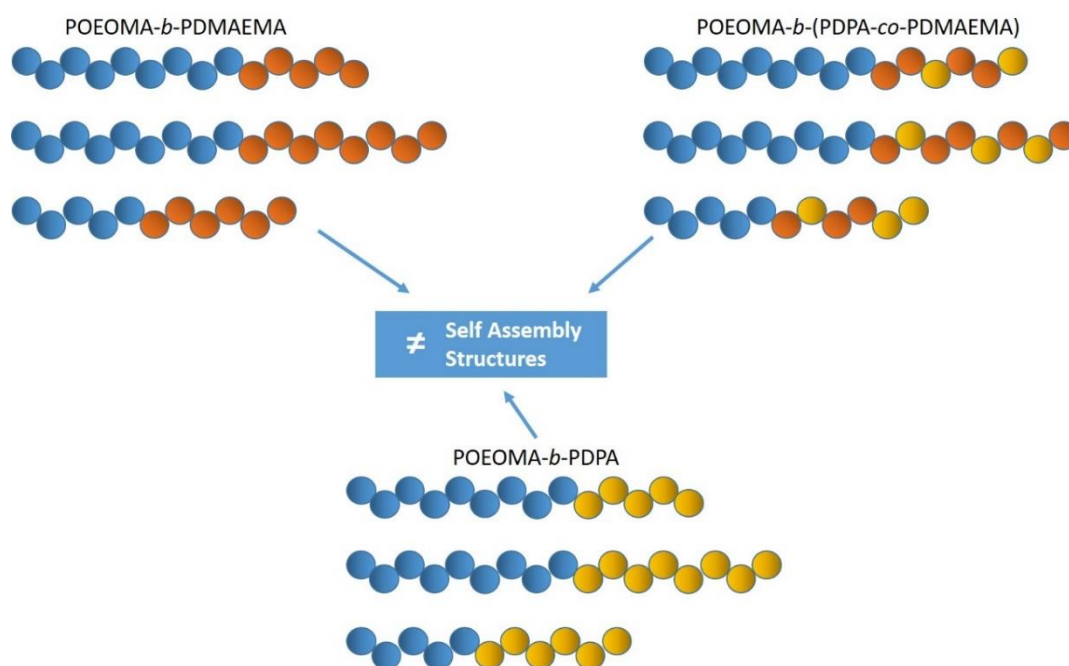
Figure 13. Schematic representation of the block copolymers.

Experimental Section

Chapter 3

30

3. Experimental Section

3.1.   Materials

2-(Diisopropylamino)ethyl methacrylate (DPA, 97%, Scientific Polymer Products Inc.), oligo(ethylene oxide) methyl ether methacrylate (OEOMA, 99%, average molecular weight 475, Aldrich) and 2-(dimethylamino)ethyl methacrylate (DMAEMA, 98%, Aldrich) were passed over a column of basic alumina to remove the inhibitor prior to use. Sodium dithionite ($Na_2S_2O_4$, 85%, ACROS Organics), copper($_{II}$) bromide ($Cu^{II}Br_2$, 99.999%, Aldrich), ethyl α-bromophenyl acetate (EBPA, 97%, Alfa Aesar), isopropanol (IPA, ACS grade, Fisher Scientific), tetrahydrofuran (THF, ACS grade, Fisher Scientific), deuterated chloroform ($CDCl_3$) (99.8%, Cambridge Isotope Laboratories), Deuterium oxide (D_2O) (99,9%, Aldrich) anhydrous magnesium sulphate ($MgSO_4$) (99%, Aldrich), methanol (MeOH) and sodium hydroxide (NaOH) were used as received. Tris(2-(dimethylamino)ethyl)amine (Me_6TREN) and tris(pyridin-2-ylmethyl)amine (TPMA) were synthesized as reported in the literature.[18, 24] Purified water (Milli-Q®, Millipore, resistivity >18 MΩ cm) was obtained by reverse osmosis.

3.2.   Techniques
3.2.1.   Size Exclusion Chromatography

For PDPA homopolymers and all of block copolymers, SEC analysis was performed using a system equipped with an online degasser, a refractive index detector and a set of columns: Shodex OHpak SB-G guard column, OHpak SB-802.5HQ and OHpak SB-804HQ columns. The polymers were eluted at a flow rate of 0.5 mL min^{-1} with 0.1 M Na_2SO_4 (aq)–1 wt% acetic acid–0.02% NaN_3 at 40 °C. Before injection (50 µL) the samples were filtered through a polyester membrane with 0.45 µm pores. The system was calibrated with narrow Đ (M_w/M_n) PEG standards. The number average molecular weight (M_n^{SEC}) and Đ of the synthesized polymers were determined by conventional calibration using Clarity software version 2.8.2.648.

High performance gel permeation chromatography (HPSEC) was performed in POEOMA samples, using a Viscotek (ViscotekTDAmax) with a differential viscometer, right-angle laser-light scattering (RALLS, Viscotek), and refractive index detectors, using a column set of a PL 10 µm guard column followed by one MIXED-E PLgel column and one MIXED-C PLgel column. Previously filtered THF was used as an eluent at a flow rate of 1.0 mL min^{-1} at 30 °C. The samples were filtered through a polytetrafluoroethylene membrane with 0.2 µm pores before injection and the system was calibrated with narrow PS standards. The M_n^{SEC} and $Đ$ of the synthesized polymers were determined by using a multidetector calibration system (OmniSEC software version: 5.0).

3.2.2.   Nuclear Magnetic Resonance Spectroscopy

^{1}H NMR (400 MHz) spectra of reaction mixture and pure copolymers samples were recorded on a Bruker Avance III 400 MHz spectrometer, with a 5-mm TXI triple resonance detection probe, in CDCl$_3$ or D$_2$O with tetramethylsilane (TMS) as an internal standard. Conversion of monomers was determined by integration of monomer and polymer signals using MestReNova software version: 6.0.2-5475.

3.2.3.   Acid-base titration

Potentiometric titration curves of polymers were obtained in Milli-Q purified water. Samples of the pure (co)polymers (10 mg) were dissolved in 0.1 M HCl solution (5 mL) (2.0 mg mL^{-1}). The solution was then titrated with 100 µL aliquots of 0.02 M NaOH. Titration curve of Milli-Q purified water (without polymer) was used as background control. Measurements were taken using a Jenway 3510 pH meter (Stone, Staffs, UK). The pK$_a$ was calculated using the first-derivate of the titration curve.[41]

3.2.4. Dynamic Light Scattering and Zeta Potential Analysis

Dynamic light scattering (DLS) measurements were performed on a Zetasizer Nano-ZS (Malvern Instruments Ltd., UK). The particle size distribution (in intensity), average hydrodynamic particle size average (z-average), and polydispersity index (PDI) were determined with Zetasizer 7.11 software. Measurements were made at 25 °C and at a backward scattering angle of 173°. Zeta-potential measurements were performed using a Zetasizer Nano-ZS (Malvern Instruments Ltd.), coupled to laser Doppler electrophoresis and determined using a Smoluchovski model. The aggregates were prepared before analysis and independent experiments were performed in triplicate for size and zeta potential.

3.2.5. Atomic Absorption Spectroscopy

An atomic absorption spectrometer 3300 (Perkin Elmer, USA) flame atomic absorption spectrometer was used for the analysis of residual copper content. The copper hollow cathode lamp was run under the conditions suggested by the manufacturer (current: 4.0 mA). Also, the wavelength (324.8 nm) and the bandwidth of the slit (0.7 nm) had conventional values. The flame composition was: acetylene (flow rate: 2.0 L min^{-1}) and air (flow rate: 10.0 L min^{-1}). Aspiration flow rate was 5.0 L min^{-1}. At least, eight measurements were taken for each sample. 50 mg of each copolymer/homopolymers was dissolved in a volume with 10 mL of 0.1 M HCl at a pH 5.

3.2.6. Formulation of pDNA loaded nanoparticles

Plasmid DNA (pDNA) loaded nanoparticles were synthesized by the ionotropic gelation technique. For this synthesis a 1.0/0.1/0.01 mg mL^{-1} (pH 4.9) copolymer solution were prepared. All the solutions were then filtered with a 0.22 μm filter to remove traces of solid particles. In order to promote encapsulation, pDNA (20 μg mL^{-1}) was added to

the copolymer solution prior to particle formation, under magnetic stirring (300 ± 50 rpm), at room temperature, for 30 min. The formulated nanoparticles were then pelleted by centrifugation at 17,000 g for 30 min.

3.2.7. Encapsulation efficiency of pDNA

To determine pDNA encapsulation efficiency (EE) nanoparticle samples were isolated by centrifugation, and the supernatant recovered for further analysis. The concentration of unbound pDNA was measured by UV–vis analysis (Shimadzu UV–vis spectrophotometer, Shimadzu Inc, Japan) as reported in the literature.[42]

3.2.8. Agarose gel electrophoresis

The agarose gel electrophoresis experiments were performed using a 1% agarose gel with ethidium bromide ($0.5~\mu g~mL^{-1}$). Electrophoresis was carried out at 100 V for 45 min in Tris–Acetate–Ethylene Diamine (TAE) buffer. The agarose gels were revealed under UV light. Lane density measurements were performed in the software Bio-Rad Quantity One® (Hercules, USA).

3.2.9. Cytotoxicity assays

The cellular toxicity of nanoparticles was determined by the MTS assay, which was performed both in A549 (cell line human lung carcinoma) and rat skin Fibroblasts, according to the manufacturer instructions. Twenty four hours prior to the experiment the cells were seeded at a density of 2×10^4 cells per well into 96-well flat bottom culture plates with 200 μL of cell culture medium supplemented with 10% fetal bovine serum (FBS), without antibiotics. On the day of the experiment the culture medium was aspirated and replaced by fresh medium. The cells were then incubated with 30 μL of nanoparticle formulations for 48 h. All the formulations of nanoparticles were resuspended in pre-warmed culture medium containing 10% FBS and then added to each well. A total of five replicates were considered for each formulation.

3.3. Procedures
3.3.1. Typical procedure for the SARA ATRP of DPA

PDPA was synthesized by SARA ATRP of DPA using EBPA as an initiator (Figure 14). A mixture of $CuBr_2$ (0.10 mg, 0.47 µmol), TPMA (0.27 mg, 0.94 µmol), water (56 µL), $Na_2S_2O_4$ (1.92 mg, 11.03 µmol), DPA (1.00 g, 4.70 mmol), EBPA (11.40 mg, 46.88 µmol) and IPA (1.056 mL) were added to the Schlenk flask reactor and frozen in liquid nitrogen. The reaction mixture was deoxygenated by three freeze–pump–thaw cycles and purged with nitrogen. The reactor was placed in an oil bath at 40 °C with magnetic stirring (600 rpm). In case of kinetics, aliquots of the reaction mixture were collected periodically during the polymerization by using an airtight syringe and purging the side arm of the Schlenk tube reactor with nitrogen and analysed by SEC and ^{1}H NMR. To obtain pure polymers the resultant solution was dissolved in SEC (H_2O) eluent and dialyzed against distilled water. PDPA was obtained after freeze drying.
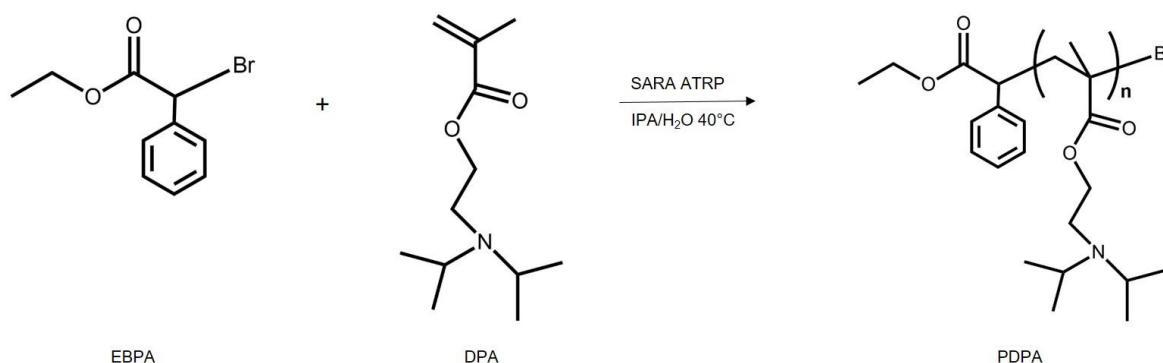
Figure 14. Typical synthesis of PDPA via SARA ATRP.

3.3.2. Typical procedure for the SARA ATRP of OEOMA

The procedures for the SARA ATRP of OEOMA (Figure 15) using $Na_2S_2O_4$ were similar to that used for the DPA, but the monomer concentration was adjusted to 54% (w/w). A mixture of $CuBr_2$ (0.27 mg, 1.20 µmol), TPMA (0.70 mg, 2.40 µmol), water (161 µL), $Na_2S_2O_4$ (6.15 mg, 35.29 µmol), $OEOMA_{500}$ (3.0 g, 6.0 mmol), EBPA (29.17 mg, 120.0 µmol) and IPA (3.061 mL) were added to the Schlenk flask reactor and frozen

in liquid nitrogen. The reaction mixture was deoxygenated by three freeze–pump–thaw cycles and purged with nitrogen. The reactor was placed in an oil bath at 40 °C with stirring (600 rpm). For kinetics, aliquots of the reaction mixture were collected periodically during the polymerization by using an airtight syringe and purging the side arm of the Schlenk tube reactor with nitrogen and analysed by SEC and ^{1}H NMR. To purify the polymers the resultant solution was dissolved in THF and dialyzed against distilled water. The pure POEOMA was obtained after freeze drying.
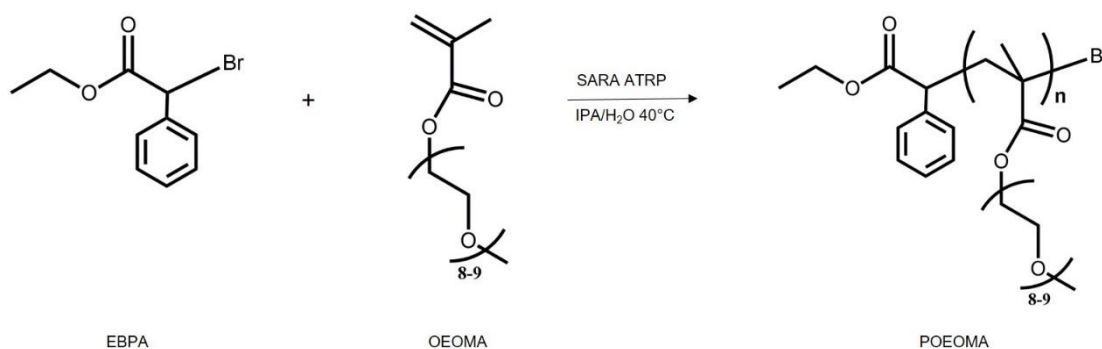
Figure 15. Typical synthesis of POEOMA via SARA ATRP.

3.3.3. Synthesis of POEOMA-*b*-PDPA block copolymers

The pH-sensitive block polymers of POEOMA-*b*-PDPA were prepared by SARA ATRP (Figure 16) using POEOMA-Br as the macromolecular initiator in a solution of IPA/water = 95/5 (v/v). In a typical reaction a mixture of CuBr$_2$ (0.33 mg, 1.50 µmol), water (10 µL), TPMA (0.69 mg, 2.39 µmol), DPA (0.35 g, 1.64 mmol), POEOMA (0.24 mg, 29.83 µmol) (29% conversion, $M_n^{th} = 4.507 \times 10^3$ g mol^{-1}, $M_n^{SEC} = 7.57 \times 10^3$ g mol^{-1}, Đ = 1.20) in IPA (3.325 mL) was placed in a Schlenk tube reactor that was sealed by using a rubber septum. The reactor was bubbled with nitrogen for about 15 minutes. A mixture of Na$_2$S$_2$O$_4$ (1.53 mg, 8.78 µmol) in water (165 µL) (previously bubbled with nitrogen for about 15 minutes) was slowly fed into the reaction mixture using a syringe pump at a feed rate of 229 nL min^{-1}. The polymerization proceeded for 12 h at 40 °C. The resultant solution was dialyzed against distilled water. Then, the solution was freeze-dried from water to yield POEOMA-*b*-PDPA.
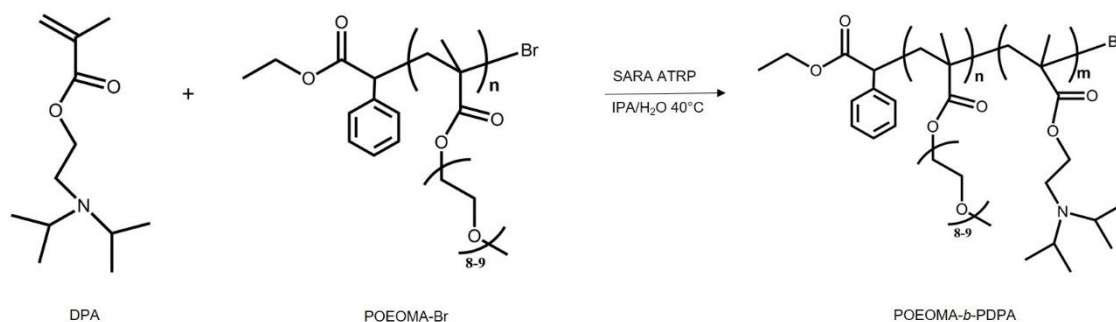
Figure 16. Typical synthesis of POEOMA-b-PDPA via SARA ATRP.

3.3.4. Synthesis of POEOMA-*b*-PDMAEMA block copolymers

The pH-sensitive block polymers of POEOMA-*b*-PDMAEMA were prepared by SARA ATRP (Figure 17) using POEOMA-Br as the macromolecular initiator in a solution of IPA/water = 95/5 (v/v). In a typical reaction a mixture of CuBr$_2$ (0.12 mg, 0.53 µmol), water (10 µL), TPMA (0.25 mg, 0.85 µmol), DMAEMA (0.20 g, 1.27 mmol), POEOMA (0.22 mg, 10.59 µmol) (53% conversion, M_n^{th} = 13.561×10^3 g mol^{-1}, M_n^{SEC} = 20.99×10^3 g mol^{-1}, Đ= 1.09) in IPA (1.833 mL) was placed in a Schlenk tube reactor that was sealed by using a rubber septum. The reactor was bubbled with nitrogen for about 15 minutes. A mixture of Na$_2$S$_2$O$_4$ (0.54 mg, 3.12 µmol) in water (85 µL) (previously bubbled with nitrogen for about 15 minutes) was slowly fed into the reaction mixture using a syringe pump at a feed rate of 120 nL min^{-1}. The polymerization proceeded for 12 h at 40 °C. The resultant solution was dialyzed against distilled water. Then, the solution was freeze-dried from water to yield POEOMA-*b*-PDMAEMA.
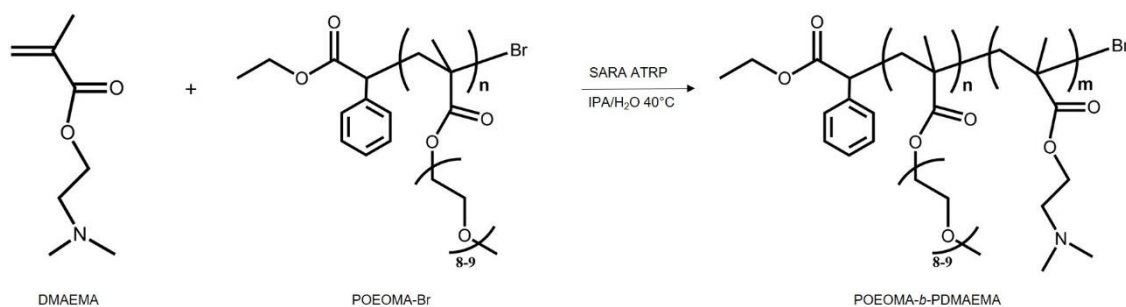
Figure 17. Typical synthesis of POEOMA-*b*-PDMAEMA via SARA ATRP.

3.3.5. Synthesis of POEOMA-*b*-(PDMAEMA-*co*-PDPA) block copolymers

The pH-sensitive block polymers of POEOMA-*b*-(PDMAEMA-*co*-PDPA) were prepared by SARA ATRP (Figure 18) using POEOMA-Br as the macromolecular initiator in a solution IPA/water = 95/5 (v/v). In a typical reaction a mixture of CuBr$_2$ (0.31 mg, 1.38 µmol), water (10 µL), TPMA (0.64 mg, 2.21 µmol), DMAEMA (0.50 g, 3.18 mmol), DPA (0.50 g, 2.34 mmol), POEOMA (0.37 mg, 27.61 µmol) (56% conversion, $M_n^{th} = 8.638 \times 10^3$ g mol^{-1}, $M_n^{SEC} = 13.53 \times 10^3$ g mol^{-1}, Đ= 1.23) in IPA (4.582 mL) was placed in a Schlenk tube reactor that was sealed by using a rubber septum. The reactor was bubbled with nitrogen for about 15 minutes. A mixture of Na$_2$S$_2$O$_4$ (0.54 mg, 3.12 µmol) in water (231 µL) (previously bubbled with nitrogen for about 15 minutes) was slowly fed into the reaction mixture using a syringe pump at a feed rate of 321 nL min^{-1}. The polymerization proceeded for 12 h at 40 °C. The resultant solution was dialyzed against distilled water. Then, the solution was freeze-dried from water to yield POEOMA-*b*-(PDMAEMA-*co*-PDPA).
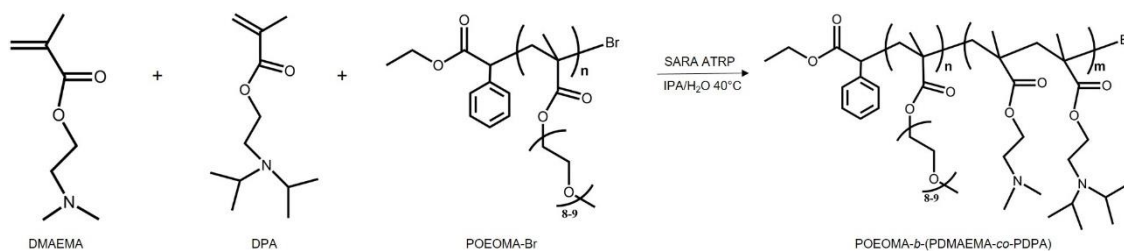
Figure 18. Typical synthesis of POEOMA-*b*-(PDMAEMA-*co*-PDPA) via SARA ATRP.

3.3.6. Typical procedure for the synthesis of PDMAEMA-*co*-PDPA copolymers

PDMAEMA-*co*-PDPA copolymers were synthesized by SARA ATRP of DPA and DMAEMA using EBPA as an initiator (Figure 19). A mixture of CuBr$_2$ (0.18 mg, 0.79 µmol), TPMA (0.46 mg, 1.57 µmol), water (56 µL), Na$_2$S$_2$O$_4$ (3.22 mg, 18.51 µmol), DPA (0.50 g, 2.34 mmol), DMAEMA (0.50 g, 3.18 mmol), EBPA (19.13 mg, 78.68 µmol) and IPA (2.074 mL) were added to the Schlenk flask reactor and frozen in liquid

nitrogen. The reaction mixture was deoxygenated by three freeze–pump–thaw cycles and purged with nitrogen. The reactor was placed in an oil bath at 40 °C with magnetic stirring (600 rpm). To obtain the pure polymer the resultant solution was dissolved in the SEC (H_2O) eluent (H_2O at acidic pH) and dialyzed against distilled water. PDMAEMA-*co*-PDPA was obtained after freeze drying.
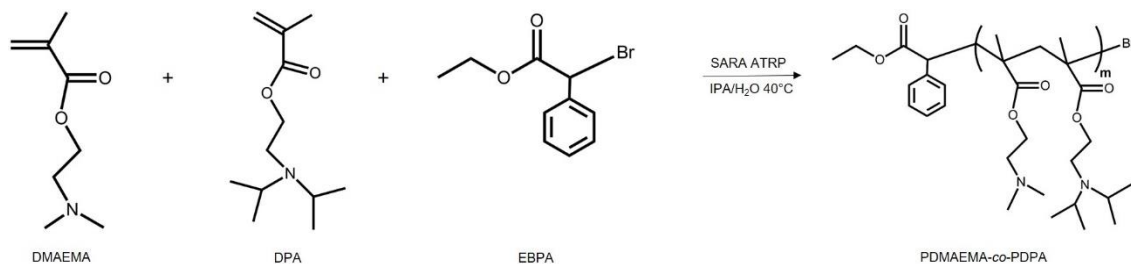
Figure 19. Typical synthesis of PDMAEMA-*co*-PDPA.

3.3.7.   Self-assembly of block copolymers

The self-assembly of block copolymers was carried out by both titration and solvent exchange methods to afford 1 mg mL^{-1} of aqueous solutions. In the titration method, the block copolymer was previously dissolved in an aqueous solution of HCl (0.1 M). The solution was then titrated using a very slow dropwise addition of 0.02 M NaOH aqueous solution. The change in the pH with respect to the added volume of the NaOH solution was recorded. The titration was stopped when the pH stabilized at 7.4. This method was not effective because the copolymer precipitated in solution, preventing the measurement of the size of the particles formed at a pH above the pK$_a$ of the different copolymers. Thus, solvent exchange method has been investigated.

In the solvent exchange method[43], to prepare samples for DLS, the block copolymer was previously dissolved in THF at a concentration of 10 mg mL^{-1}. 500 µL of the block copolymer solution were then added dropwise to 5 mL of Milli-Q water at a pH of 7.4, under vigorous stirring. The other 500 µL were added dropwise to 5 mL of a PBS solution at a pH of 7.4. The nanoparticles were formed and THF was removed through 12 h evaporation at room temperature.[44] The same method was used in MeOH for PBS and Milli-Q water.

In case of ζ-potential[43], the block copolymers were previously dissolved only in THF at a concentration of 20 mg mL^{-1}. 375 µL of the block copolymer solution were then added dropwise to 1.5 mL of Milli-Q water, under vigorous stirring, reaching a final concentration of 5 mg mL^{-1}.

Results and Discussion

Chapter 4

42

4. Results and Discussion

The molecular weight or chain length of polymers has been shown to have significant impact on DNA delivery. Controlled polymerization techniques such as ATRP make possible to prepare amphiphilic polymers with defined chain length in a facile way.[45] Because $Na_2S_2O_4$ was proven to be an efficient reducing agent, it was used in these studies.[46] The use of $Na_2S_2O_4$ in SARA ATRP acts as a powerful reducing agent for X–Cu^{II}/L species allowing efficient regeneration of Cu^I/L species, as well as generating radicals through the activation of halogen-carbon bonds by its role as a supplemental activator.[18] It should be mentioned that due to the poor solubility of sodium dithionite in isopropanol, the polymerization should always be carried out in the presence of a small amount of water.[24] The reports available in the literature concerning the ATRP of DPA based polymers involve the use of high concentration of copper catalysts and, in some cases, toxic solvents, such as THF or MeOH. However, polymers proposed to be applied in the biomedical field require the use of safer solvent mixtures and stringent removal of the catalyst from the final product. The capacity to control the polymerization with small amounts of copper/ligand complex in an alcohol–water mixture makes these systems very promising for the synthesis of polymers intended for biomedical applications.[24]

Therefore, a series of variables associated with SARA ATRP were taken into account in this work, to allow the synthesis of PDPA, POEOMA-*b*-PDPA, POEOMA-*b*-PDMAEMA and POEOMA-*b*-(PDMAEMA-*co*-PDPA) with defined chain length and narrow molecular weight distribution, under environmentally friendly reaction conditions.[15]

4.1. Synthesis of homopolymers

4.1.1. SARA ATRP of DPA

PDPA is highly biocompatible and pH sensitive with a pK_a of around 6.2. This monomer is hydrophobic when the pH is higher than pK_a due to its deionization, and becomes hydrophilic when ionized at low pH. PDPA has been used as a copolymer to develop pH sensitive nanomicelles.[47]

The kinetics of SARA ATRP of DPA were investigated. SARA ATRP using $Na_2S_2O_4$ was used to create well controlled polymers of PDPA (Figure 20). In SARA ATRP mediated by Cu(II)Br₂/ligand catalytic system employing inorganic sulphites, the use of small amounts of water in the reaction mixture can enhance the solubilisation of the inorganic salts leading to faster reactions.[24] Góis and co-authors have found that for the system $[DPA]_0/[EBiB]_0/[Na_2S_2O_4]_0/[Cu(II)Br_2]_0/[Me_6TREN]_0$ polymerization of DPA in a IPA/water mixture, the optimum content of water was 5 (v/v). Up to this value, the polymerization rate increased with the water content maintaining the control over the M_w and $Đ$.[24]
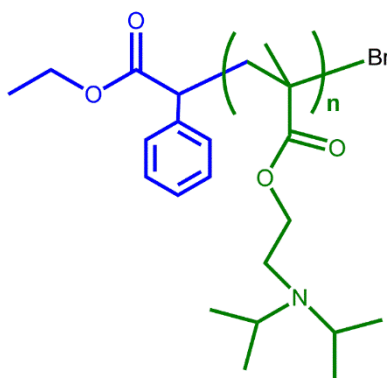
Figure 20. PDPA homopolymer synthesized by SARA ATRP with $Na_2S_2O_4$.

The kinetic results of SARA ATRP of DPA (Figure 21) indicate that the polymerization proceeds with only small deviations from the expected linear kinetics of typical RDRP systems. The observed induction period may be attributed to the significant rate of deactivation at the beginning of the polymerization due to the presence of Cu(II), whereas the deviation from linearity in CuBr₂ systems at high monomer conversion

reflects a significant decrease of active species.[22] After the induction period, a linear dependence of the $\ln[M]_0/[M]$ on the polymerization time was observed, and low $Đ$ values were obtained at all monomer conversions. The lower $Đ$ values indicate that an improved level of control over PDPA chain growth was achieved. The rate of polymerization achieves nearly full conversion of DPA in 24 hours, while forming PDPA with low $Đ$ values. In fact, very low $Đ$ values were obtained even for monomer conversions as high as 90%, which suggests that deviations from "living" polymerization conditions were negligible.

$$[DPA]_0/[EBPA]_0/[Na_2S_2O_4]/[CuBr_2]_0/[TPMA]_0=100/1/0.5/0.01/0.02$$
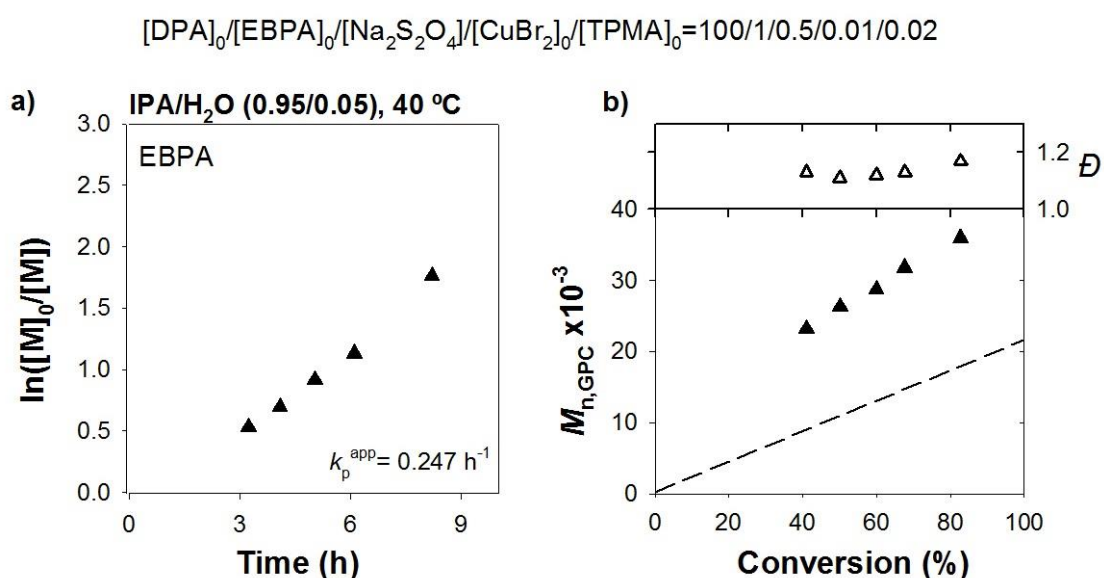
Figure 21. Kinetic plot of SARA ATRP of DPA in IPA/water (0.95/0.5 (v/v)) at 40 °C.

The SEC traces (Figure 22) of the samples that were taken at different reaction times show a unimodal distribution and a gradual shift towards high M_w with time. The polymerization reaches high monomer conversion (92%) in 24 hours with relatively low dispersity ($Đ = 1.17$). These results demonstrate the excellent degree of control achievable with the SARA ATRP process.
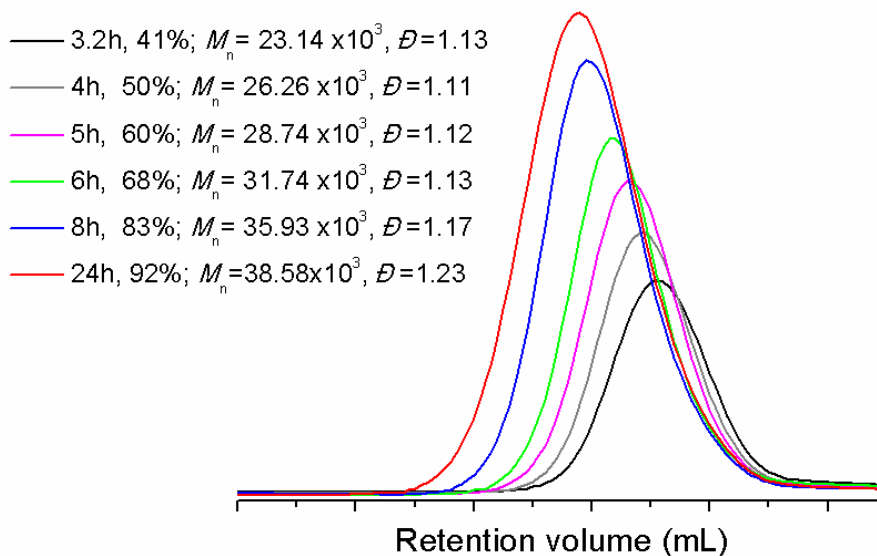
Figure 22. SEC traces with conversion of SARA ATRP of DPA in IPA/water=95/5 (v/v) at 40°C. Reaction conditions: $[DPA]_0/[EBPA]_0/[Na_2S_2O_4]_0/[CuBr_2]_0/[TPMA]_0=100/1/0.5/0.01/0.02$.

The chemical structure of the PDPA synthesized using EBPA as the SARA ATRP initiator, in D_2O, was determined using ^{1}H NMR technique. A ^{1}H NMR spectrum of a PDPA sample is shown in Figure 23. The peaks observed 4.27 ppm (t, $-OCH_2CH_2-$), 3.75 ppm (x, $-(CH-N)_2-$), 3.45 ppm (u, $-CH_2CH_2N-$), 1.95 ppm (s, $-CH_2-$ of the polymer backbone), resonances at 1.35 ppm (v, $-CH(CH_3)_2-$) and at 1 ppm (p, "methacrylic" CH_3) are in agreement with the expected PDPA chemical structure.[48] The peak of the methylene group (d) of the initiator fragment (CH_2) and the peak (r) of protons of the methine from the EBPA can be found at 4.82 ppm and its methyl resonances (h) are overlapped with other methyl group signals in the region around 1.08 ppm. The chemical shifts at 7.25-7.45 ppm correspond to the aromatic protons of the initiator.[49] The percentage of the bromine-chain-end functionality cannot be determined since the PDPA signals of the protons near the terminal bromine group are overlapped with the proton signals of the main polymeric chain (p).
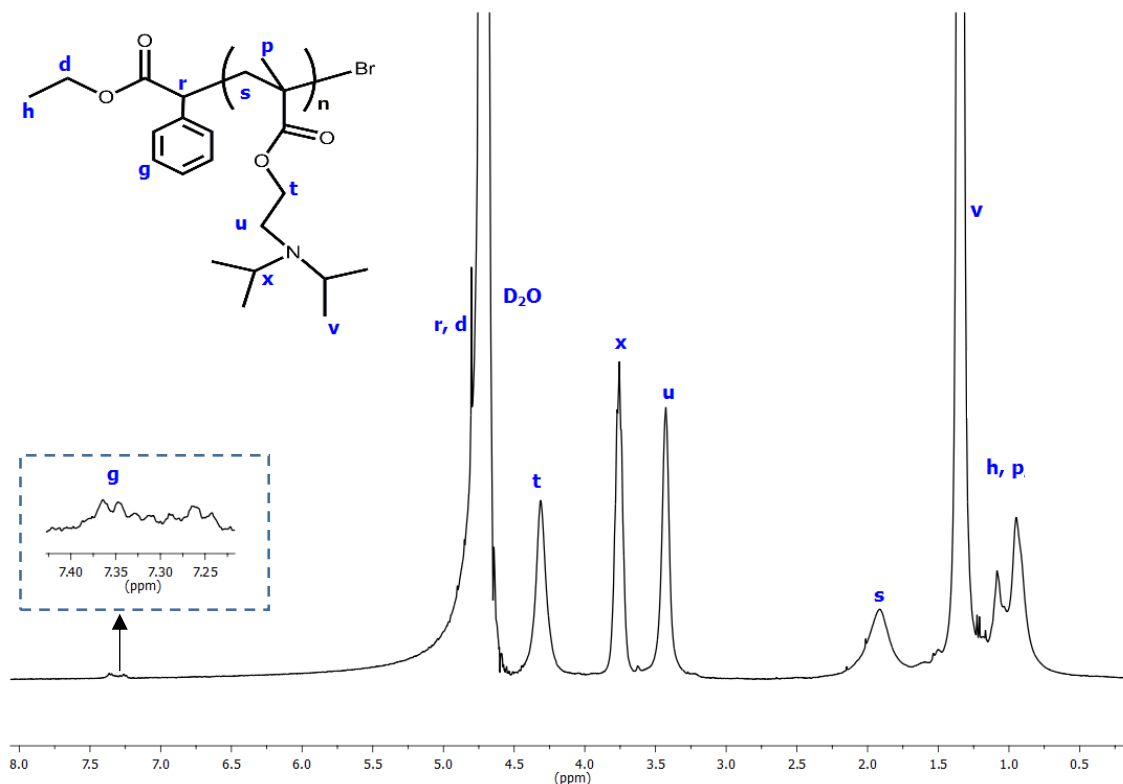
Figure 23. ^{1}H NMR spectrum, in D_2O of a pure PDPA sample (M_n^{SEC}= 25.0 x 10^3 ; Đ=1.1) obtained by SARA ATRP. Reaction conditions: [DPA]$_0$/[EBPA]$_0$/[Na$_2$S$_2$O$_4$]$_0$/[CuBr$_2$]$_0$/[TPMA]$_0$ = 84/1/0.2/0.01/0.02 (molar), Solv./Mon=1/1 (v/v), IPA/water = 95/5 (v/v), 40 °C.

Due to the overlapping of signals the degree of polymerization was determined by comparing integrals of t at 4.27 ppm (t) (PDPA), and of g at 7.35 ppm (g) (EBPA). From the ratio 2n/5 = I(t)/I(g), n = 84 was obtained. The molecular weight and the dispersity of the polymers were also determined by SEC analysis (Table 6).

Table 6. Molecular weight parameters of homopolymers of DPA synthesized by SARA ATRP with Na$_2$S$_2$O$_4$ based on ^{1}H NMR and SEC analysis.

Ref	Samples	$M_n^{th} \times 10^{-3}$	$M_n^{SEC} \times 10^{-3}$	Đ
FR 01	PDPA$_{84}$	18.14	24.84	1.10

The results listened in Table 6 indicate that very well-controlled DPA polymers can be synthesized using just 100 ppm of the Cu^{II}Br$_2$/TPMA complex with DP ≈ 84.

4.1.2.   SARA ATRP of OEOMA

Although DPA is an important monomer for biomedical applications, it is also relevant to investigate other water soluble methacrylates, and determine whether the conditions developed can be used polymerize other monomers. Therefore, the Cu/TPMA system was applied to polymerize OEOMA (Figure 24). The reactions were performed using the following conditions: IPA/water = 95/5 (v/v), $[OEOMA]_0/[EBPA]_0/[Na_2S_2O_4]_0/[CuBr_2]_0/[TPMA]_0 = 50/1/0.25/0.01/0.02$ (molar) and the monomer concentration was adjusted to 54% (w/w).
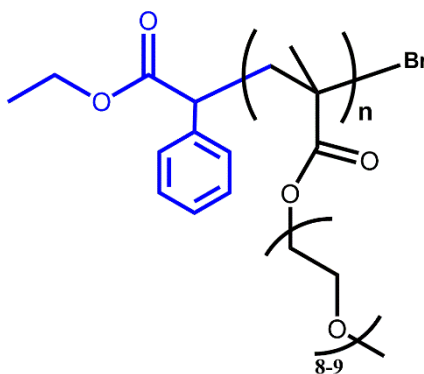
Figure 24. POEOMA-Br synthesized by SARA ATRP with $Na_2S_2O_4$.

The kinetic plots for the homopolymerization of OEOMA are presented in Figure 25, and they show a linear first order kinetics. The evolution of M_w is linear with conversion, and Đ were close to 1.20 throughout the polymerization, indicate that an improved level of control over POEOMA chain growth was achieved. The observed induction period may be attributed to the significant rate of deactivation at the beginning of the polymerization due to the presence of Cu(II), whereas the deviation from linearity in $CuBr_2$ systems at high monomer conversion reflects a significant decrease of active species.[22]

$$[OEOMA]_0/[EBPA]_0/[Na_2S_2O_4]/[CuBr_2]_0/[TPMA]_0 = 50/1/0.25/0.01/0.02$$
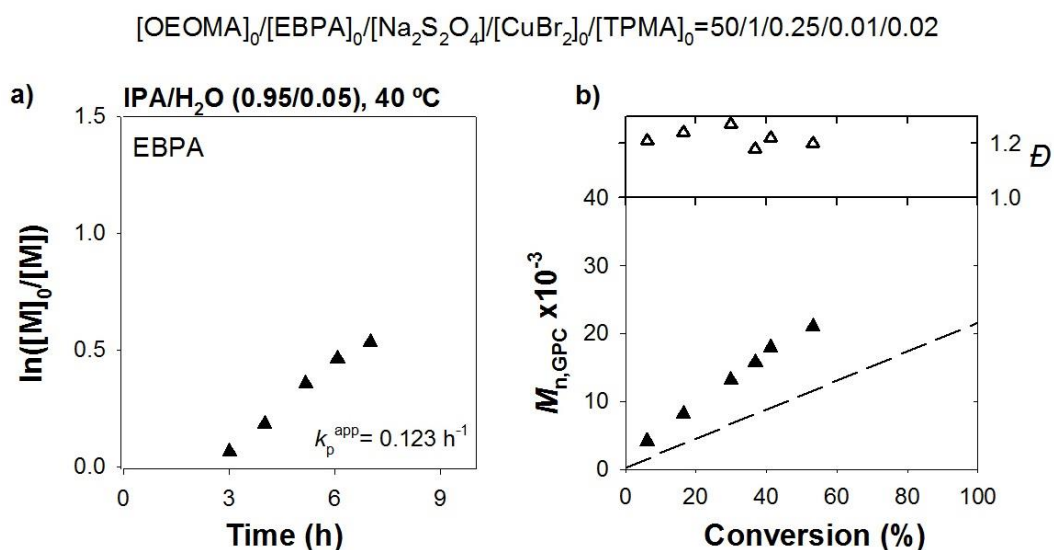
Figure 25. Kinetic plot of SARA ATRP of OEOMA in IPA/water (0.95/0.5 (v/v)) at 40 °C.

The SEC traces (Figure 26) of the samples that were taken at different reaction times show a unimodal distribution and a gradual shift towards M_w with time. The polymerization reaches low monomer conversion (53%) in 24 hours with relatively low dispersity ($Đ = 1.20$). These results demonstrate the excellent degree of control achievable with the SARA ATRP process.
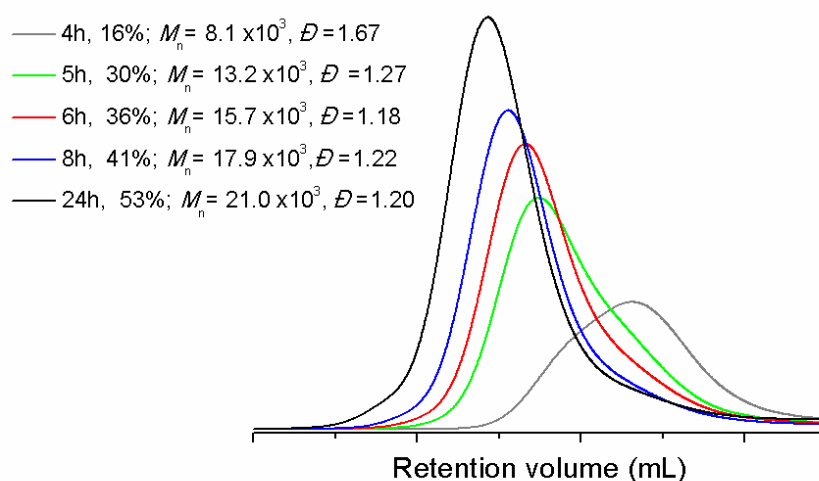
Figure 26. SEC traces with conversion of the SARA ATRP of POEOMA in IPA/water=95/5 (v/v) at 40°C. Reaction conditions: $[OEOMA]_0/[EBPA]_0/[Na_2S_2O_4]_0/[CuBr_2]_0/[TPMA]_0 = 50/1/0.25/0.01/0.02$.

Figure 27 presents the ^{1}H NMR spectrum, in CDCl$_3$, of the purified POEOMA synthesized using EBPA as the initiator, and prepared at 40 °C with the Na$_2$S$_2$O$_4$/CuBr$_2$/TPMA catalytic system. No peaks were observed between 5.5 and 6.5 ppm, indicating the complete removal of the unreacted monomer molecules of OEOMA$_{500}$.[39] The peaks ascribed to repeating OEOMA$_{500}$ units at 3.4 ppm (j, –O-CH$_3$–), 3.7 ppm (a,e,i, –O-CH$_2$–), the methylene of ending OEOMA$_{500}$ unit at 4.1 ppm (f, –CH$_2$-O–), 1.51-1.98 ppm (b) and 0.62-1.00 ppm (c) are in agreement with the expected POEOMA chemical structure.[50] The peak of the methylene group (d) of the initiator fragment (CH$_2$) can be found at 4.25 ppm and the peak (r) of protons of the methine from the EBPA can be found at 5.5 ppm; its methyl resonances (h) are overlapped with other methyl group signals in the region around 1 ppm. The chemical shifts at 7.25-7.46 ppm (g) correspond to the aromatic protons of the initiator.[49] Due to the overlapping of signals and low intensity of the resonances of the initiator moieties, the degree of polymerization was determined by comparing integrals of h at 1.20 ppm, and of f at 4.1 ppm. From the ratio $2n/3 = I(f)/I(h)$, n = 26 was obtained.
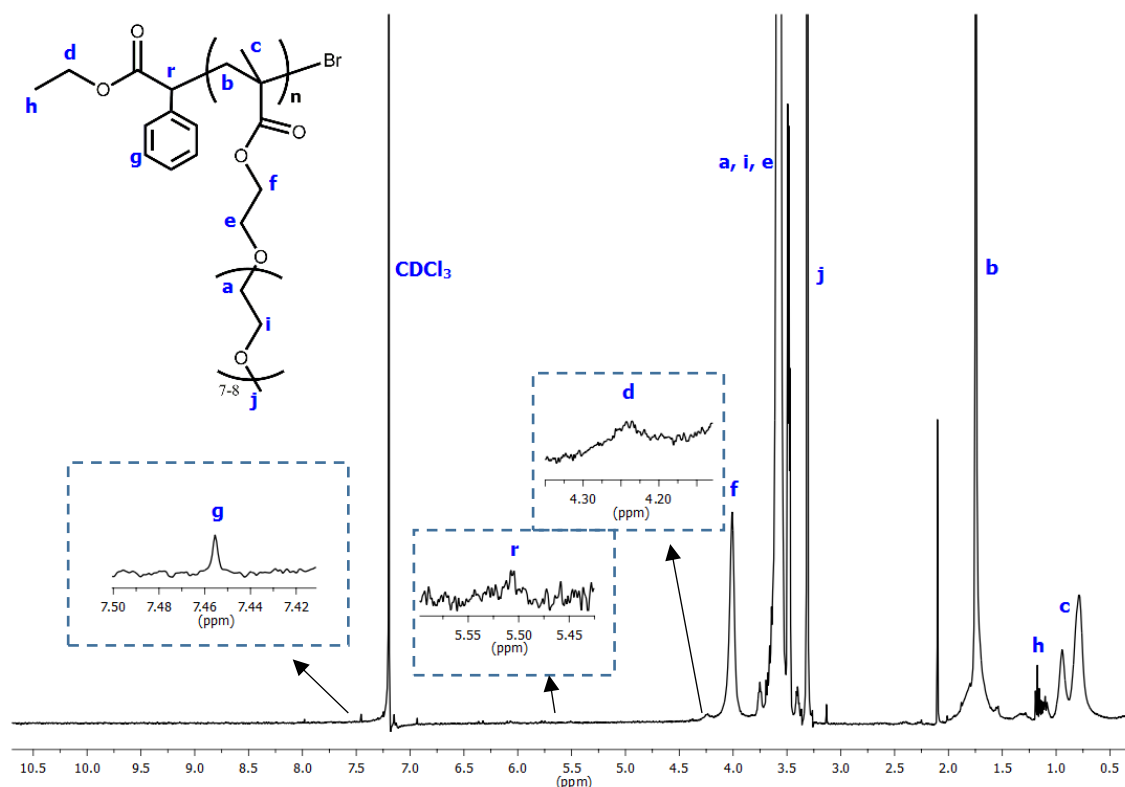
Figure 27. ^{1}H NMR spectrum, in CDCl$_3$ of a pure POEOMA sample (M_n^{SEC}= 21.0 x 10^3; Đ=1.09) obtained by SARA ATRP. Reaction conditions: [OEOMA]$_0$/[EBPA]$_0$/[Na$_2$S$_2$O$_4$]$_0$/[CuBr$_2$]$_0$/[TPMA]$_0$ = 26/1/0.25/0.01/0.02 (molar), [OEOMA]=54 wt%, IPA/water = 95/5 (v/v), 40 °C.

4.1.3.   Evaluation of the POEOMA "livingness"

One of the key advantages of SARA ATRP over conventional radical processes is their ability to create polymers with active chain-ends, which can be extended with either the same or a different monomer. The chain-end functionality of the synthesized polymers was confirmed by a chain extension reaction of a POEOMA macroinitiator with DPA. The complete shift of the SEC trace towards higher molecular weights after the copolymerization proves the "living" character of the POEOMA and the possibility of using this catalytic system in the synthesis of block copolymers (Figure 28).[15, 22, 46] No tailing was observed in the block copolymer molecular weight distribution, which suggests that the POEOMA have high chain-end functionality, allowing the successful extension of the polymer. This result was attributed to the lower concentration of metal catalyst/ligand complex used in SARA ATRP, in comparison with normal ATRP, which decreased the rate of catalyst induced side reactions.
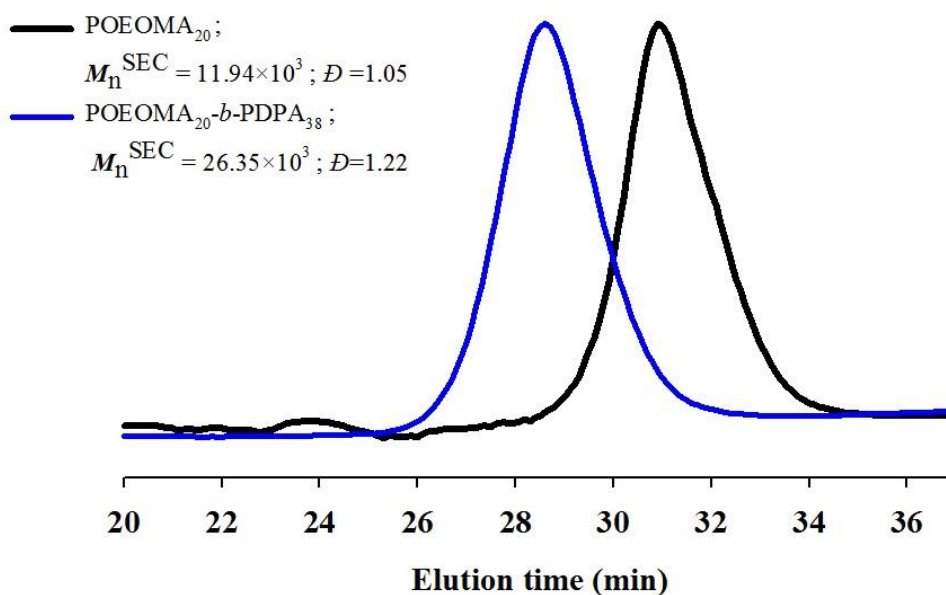
Figure 28. SEC traces of POEOMA$_{500}$ before and after extension with DPA: macroinitiator obtained at 40% of monomer conversion (black line) and block copolymer at 76% of DPA conversion (blue line). First block: [OEOMA]$_0$/[EBPA]$_0$/[Na$_2$S$_2$O$_4$]$_0$/[CuBr$_2$]$_0$/[TPMA]$_0$ = 50/1/0.25/0.01/0.02 (molar), [OEOMA]=54 wt%, IPA/water = 95/5 (v/v), 40 ^{0}C ; second block: [DPA]$_0$/[POEOMA-Br]/ [Na$_2$S$_2$O$_4$]$_0$/[CuBr$_2$]$_0$/[TPMA]$_0$ = 50/1/0.25/0.01/0.02 (molar), Solv./Mon(V)=9, IPA/water = 95/5 (v/v) and slow feeding of Na$_2$S$_2$O$_4$ solution, 40 ^{0}C.

4.2. Synthesis and characterization of block copolymers
4.2.1. POEOMA-*b*-PDPA copolymers

POEOMA-*b*-PDPA (Figure 29) is a pH-responsive diblock copolymer that can self-assemble to form micelles. The pH-responsive nature of the PDPA block means that these chains protonate, becoming cationic and water-soluble below its pK$_a$, but deprotonate, becoming hydrophobic and water-insoluble above its pK$_a$. The POEOMA is the permanent hydrophilic segment and thus, the amphiphilic character of this copolymer can be switched on or off via pH modulation. The well-defined block copolymers were obtained by a two-step SARA ATRP. Firstly, the POEOMA was obtained and purified to remove the monomer contamination. Then, the macro-POEOMA was chain extended with a second monomer, DPA, to obtain the POEOMA-*b*-PDPA copolymer. The copolimerization was performed at 40 °C, using a monomer to solvent ratio of 1/9 (v/v) and a solvent mixture of IPA-water of [95/5 (v/v)].
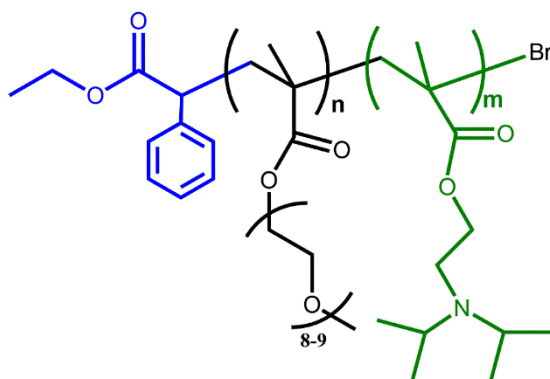
Figure 29. POEOMA-*b*-PDPA block copolymer synthesized by SARA ATRP with Na$_2$S$_2$O$_4$.

Figure 30 show the ^{1}H NMR spectrum of the pure POEOMA-*b*-PDPA copolymer, in CDCl$_3$. The peaks observed at 3.82 ppm (t, –OCH$_2$CH$_2$–), 2.98 ppm (x, –(CH–N)$_2$–), 2.62 ppm (u, –CH$_2$CH$_2$N–), 1.7–2.1 ppm (s, –CH$_2$– of the polymer backbone), resonances at 1 ppm (p, –CH(CH$_3$)$_2$–; v, "methacrylic" CH$_3$) are in agreement with the expected PDPA chemical structure. As mentioned above, the relative intensities of the peaks at 4.1 ppm (f), 3.40 ppm (j), 3.70 ppm (a,e,i), 1.7 ppm (b) and 0.62-1.5 ppm (c) are in agreement with the expected POEOMA chemical structure.[24, 39, 48, 51, 52] In addition, the mass percentages of each monomer unit of the POEOMA-*b*-PDPA block copolymer were calculated from

the comparison of the integral values of their characteristic peaks ((x, –(CH–N)$_2$–) of PDPA at 2.98 ppm and (j, –O-CH$_3$–) of POEOMA at 3.4 ppm), which allowed the estimation of the average DP of each segment. Knowing the DP of the POEOMA segment (calculated as explained in section 4.1.2), the DP of the PDPA segment is obtained from the ratio (DP(PDPA)/DP(POEOMA) = [I(x)/2]/[I(j)/3]).
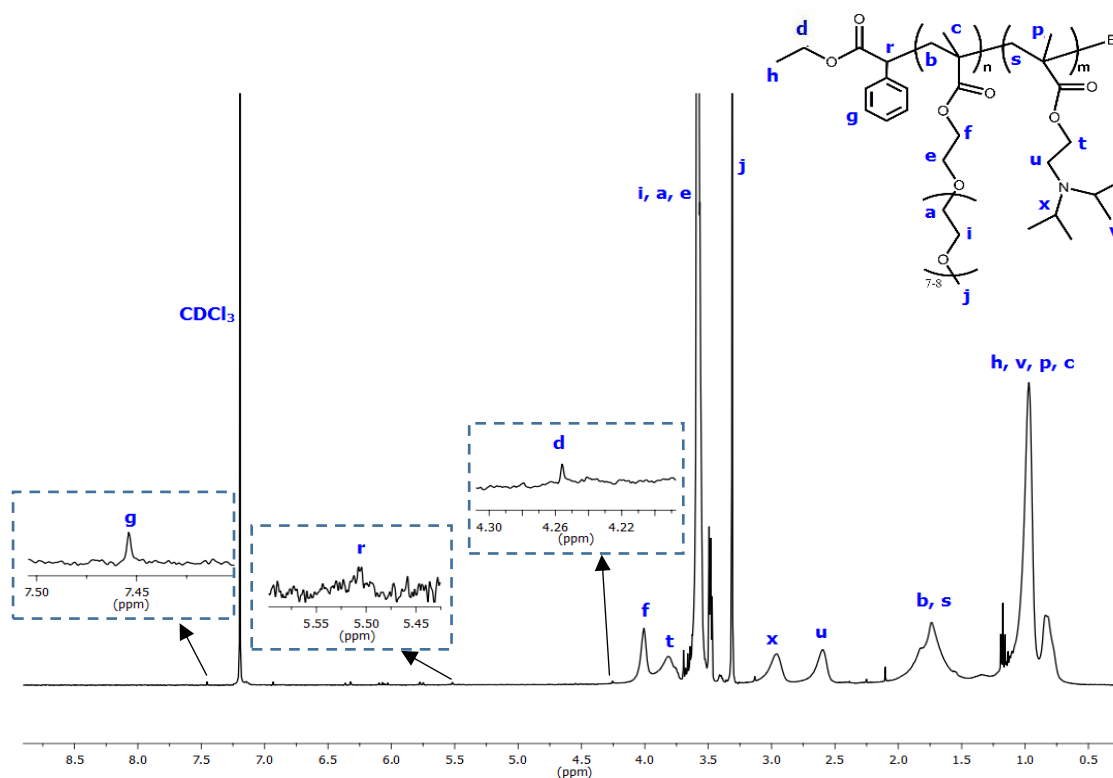
Figure 30. ^{1}H NMR spectrum, in CDCl$_3$ of a pure POEMA-*b*-PDPA sample (M_n^{SEC}= 26.0 x 10^3 ; Đ=1.21) obtained by SARA ATRP. Reaction conditions: [DPA]$_0$/[POEOMA-Br]/[Na$_2$S$_2$O$_4$]$_0$/[CuBr$_2$]$_0$/[TPMA]$_0$ = 38/1/0.25/0.01/0.02 (molar), Solv./Mon(V)=9, IPA/water = 95/5 (v/v) and slow feeding of Na$_2$S$_2$O$_4$ solution, 40 ^{0}C.

Initial attempts of the SARA ATRP synthesis of POEOMA-*b*-PDPA were done by adding the total amount of Na$_2$S$_2$O$_4$ at the beginning of the polymerization. This resulted in an uncontrolled polymerization (Đ > 1.5) with limited monomer conversion of 50% (all the reactions are present in table 18 (Attachments)). Alternatively, Na$_2$S$_2$O$_4$ was fed to the reaction via a syringe pump to regenerate the Cu(I) activator species in a slow and controlled manner because, as referenced in literature, higher feeding rates led to faster polymerization reactions with inferior control.[18] Using this strategy, it was possible to achieve high monomer conversion (≈ 85%) and more controlled polymerizations (Đ ≈ 1.3).

The average DP of each purified block was calculated based on ^{1}H NMR analysis. The molecular weight and the dispersity of the polymers synthesized with this new strategy were also determined by SEC analysis (Table 7).

Table 7. Molecular weight parameters of copolymers of POEOMA-*b*-PDPA synthesised by SARA ATRP with Na$_2$S$_2$O$_4$, and respective POEOMA macroinitiators based on ^{1}H NMR (M_n^{th}) and SEC analysis (M_n^{SEC}).

Ref	Samples	1st segment			Block copolymer		
		$M_n^{th} \times 10^{-3}$	$M_n^{SEC} \times 10^{-3}$	Đ	$M_n^{th} \times 10^{-3}$	$M_n^{SEC} \times 10^{-3}$	Đ
FR 37	POEOMA$_{26}$-*b*-PDPA$_{60}$	13.56	20.99	1.09	34.42	30.90	1.30
FR 39	POEOMA$_{30}$-*b*-PDPA$_{96}$	15.02	25.18	1.14	43.93	31.01	1.29
FR 41	POEOMA$_{15}$-*b*-PDPA$_{99}$	6.82	13.26	1.11	33.00	34.91	1.32
FR 43	POEOMA$_{15}$-*b*-PDPA$_{82}$	6.96	17.30	1.04	28.84	36.04	1.35
FR 46	POEOMA$_{20}$-*b*-PDPA$_{38}$	9.96	16.15	1.20	24.23	25.62	1.22
FR 19	POEOMA$_4$-*b*-PDPA$_{168}$	2.00	8.00	1.18	42.76	54.95	1.36
FR 66	POEOMA$_8$-*b*-PDPA$_{35}$	4.51	7.57	1.20	15.49	29.16	1.20

The main conclusion of the data in Table 7 is that SARA ATRP of DPA can yield well controlled polymers if the Na$_2$S$_2$O$_4$ solution is slowly and continuously fed into the reaction mixture. The resultant copolymers have controlled M_w values and low dispersity values ($1.20 \leq Đ \leq 1.36$). The results also indicate that very well-controlled polymers can be synthesized using just 246 ppm of the Cu^{II}Br$_2$/TPMA complex.

4.2.2.   POEOMA-*b*-PDMAEMA copolymers

New block copolymers containing both POEOMA and PDMAEMA segments (Figure 31) were reported. These copolymers were synthesized by SARA ATRP of DMAEMA initiated with a macro POEOMA–Br using the much more environmentally friendly catalytic system and a non-toxic solvent medium than those traditionally used for ATRP. Firstly, the POEOMA was obtained and purified to remove the monomer contamination. Then, the macro-POEOMA was chain extended with a second monomer, DMAEMA, to obtain the POEOMA-*b*-PDMAEMA copolymer. The chain length of the cationic segment, which may affect DNA binding capability and gene transfection efficacy, can be easily tuned by changing molar ratio of macroinitiator to monomer DMAEMA.[36]
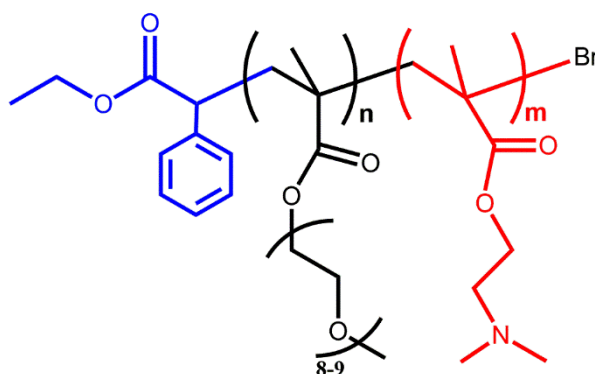
Figure 31. POEOMA-*b*-PDMAEMA block copolymer synthesized by SARA ATRP with $Na_2S_2O_4$.

^{1}H NMR analysis of the block copolymers was carried in order to compare the integrals of the macroinitiator with those of PDMAEMA. Figure 32 presents the ^{1}H NMR spectra of POEOMA-*b*-PDMAEMA prepared at 40 °C. The peaks observed at 4.07 ppm (y) (2H, –OCH_2CH_2N–), 2.58 ppm (q) (2H, –OCH_2CH_2N–), 2.35–2.20 ppm (k) (6H, –$N(CH_3)_2$), 2.00–1.75 ppm (z) (2H, –CCH_2C–) and 1.10–0.80 ppm (w) (3H, –CCH_3Br) are in agreement with the expected PDMAEMA chemical structure. Additionally, as mentioned above, the relative intensities of the peaks at 4.1 ppm (f), 3.40 ppm (j), 3.70 ppm (a,e,i), 1.7 ppm (b) and 0.62-1.5 ppm (c) are in agreement with the expected POEOMA chemical structure.[39, 48, 51]

The mass percentages of each monomer unit of the POEOMA-*b*-PDMAEMA block copolymer were calculated from the integral values of their characteristic peaks ((q, –OCH$_2$CH$_2$N–) of PDMAEMA at 2.58 ppm and (j, –O-CH$_3$–) of POEOMA at 3.4 ppm), which allowed the estimation of the average DP of each segment. Knowing the DP of the POEOMA segment (calculated as explained in section 4.1.2), the DP of the PDMAEMA segment is obtained from the ratio DP(PDMAEMA)/DP(POEOMA) = [I(k)/6]/[I(j)/3]. The amount of active chain ends could not be determined from ^{1}H NMR analysis, since the protons in the PDMAEMA unit adjacent to the bromine chain end do not have a distinct signal that allows integration as a single unit.[22, 53]
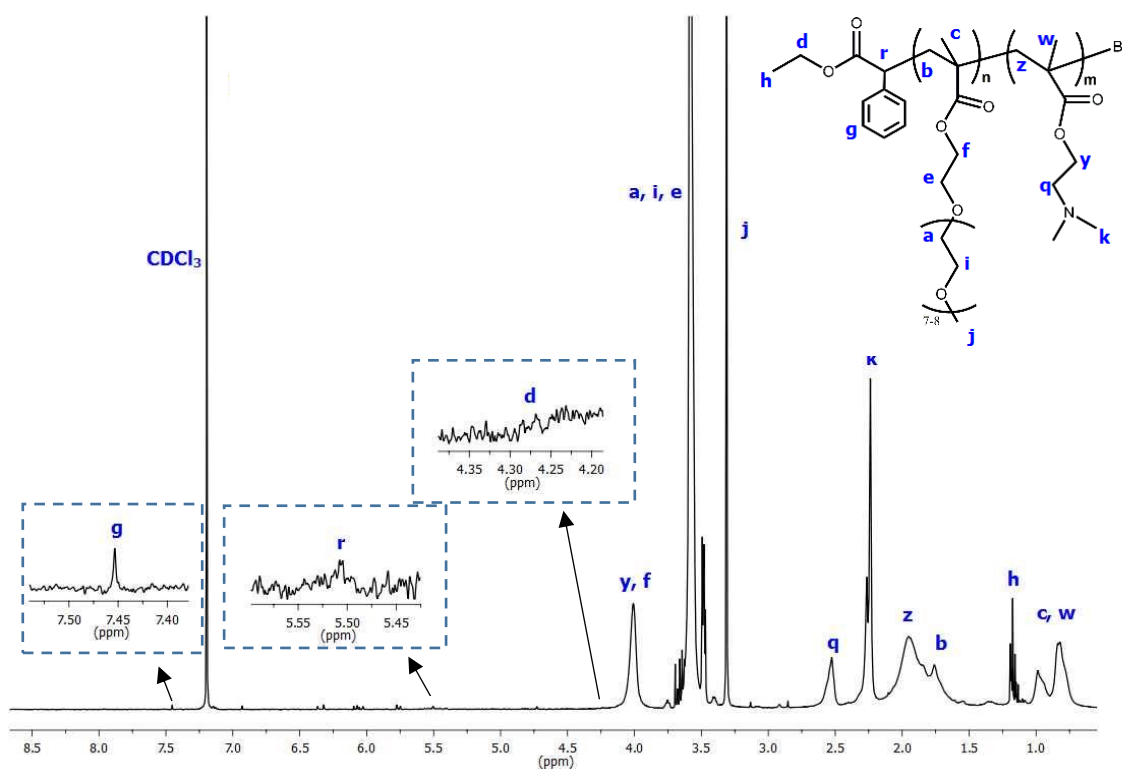
Figure 32. ^{1}H NMR spectrum, in CDCl$_3$ of a pure POEMA-*b*-PDMAEMA sample (M_n^{SEC}= 26.0 x 10^3 ; *Đ*=1.19) obtained by SARA ATRP. Reaction conditions: [DMAEMA]$_0$/[POEOMA-Br]/[Na$_2$S$_2$O$_4$]$_0$/[CuBr$_2$]$_0$/[TPMA]$_0$ = 90/1/0.25/0.01/0.02 (molar), Solv./Mon(V)=9, IPA/water = 95/5 (v/v) and slow feeding of Na$_2$S$_2$O$_4$ solution, 40 ^{0}C.

The average DP of each purified block was calculated based on the ^{1}H NMR analysis. The molecular weight and the dispersity of the polymers were also obtained by SEC analysis (Table 8).

Table 8. Molecular weight parameters of copolymers of POEOMA-*b*-PDMAEMA synthesised by SARA ATRP with Na$_2$S$_2$O$_4$ based on ^{1}H NMR and SEC analysis.

Ref	Samples	1st segment			Block copolymer		
		$M_n^{th} \times 10^{-3}$	$M_n^{SEC} \times 10^{-3}$	Đ	$M_n^{th} \times 10^{-3}$	$M_n^{SEC} \times 10^{-3}$	Đ
FR 38	POEOMA$_{26}$-*b*-PDMAEMA$_{90}$	13.56	20.99	1.09	34.48	25.91	1.19
FR 42	POEOMA$_{15}$-*b*-PDMAEMA$_{120}$	6.82	13.26	1.11	30.74	23.75	1.18
FR 61	POEOMA$_{16}$-*b*-PDMAEMA$_{78}$	8.64	13.53	1.23	25.58	29.94	1.22
FR 62	POEOMA$_{16}$-*b*-PDMAEMA$_{96}$	8.64	13.53	1.23	28.42	32.09	1.29
FR 65	POEOMA$_8$-*b*-PDMAEMA$_{30}$	4.51	7.57	1.20	12.80	24.25	1.14
FR 67	POEOMA$_{28}$-*b*-PDMAEMA$_{55}$	14.35	21.29	1.10	29.91	36.53	1.21

The main conclusion is that SARA ATRP of POEOMA-*b*-PDPA can yield well controlled copolymers if the Na$_2$S$_2$O$_4$ solution is slowly and continuously fed into the reaction mixture. The control over the polymerization was worse for PDMAEMA block copolymers of higher molecular weight, but still possessed acceptable Đ values. Another key conclusion from these experiments is that very well-controlled polymers can be synthesized using around of 250 ppm of the CuBr$_2$/TPMA complex.

4.2.3.   POEOMA-*b*-(PDMAEMA-*co*-PDPA) copolymers

Well-defined block copolymers, of POEOMA-*b*-(PDMAEMA-*co*-PDPA) (Figure 33) were obtained by a two-step SARA ATRP reaction. The copolimerization were performed at 40 °C, using a monomer to solvent ratio 1/9 (v/v) and a solvent mixture of IPA-water of [95/5 (v/v)]. It should be noted that these copolymers are composed by one first block of POEOMA and a second random segment composed of DPA and DMAEMA.
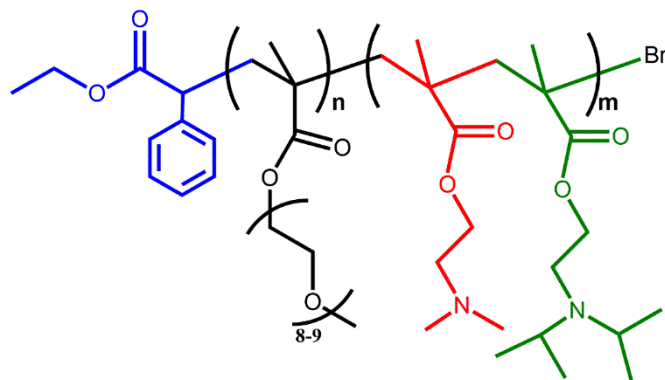
Figure 33. POEOMA-*b*-(PDMAEMA-*co*-PDPA) block copolymer synthesized by SARA ATRP with $Na_2S_2O_4$.

Figure 34 presents the ^{1}H NMR spectrum of a pure POEOMA-*b*-(PDMAEMA-*co*-PDPA) prepared at 40 °C. The peaks observed at 4.07 ppm (y) (2H, $-OCH_2CH_2N-$), 2.58 ppm (q) (2H, $-OCH_2CH_2N-$), 2.35–2.20 ppm (k) (6H, $-N(CH_3)_2$), 2.00–1.75 ppm (z) (2H, $-CCH_2C-$) and 1.10–0.80 ppm (w) (3H, $-CCH_3Br$) are in agreement with the expected PDMAEMA chemical structure. Additionally, as mentioned above, the relative intensities of the peaks at 4.1 ppm (f), 3.40 ppm (j), 3.70 ppm (a,e,i), 1.7 ppm (b) and 0.62-1.5 ppm (c) are in agreement with the expected POEOMA chemical structure.[39, 48, 51] Moreover, the relative intensities of the peaks at 3.82 ppm (t), 2.98 ppm (x), 2.62 ppm (u), 1.7–2.1 ppm (s) and resonances at 1 ppm (p, v) are also in agreement with the expected PDPA chemical structure. In addition, the mass percentages of each monomer unit in the of POEOMA-*b*-(PDMAEMA-*co*-PDPA) block copolymer were calculated from the integral values of their characteristic peaks ((k, $-N(CH_3)_2$) of PDMAEMA at 2.58 ppm, (x, $-(CH-N)_2-$) of PDPA at 2.98 ppm and (j, $-O-CH_3-$) of POEOMA at 3.4 ppm), which allowed the estimation of the average DP of each segment. Knowing the DP of the POEOMA segment (calculated as explained in section 4.1.2), the DP of the PDMAEMA segment is obtained from the ratio DP(PDMAEMA)/DP(POEOMA) = [I(k)/6]/[I(j)/3], and the DP of the PDPA segment is obtained from the ratio DP(PDPA)/DP(POEOMA) = [I(x)/2]/[I(j)/3].
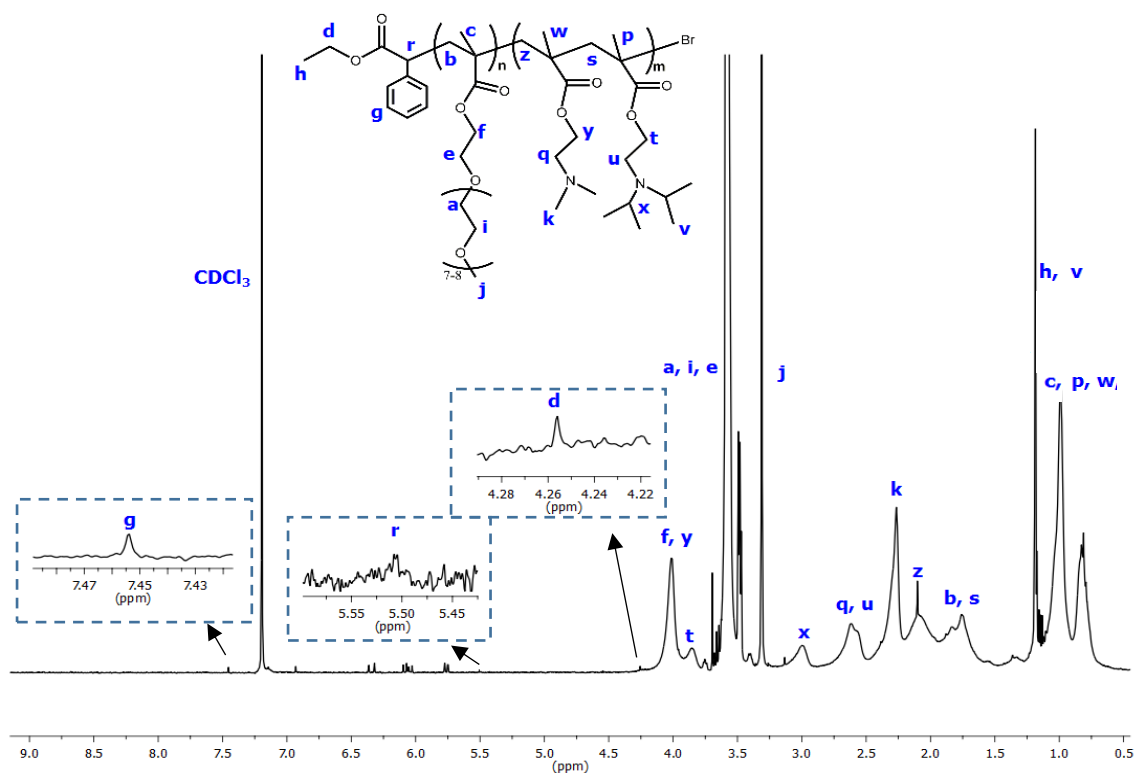
Figure 34. ^{1}H NMR spectrum, in CDCl$_3$ of a pure POEMA-*b*-(PDMAEMA-*co*-PDPA) sample (M_n^{SEC}= 27.0 x 10^3 ; *Đ*=1.2) obtained by SARA ATRP. Reaction conditions: [DPA]$_0$/[DMAEMA]$_0$/[POEOMA-Br]/[Na$_2$S$_2$O$_4$]$_0$/[CuBr$_2$]$_0$/ [TPMA]$_0$ = 200/200/1/0.26/0.05/0.08 (molar), Solv./Mon(V)=9, IPA/water = 95/5 (v/v) and slow feeding of Na$_2$S$_2$O$_4$ solution, 40 ^{0}C.

The average DP of each segment was estimated using the ^{1}H NMR analysis. The molecular weight and the dispersity of the block copolymers were determined by SEC analysis (Table 9).

Table 9. Molecular weight parameters of copolymers of POEOMA-*b*-(PDMAEMA-*co*-PDPA) synthesised by SARA ATRP with Na$_2$S$_2$O$_4$ based on ^{1}H NMR and SEC analysis.

Ref	Samples	1st segment			Block copolymer		
		$M_n^{th} \times 10^{-3}$	$M_n^{SEC} \times 10^{-3}$	*Đ*	$M_n^{th} \times 10^{-3}$	$M_n^{SEC} \times 10^{-3}$	*Đ*
FR 40	POEOMA$_{26}$-*b*-(PDMAEMA$_{27}$-*co*-PDPA$_{21}$)	15.02	25.18	1.14	32.51	26.72	1.22
FR 64	POEOMA$_{16}$-*b*-(PDMAEMA$_{44}$-*co*-PDPA$_{37}$)	8.64	13.53	1.23	43.17	44.70	1.31
FR 68	POEOMA$_{15}$-*b*-(PDMAEMA$_{30}$-*co*-PDPA$_{27}$)	7.97	11.85	1.12	39.60	52.30	1.57

These results suggest that for the first two block copolymers, the values of molecular weight and dispersity are indicative of a good control over the polymerization. However,

in the case of the last block copolymer (FR 68), the values of the molecular weights determined by SEC were not in agreement with the theoretical values, indicating a poor control during polymerization. This observation was confirmed by an higher dispersity value ($Đ$ >1.5). Furthermore, it was noted that the obtained DP of each PDMAEMA segment is always greater than the PDPA as expected, since, as shown above, the PDPA takes about 24 hours to reach a conversion of 92 % while PDMAEMA takes about 12 hours to achieve a 91% conversion. This proves that the PDMAEMA has a conversion time faster than the PDPA.

4.2.4. (PDMAEMA-*co*-PDPA) copolymers

The use of $Na_2S_2O_4$ in SARA ATRP of PDMAEMA-*co*-PDPA (Figure 35) acts as a powerful reducing agent for X–Cu^{II}/L species allowing efficient regeneration of Cu^{I}/L species, as well as generating radicals by its role as a supplemental activator. The synthesis of well controlled (PDMAEMA-*co*-PDPA) copolymers was applied by a one-pot polymerization reaction. The reaction was performed at 40 °C, using a monomer to solvent ratio 1/9 (v/v) and a solvent mixture of IPA–water of [95/5 (v/v)]. It must be noted that these copolymers are composed of a random PDPA and PDMAEMA segment.
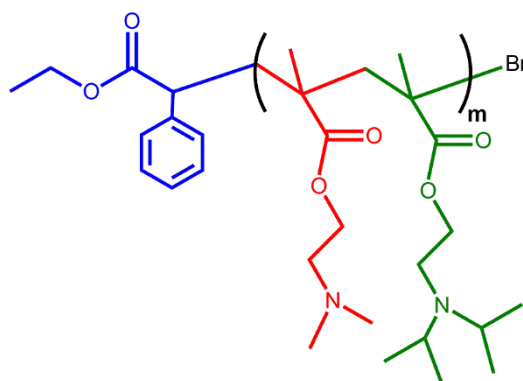
Figure 35. PDMAEMA-*co*-PDPA copolymer synthesized by SARA ATRP with $Na_2S_2O_4$.

Figure 36 presents the ^{1}H NMR spectrum of the pure PDMAEMA-*co*-PDPA. The peaks observed at 4.07 ppm (y) (2H, –OCH$_2$CH$_2$N–), 2.58 ppm (q) (2H, –OCH$_2$CH$_2$N–),

2.35–2.20 ppm (k) (6H, $-N(CH_3)_2$), 2.00–1.75 ppm (z) (2H, $-CCH_2C-$) and 1.10–0.80 ppm (w) (3H, $-CCH_3Br$) are in agreement with the expected PDMAEMA chemical structure. Additionally, as mentioned above, the relative intensities of the peaks at 3.82 ppm (t), 2.98 ppm (x), 2.62 ppm (u), 1.7–2.1 ppm (s) and resonances at 1 ppm (p, v) are also in agreement with the expected PDPA chemical structure. In addition, the mass percentages of each monomer unit of the PDMAEMA-*co*-PDPA block copolymer were calculated from the integral values of their characteristic peaks ((k, $-N(CH_3)_2$) of PDMAEMA at 2.58 ppm and (x, $-(CH-N)_2-$) of PDPA), which allowed the estimation of the average DP of each segment. The degree of polymerization was determined by comparing integrals of x at 3.80 ppm (x) (PDPA), and of g at 7.35 ppm (g) (EBPA). From the ratio $2n/5 = I(x)/I(g)$, the DP of PDPA segment was obtained. Knowing the DP of the PDPA segment, the DP of the PDMAEMA segment is obtained from the ratio (DP(PDMAEMA)/DP(PDPA) = [I(k)/6]/[I(x)/2].
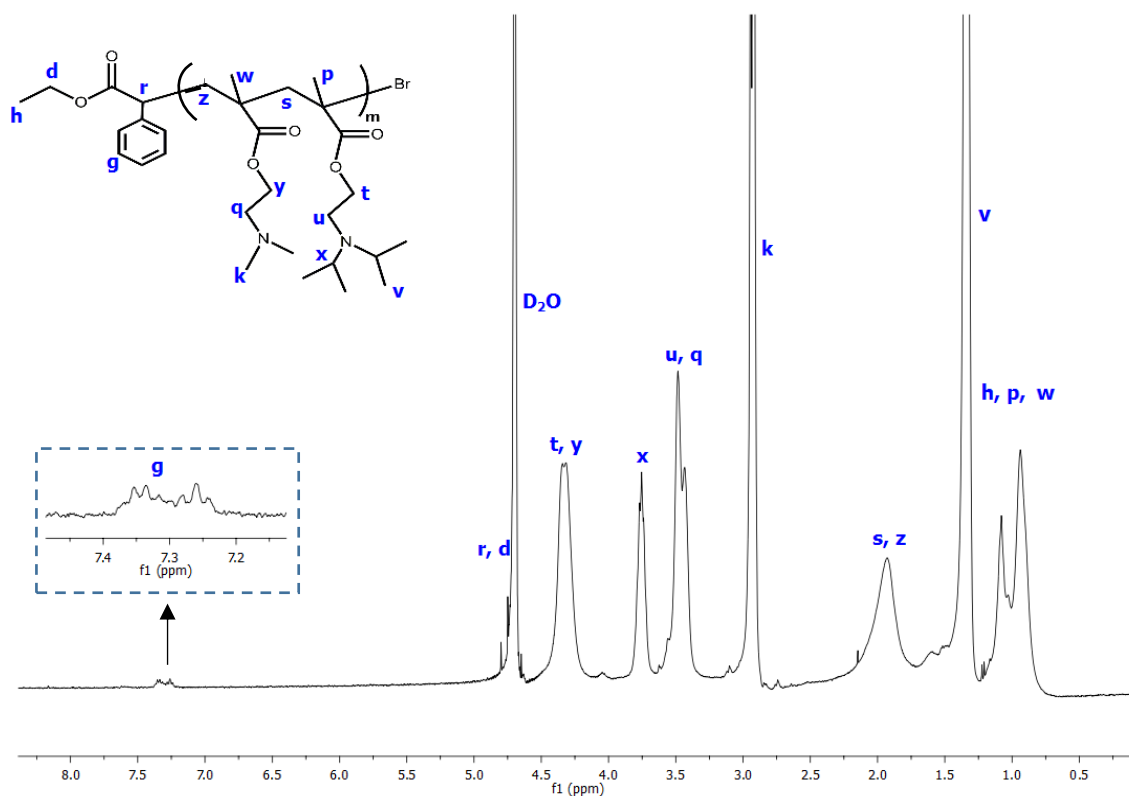
Figure 36. ^{1}H NMR spectrum, in D_2O of a pure PDMAEMA-*co*-PDPA sample (M_n^{SEC}= 23.0 x 10^3 ; Đ=1.08) obtained by SARA ATRP. Reaction conditions: [DPA]$_0$/[DMAEMA]$_0$/[EBPA]$_0$/[Na$_2$S$_2$O$_4$]$_0$/[CuBr$_2$]$_0$/[TPMA]$_0$ = 50/100/1/0.2/0.01/0.02 (molar), Solv./Mon=2 (v/v), IPA/water = 95/5 (v/v), 40 ^{0}C.

The DP of each block was calculated based on the ^{1}H NMR analysis of the pure polymer. The molecular weight and the dispersity of the block copolymers were obtained by SEC analysis (Table 10).

Table 10. Molecular weight parameters of PDMAEMA-*b*-PDPA synthesised by SARA ATRP with $Na_2S_2O_4$ based on ^{1}H NMR and SEC analysis.

Ref	Samples	$M_n^{th} \times 10^{-3}$	$M_n^{SEC} \times 10^{-3}$	Đ
FR 10	PDMAEMA$_{70}$-*co*-PDPA$_{57}$	25.88	23.23	1.08

The results in Table 10 indicate that very well-controlled polymers can be synthesized using just 85 ppm of the $Cu^{II}Br_2$/TPMA complex.

4.3.   Polymer Buffering Capacity

The release ability at intracellular level is a critical parameter for polymers intended to be used for the preparation of delivery systems. Polymers, which contain secondary and tertiary amine groups have been shown to have the ability to buffer the endosome, acting as "proton sponge", and enhancing the release process of materials to cytoplasm.[53] Thereby, since PDMAEMA and PDPA have a pH-dependent protonation, potentiometric titration curves (Figure 37) were carried out in order to evaluate their acid dissociation constant (pK_a). For biomedical applications, these curves were obtained at 37°C, a physiological temperature.
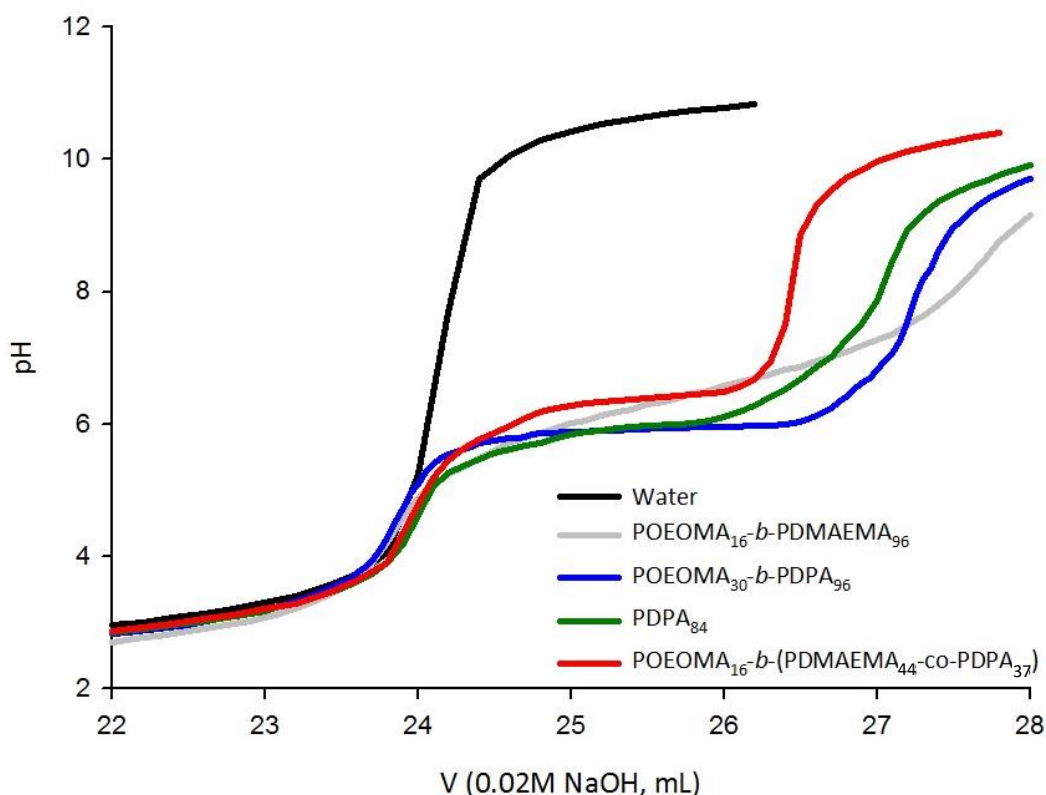
Figure 37. Potentiometric titration curves at 37°C of POEOMA$_{16}$-b-PDMAEMA$_{96}$ (grey line), POEOMA$_{30}$-b-PDPA$_{96}$ (blue line), PDPA$_{84}$ (green line), POEOMA$_{16}$-b-(PDMAEMA$_{88}$-co-PDPA$_{73}$) (red line) in milli-Q water. The x-axis label of the plot, V_{NaOH}, denotes the total volume of added NaOH. Horizontal lines correspond to pH. The titration data for pure water obtained under an identical set of conditions (grey line) are also shown for reference. For correction and better visualization, the original titration curves (Figure 45-47, Attachments) have been shifted with respect to water data using the procedure described in literature.[54, 55]

The plot of the 1st derivate ($\frac{d\,Vol}{d\,pH}$) of the titration curve versus pH (Figure 38), clearly reveals a strong peak due to buffering, which allows the determination of the pK$_a$ value.[41, 54]
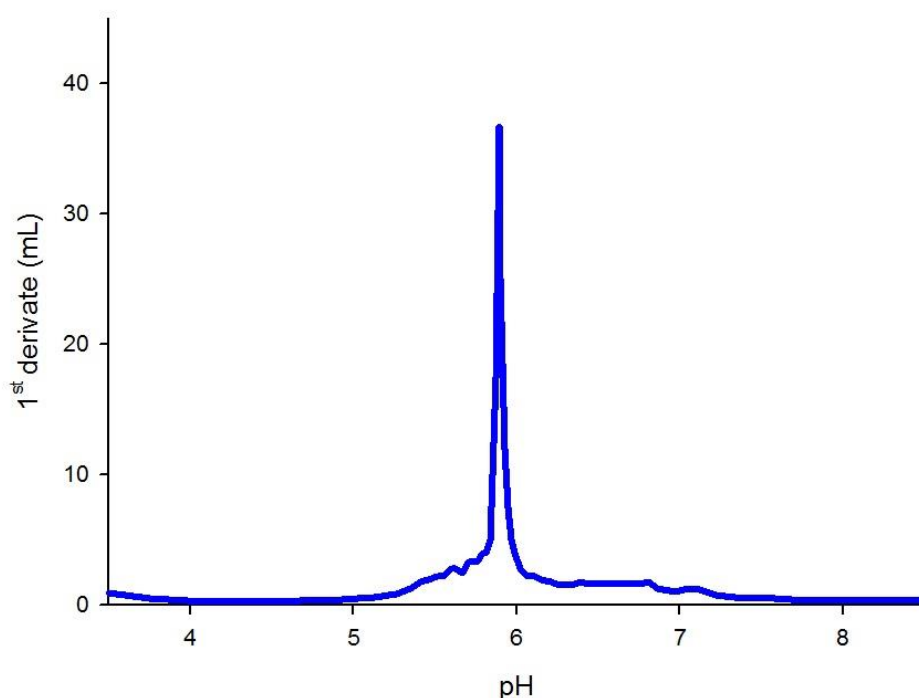
Figure 38. Determination of pK$_a$ (5.89) of the POEOMA$_{15}$-b-PDPA$_{99}$ thorough the plot of (dVol/ dpH)=(Vol$_2$-Vol$_1$)/(pH$_2$-pH$_1$) versus pH. A strong peak due to buffering, permits a fairly certain determination of the pK$_a$ value.

The results obtained from the titration curves suggest that the length of the hydrophilic and hydrophobic segment not significantly affected the pK$_a$ values of the representative PDPA-based and PDMAEMA-based samples investigated (Table 11).

Moreover, the pK$_a$ value obtained for the block copolymers POEOMA-b-PDPA and POEOMA-b-PDMAEMA are in agreement with those reported in the literature.[53, 56] The values between 5.83–5.96 and 6.23-6.47 for the POEOMA-b-PDPA and POEOMA-b-PDMAEMA, respectively suggest that a pH below their pK$_a$ the amine groups will be protonated inducing the endosomal swelling and/or enhancing the interaction with the endosomal/lysosomal membranes, which can be essential to induce membrane rupture and leakage of the transported material to the cytoplasm. For pH values higher than the pK$_a$, the PDPA/PDMAEMA segment becomes hydrophobic. In the block copolymers,

the linkage of the PDPA/PDMAEMA with an hydrophilic segment like POEOMA renders the copolymers stable in water, even for high pH values (pH $\gg$ pK$_a$).[47, 57]

Table 11. Buffer capacities and acid dissociation constant (pK$_a$) values of synthesized block copolymers and homopolymers.

Ref.	Polymer	pK$_a$	$M_n^{SEC} \times 10^{-3}$	Đ
FR 37	POEOMA$_{26}$-*b*-PDPA$_{60}$	5.96	30.90	1.30
FR 39	POEOMA$_{30}$-*b*-PDPA$_{96}$	5.94	31.01	1.29
FR 41	POEOMA$_{15}$-*b*-PDPA$_{99}$	5.89	34.91	1.32
FR 43	POEOMA$_{15}$-*b*-PDPA$_{82}$	5.83	36.04	1.35
FR 46	POEOMA$_{20}$-*b*-PDPA$_{38}$	5.99	25.62	1.22
FR 19	POEOMA$_{4}$-*b*-PDPA$_{168}$	5.90	54.95	1.36
FR 66	POEOMA$_{8}$-*b*-PDPA$_{35}$	5.92	29.16	1.20
FR 38	POEOMA$_{26}$-*b*-PDMAEMA$_{90}$	6.23	25.91	1.19
FR 42	POEOMA$_{15}$-*b*-PDMAEMA$_{120}$	6.39	23.75	1.18
FR 61	POEOMA$_{16}$-*b*-PDMAEMA$_{78}$	6.47	29.94	1.22
FR 62	POEOMA$_{16}$-*b*-PDMAEMA$_{96}$	6.34	32.09	1.29
FR 65	POEOMA$_{8}$-*b*-PDMAEMA$_{30}$	6.46	24.25	1.14
FR 67	POEOMA$_{28}$-*b*-PDMAEMA$_{55}$	6.31	36.53	1.21
FR 40	POEOMA$_{26}$-*b*-(PDMAEMA$_{27}$-*co*-PDPA$_{21}$)	6.50	26.72	1.22
FR 64	POEOMA$_{16}$-*b*-(PDMAEMA$_{44}$-*co*-PDPA$_{37}$)	6.39	44.70	1.31
FR 68	POEOMA$_{15}$-*b*-(PDMAEMA$_{30}$-*co*-PDPA$_{27}$)	6.40	52.30	1.57
FR 01	PDPA$_{84}$	5.97	24.84	1.10
FR 10	PDMAEMA$_{70}$-*co*-PDPA$_{57}$	6.77	23.23	1.08

4.4. Solution self-assembly of pH-responsive block copolymers

In order to take advantage of the special growth microenvironment of tumour tissue, which has lower pH (5.7–7.8) and higher temperature than that of normal tissues, several kinds of thermo-sensitive, pH-sensitive and dual-sensitive copolymer nanoparticles (NPs) have been prepared by incorporating pH and/or temperature-sensitive components. Amphiphilic cationic copolymers can self-assemble into stable, size-controlled and dispersive NPs with a hydrophobic core and a cationic shell with a high surface charge density. [44] This kind of amphiphilic block copolymer is assumed to hold several advantages. Firstly, it can self-assemble into core-shell nanoparticles with ultralow critical association concentrations. Secondly, cationic core-shell nanoparticles can carry two payloads simultaneously, anionic nucleic acid and hydrophobic anticancer drugs. Thirdly, POEOMA-*b*-PDPA and POEOMA-*b*-PDMAEMA NPs could release the drug payload faster in an acidic environment than that in a neutral environment (due to their sensitivity to pH), which is very useful to effectively treat tumours with acidic microenvironments and reduce the side effects of the drug on normal tissues *in vivo*.[44]

Considering the pH-responsive character of PDPA and PDMAEMA, one way of preparing the block copolymer micelles involves aqueous self-assembly as a result of pH change, the pH titration method.[43] As represented in Figure 39, these block copolymers are soluble under acidic conditions, but form core–shell micelles when the solution pH is above the pK_a of each copolymer, at which point the PDMAEMA and PDPA chains are deprotonated and these segments become hydrophobic. The self-assembly of POEOMA-*b*-PDPA, POEOMA-*b*-PDMAEMA and POEOMA-*b*-(PDMAEMA-*co*-PDPA) could be monitored by the titration of HCl-acidic aqueous dispersions of the block copolymer, using a NaOH solution. Change from unimers to the micellized state was indicated by an increase in the solution turbidity (Figure 39-40) when the pK_a of these copolymers was reached, and could be confirmed by the significant increase in their hydrodynamic size, as determined by DLS. However, in this work the titration method was not an effective strategy to obtain the nanoparticles because the copolymer tends to precipitated in solution which compromises the DLS measurement.[43]
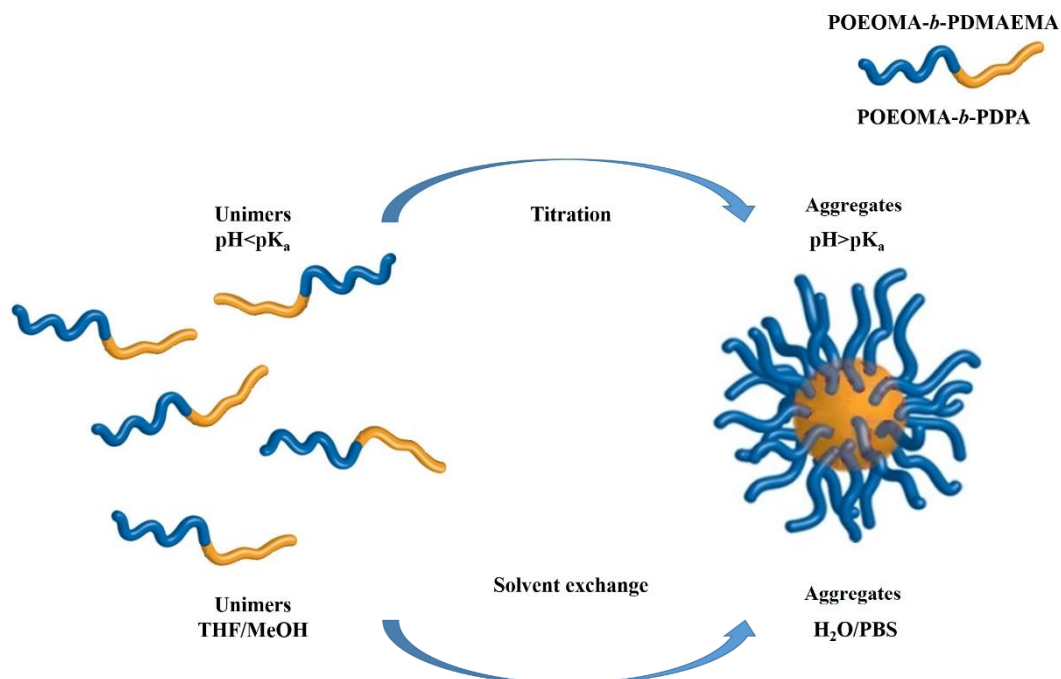
Figure 39. Representation of POEOMA-*b*-PDPA/POEOMA-*b*-PDMAEMA self-assembly in aqueous media via titration and solvent exchange methods. Adapted from ref. [43]

With the aim to visually observe the aggregation transition of polymeric nanomicelles, **POEOMA-*b*-PDMAEMA**, **POEOMA-*b*-PDPA** and **POEOMA-*b*-(PDMAEMA-*co*-PDPA)** were investigated at different pH conditions (pH 7.4 and pH 5). Note that, for the intracellular region of a tumour cell the pH is around 5 and for the intracellular region of a normal cell the pH is around 7.4. As can be seen, POEOMA-*b*-PDMAEMA has a similar turbidity for all of the pH conditions that were tested (Figure 40-A), indicating that there is no aggregation of micelles. On the contrary, POEOMA-*b*-PDPA (Figure 40-B) and POEOMA-*b*-(PDMAEMA-*co*-PDPA) (Figure 40-C) exhibit an apparent pH-induced aggregation transition with significant turbidity changes.
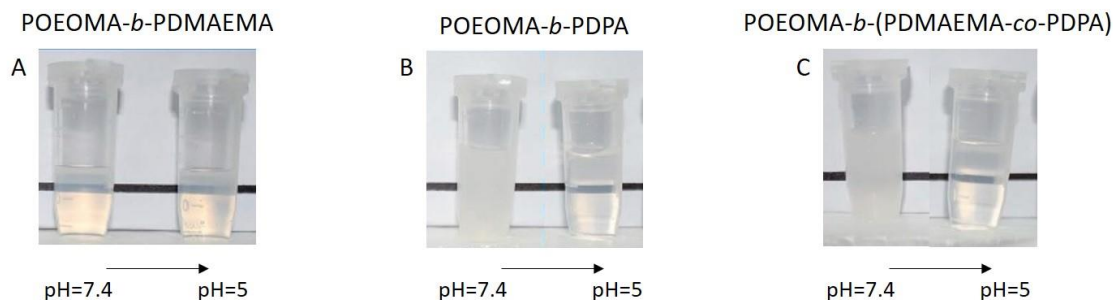
Figure 40. Digital images of POEOMA-*b*-PDMAEMA (A), POEOMA-*b*-PDPA (B) and POEOMA-*b*-(PDMAEMA-*co*-PDPA) (C) at different pH conditions. The differences of turbidity of the samples indicated the formation of well-dispersed nanomicelles and their aggregates.

This phenomenon supports the hypothesis that PDPA is more sensitive than PDMAEMA to pH changes, since it has a much more defined buffer zone compared to the PDMAEMA, as shown in Figure 40. Furthermore, this result suggests that the self-assemblies (nanomicelles) further aggregate into larger size nanostructures under neutral/basic pH condition. The degree of protonation of the PDPA block is 5.5%, 11.8%, 26.2% and 97.2% at pH 7.4, 6.8, 6.5 and 5.0, respectively, which indicate that the protonation of PDPA is greatly affected by the pH.[31] Moreover, the pH value of the aggregation transition (6.4) is close to the pK_a of PDPA block, demonstrating the possible mechanism of a secondary aggregation of primary self-assemblies caused by the enhanced electric interaction.[31]

Another route for particle formation is via a solvent exchange method, as schematically represented in Figure 39. In this method, the block copolymer is initially dissolved in a good solvent for both blocks (such as THF, MeOH, etc.) and, due to dispersibility changes caused by the dropwise addition of such organic solution into water/ PBS solution (at a specific pH), the particles are formed.

4.4.1. Determination of Particle size

The size of polymeric micelles is a key factor in determining the biodistribution of encapsulated agents.[2] The particle size distributions were determined by DLS and the average hydrodynamic diameters (D_h) and PDI of the nanoparticles obtained are listed in

Table 12. The width of the distribution of the population of particles was calculated trough the follow expression

$$\sigma = D_h \times \sqrt{PDI} \qquad (1)$$

4.4.1.1. Influence of different organic solvents (THF/MeOH)

In this work, the NPs were obtained sing the solvent exchange method. Two organic solvents were tested for the dissolution of the block copolymers: THF and MeOH. The organic solution was added dropwise to water (pH > pK$_a$, pH-responsive segment) or PBS. The NPs were formed after the organic solvent evaporation and solution stabilization overnight. The DLS results of the obtained self-assemblies are listened in Table 12 and suggest that THF is more effective than MeOH, since it leads to the formation of smaller aggregates, which is a prerequisite for avoiding the reticuloendothelial system (RES) uptake. In the case of MeOH the diameter of the nanoparticles could not be determined for the POEOMA-*b*-(PDMAEMA-*co*-PDPA) copolymers due to the formation of aggregates. For THF these copolymers displayed good results in terms of dispersion capabilities. THF is a stronger base and has a greater elution strength than methanol. [58-60] The greater effect of solvation by water in the THF-water mixture, when compared to the methanol-water mixture [61] explains why THF is more powerful than MeOH to dissolve these copolymers.

4.4.1.2. Influence of different dispersing medium (PBS/H$_2$O)

Phosphate-buffered saline (PBS) is a buffer solution commonly used in biological research. It is intended to maintain a constant pH value, when added to different environments.[62, 63] The salt concentration present in the PBS equals that of the Human Body. For these reasons, PBS and H$_2$O were compared as dispersant. Table 12 shows that for these different dispersant, the results of diameter size are quite similar.

Table 12. Hydrodynamic parameters of self-assembled nanocarriers at pH 7.4 in presence of different organic solvents and different dispersants.

Samples	Organic Solvent = THF				Organic Solvent = MeOH			
	Dispersant = H_2O		Dispersant = PBS		Dispersant = H_2O		Dispersant = PBS	
	Average Diameter (nm)	PDI	Average Diameter (nm)	PDI	Average Diameter (nm)	PDI	Average Diameter (nm)	PDI
POEOMA$_{26}$-b-PDPA$_{60}$	74.09 ± 37.26	0.253	115.60 ±45.22	0.153	124.00 ± 60.49	0.238	111.10 ± 59.93	0.291
POEOMA$_{30}$-b-PDPA$_{96}$	75.56 ± 38.53	0.260	77.01 ± 40.24	0.273	115.00 ± 66.36	0.333	113.00 ± 65.31	0.334
POEOMA$_{15}$-b-PDPA$_{99}$	68.62 ± 22.96	0.112	69.44 ± 20.01	0.083	65.72 ± 25.96	0.156	89.18 ± 52.08	0.341
POEOMA$_{15}$-b-PDPA$_{82}$	74.33 ± 22.67	0.093	112.30 ± 42.17	0.141	68.49 ± 23.82	0.121	73.71 ± 32.21	0.191
POEOMA$_{20}$-b-PDPA$_{38}$	78.16 ± 47.09	0.363	81.58 ± 52.05	0.407	80.47 ± 36.79	0.209	112.90 ± 47.23	0.175
POEOMA$_4$-b-PDPA$_{168}$	117.50 ± 47.29	0.162	107.60 ± 51.15	0.226	78.44 ± 57.59	0.541	171.70 ± 56.43	0.108
POEOMA$_8$-b-PDPA$_{35}$	145.40 ± 83.02	0.326	174.40 ± 92.78	0.283	74.85 ± 50.04	0.447	68.88 ± 37.41	0.295
POEOMA$_{26}$-b-PDMAEMA$_{90}$	---*	---	---	---	---	---	---	---
POEOMA$_{15}$-b-PDMAEMA$_{120}$	---	---	---	---	---	---	---	---
POEOMA$_{16}$-b-PDMAEMA$_{78}$	---	---	---	---	---	---	---	---
POEOMA$_{16}$-b-PDMAEMA$_{96}$	---	---	---	---	---	---	---	---
POEOMA$_8$-b-PDMAEMA$_{30}$	---	---	---	---	---	---	---	---
POEOMA$_{28}$-b-PDMAEMA$_{55}$	---	---	---	---	---	---	---	---
POEOMA$_{26}$-b-(PDMAEMA$_{27}$-co-PDPA$_{21}$)	62.79 ± 45.50	0.525	38.34 ± 24.64	0.413	---	---	---	---
POEOMA$_{16}$-b-(PDMAEMA$_{44}$-co-PDPA$_{37}$)	103.10 ± 37.60	0.133	141.10 ± 61.34	0.189	---	---	---	---
POEOMA$_{15}$-b-(PDMAEMA$_{30}$-co-PDPA$_{27}$)	83.85 ± 31.15	0.138	152.90 ± 70.23	0.211	---	---	---	---

* Bimodal distributions of the POEOMA-b-PDMAEMA aggregates were observed making the results do not meet quality criteria, indicating an absence of the aggregation.

As shown in Table 12, the hydrodynamic diameters of both POEOMA-*b*-PDPA and POEOMA-*b*-PDMAEMA-*co*-PDPA is almost always less than 100 nm, which is an interesting result considering the prerequisite for avoiding the RES uptake and increase the blood residence time. [2]

Figure 41 shows different particle size for different block copolymers. The key aspects that influence particle size are the <u>length of polymers</u> and the <u>ratio between hydrophobic and hydrophilic segments</u> of block copolymers.[43, 64]

The results presented in Figure 41 reveal that larger particles with broader distributions were formed when a smaller PDPA to POEOMA ratio is used. This behaviour was less pronounced when a longer POEOMA segment was used, with particles of similar sizes being formed. Rocha and co-authors obtained the same results involving the use of an amphiphilic block copolymer, poly(ethylene glycol)-block-poly(4-vinyl pyridine) (mPEG-b-P4VP).[43]
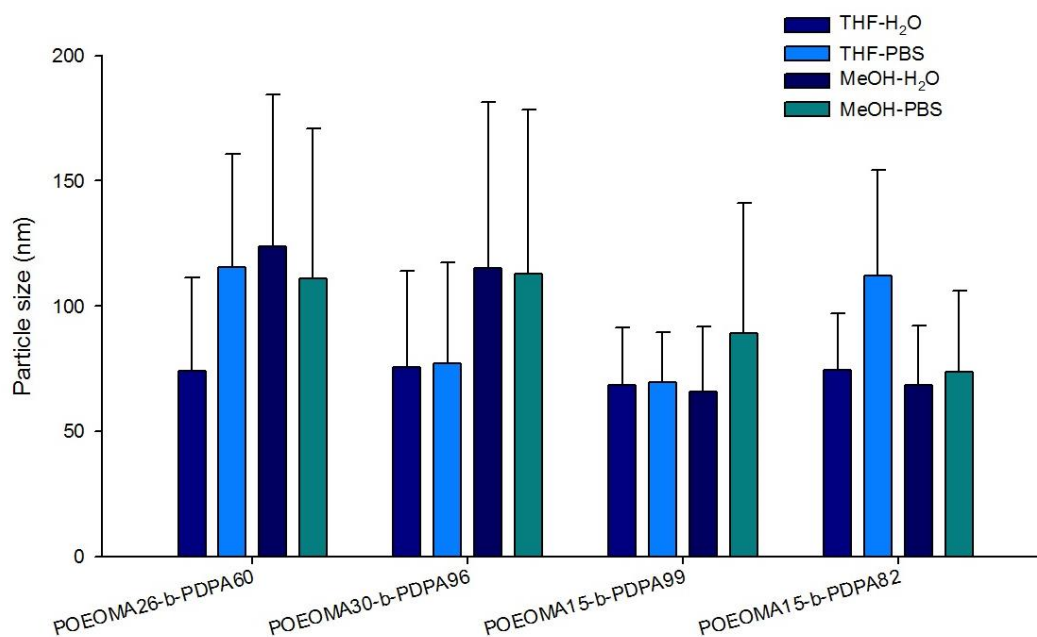
Figure 41. Particle size of POEOMA-*b*-PDPA at pH 7.4. The data are expressed as particle size in nanometer ($D_h \pm \sigma$).

In all of these different measured conditions, the hydrodynamic diameter of POEOMA-*b*-PDMAEMA copolymers could not be determined by DLS at 37ºC and pH

7.4. The absence of POEOMA-*b*-PDMAEMA aggregates indicates that the hydrophilicity/ hydrophobicity of its two blocks does not change with the pH conditions, within a range of 5.0-7.4. These results can be related with several factors: the first possibility, can be due the fact that the self-assembled nanomicelles are mainly affected by the hydrophilicity/hydrophobicity ratio of the amphiphilic block copolymers.[64] PDMAEMA exhibits both pH and temperature responsiveness. The thermo-responsive properties of the PDMAEMA can be altered by slight changes in pH and salinity, and the LCST of PDMAEMA can be tuned by changing molecular weight.[65] Ma et al.[66] studied the thermo-responsive properties of hydroxypropyl cellulose-graft-poly(*N*,*N*-dimethyl aminoethyl methacrylate) (HPC-*g*-PDMAEMA) at different pH and found that the LCST of HPC-*g*-PDMAEMA was dramatically influenced by the solution pH. Furthermore, PDMAEMA segments with a higher protonation degree at a lower pH present a stretching conformation that is hardly influenced by temperature. However, if the pH value is increased, the solubility of deprotonated PDMAEMA segments becomes temperature sensitive, i.e., the solubility is decreased with increasing temperature when the temperature is higher than the LCST. Therefore, it is rational that the average diameter of POEOMA-*b*-PDMAEMA NPs shows dual-response to temperature and pH.[44]

Hydrophobic and electrostatic interactions are the two major factors that govern the aggregation process in POEOMA-*b*-PDMAEMA aqueous solutions.[64] Because the amine residues in PDMAEMA block are protonated at low pH, the diblock in dilute solution carries many net positive charges in the PDMAEMA block, resulting in a higher positive ζ-*potential*. Due to the charge neutralization, ζ-*potential* decreases with the increase of pH and it is expected that becomes zero at pH 8.5, at which there is no net charge in the copolymers. [64] Xiong and co-authors have found that for a poly(2-(dimethylamino)ethyl methacrylate)-block-poly(acrylic acid) (PDMAEMA-*b*-PAA) at pH 8.5, it will induce aggregation of the polymer chains and phase separation due to the hydrophobic interaction.[64] When pH closed to the neutral charge, the block copolymers started to form polymeric aggregates in a pH range of 7.5–9.2.[64] Therefore, another possibility is the hydrophobic interactions are not strong enough to counteract the electrostatic repulsion, and the aggregation micelles occurs above pH 8.5.[64]

4.4.2. ζ-potential

As shown in Table 13, the ζ-potential of POEOMA-*b*-PDPA and POEOMA-*b*-(PDMAEMA-*co*-PDPA) are continuously changing with pH, since the polymers are becoming less positively charged with the increase in pH value. Under acidic conditions, the previously hydrophobic PDPA become hydrophilic after protonation. Therefore, the ζ-potential measurement provides obvious evidence that the electric interaction plays an important role in the aggregation process of nanomicelles.[31] Based on the Wu results[31], the pH-sensitive aggregation transition of POEOMA-*b*-PDPA can be divided into three stages:

i. At pH > 6.8, PDPA with a value less than 11.8% exhibits limited positive charge and sufficient hydrophobicity. Consequently, the self-assembling behaviour of POEOMA-*b*-PDPA is mainly dominated by the hydrophilic/hydrophobic ratio. [31]

ii. At pK_a 6.0 ≤ pH ≤ 6.8, with the a value ranging from 11.8% to 50%, the pH-induced protonation of diisopropylamino groups of PDPA block make it more hydrophilic and positively charged; thus, the balance of the hydrophilicity/hydrophobicity effect and the positive charge of the protonated PDPA block is important for the aggregation. [31]

iii. At 5.0 < pH < pK_a 6.0, with the change in a value ranging from 50% to 97.2%, the PDPA block is almost completely protonated and hydrophilic; thus, electric interaction will provide the main driving force for self-assembly.[31]

The presence of positive charge of POEOMA-*b*-PDPA and POEOMA-*b*-(PDMAEMA-*co*-PDPA) at pH 5 indicates that the polymer is completely soluble, distended and does not form aggregates. The PDPA segment have positive charge, and at this pH, both POEOMA and PDPA segments are hydrophilic. This conformational change allows the intracellular release of genes. However, in POEOMA-*b*-PDPA, for a pH>pK_a, these copolymers form nanoparticles. The outer layer of POEOMA-*b*-PDPA nanocarrier is rich with neutral charge (from POEOMA), and the inner layer is rich with positive charge (from PDPA), which provides not only abundant gene loading sites for the negative charged of DNA but also encapsulate hydrophobic drugs.[1, 44]

Table 13. Electrostatic characteristics of self-assembled nanocarriers at pH 7.4 and pH 5 in H_2O (nanoparticles prepared by the solvent exchange method using THF).

Ref	Samples	pH=7.4		pH=5	
		Average Diameter (nm)	ζ-potencial (mV)	Average Diameter (nm)	ζ-potencial (mV)
FR 37	POEOMA$_{26}$-b-PDPA$_{60}$	74.09 ± 37.26	15.50 ± 0.57	---*	24.30 ± 0.85
FR 41	POEOMA$_{15}$-b-PDPA$_{99}$	68.62 ± 22.96	4.64 ± 0.47	---*	21.80 ± 1.15
FR 68	POEOMA$_{15}$-b-(PDMAEMA$_{30}$-co-PDPA$_{27}$)	83.85 ± 31.15	24.00 ± 2.10	---*	39.70 ± 1.03

* The results do not meet the DLS quality criteria, indicating an absence of the aggregation.

It is expected that if the pH value decreases, an obvious increase in the gene release rate may be observed. Thus, POEOMA-b-PDPA and POEOMA-b-(PDMAEMA-co-PDPA) NPs can have an excellent tumour drug delivery character responding to mildly acidic environments. This property of both NPs should be very useful to effectively treat tumours with acidic microenvironments and reduce the side effects of the drug on the normal tissues.

4.5.   Determination of copper residual contamination (ppm)

Gene therapy shows much promise in tackling various genetic diseases and cancers, viral infection, and cardiovascular disorders. The most challenging task in gene therapy is the design of gene delivery vectors with low cytotoxicity and high transfection efficiency. In order to achieve that, several favourable attributes of amphiphilic copolymers have made them suitable as drug delivery vehicles and for this reason they have been used extensively in pharmaceutical applications.[2]

ATRP methods allow the development of block copolymers with specific properties and functionalities and can be an interesting strategy for the development of tailor-made gene delivery vehicles. However, the relatively high levels of residual Cu used in the traditional ATRP methods are problematic for biomedical applications, since it requires laborious purifications steps to reduce their cytotoxic effects. SARA ATRP operate at low levels of Cu during polymerization and therefore need minimal subsequent purification for catalyst removal. This new version of ATRP is useful to prepare well-

defined copolymers for these high value applications.[19] The amount of residual copper in the block copolymers and homopolymers synthesised in this work was determined by flame atomic absorption spectrometry and are listened in Table 14.

Table 14. Total amount of residual copper determined by flame atomic absorption spectrometry. 50 mg of each copolymer/homopolymer was dissolved in a volume with 10 mL of 0.1M HCl at pH 5.

Ref.	Polymer Sample	$M_n^{SEC} \times 10^{-3}$	$Đ$	Total [Cu] in reaction (ppm)	mg Cu/l	Residual* Cu (ppm)
FR 13	POEOMA$_{19}$	15.00	1.12	192.86	0.055	11.0
FR 58	POEOMA$_{30}$	19.86	1.17	249.80	0.032	6.4
FR 01	PDPA$_{84}$	24.84	1.10	99.50	0.059	11.8
FR 43	POEOMA$_{15}$-b-PDPA$_{82}$	36.04	1.35	499.47	0.109	21.8
FR 64	POEOMA$_{16}$-b-(PDMAEMA$_{44}$-co-PDPA$_{37}$)	44.87	1.31	249.22	0.130	26.0
FR 65	POEOMA$_8$-b-PDPA$_{30}$	24.25	1.14	1466.92	0.056	11.2

* Values after purification by dialysis.

Since the synthesis of the block copolymers and homopolymers is similar, the determination of the amount of residual copper was made for only a few representative copolymers/homopolymers. The results reveal that a very low residual amount of Cu is presented in the polymers with around 11 ppm for all macroinitiators and around 22 ppm for all copolymers, proving the safety of the final product with respect to copper contamination.[53] These results are very promising, especially when compared to the values of residual Cu presented by Ydens and co-authors[67] (177-630 ppm) after the purification of PDMAEMA synthesized by ATRP. The value of total [Cu] in the reaction is directly associated with the DP, for a given amount of monomer and a fixed molar ratio of [Cu] to initiator. The residual content of Cu in the final purified polymer was determined by Atomic Absorption (values in mg L^{-1} were converted to ppm as shown in table 17 (Attachments)).

It would be expected that for a lower value of total [Cu] in the reaction (determined by $\frac{\text{real molar ratio of CuBr2}}{\text{real molar ratio of monomer}} \times 1000000$), the residual content of Cu in the final purified polymer would also be lower when compared to polymers that have a higher value of total [Cu] in reaction mixture. However, the different times of the dialysis purification step must also be taken into account, since longer times allow larger
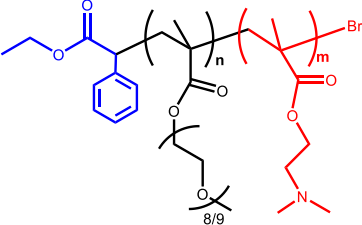
quantities of residual copper to be removed. The POEOMA$_8$-*b*-PDPA$_{30}$ dialysed for about 4 days while POEOMA$_{15}$-*b*-PDPA$_{82}$ only did so for 2 days. Thus, the POEOMA$_8$-*b*-PDPA$_{30}$ copolymer has less residual copper than the POEOMA$_{15}$-*b*-PDPA$_{82}$ despite having a greater initial concentration of Cu in the reaction mixture. Therefore a solution to further lower the values of residual copper is to increase the dialyses time, but this is accompanied by an increase in the cost of the final product. Nevertheless the polymer produced in this work already have acceptable levels of Cu for biomedical applications.
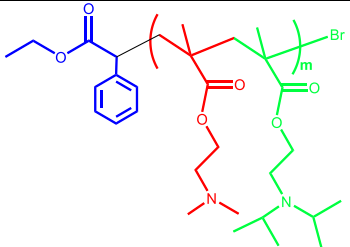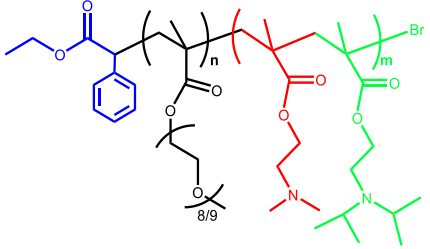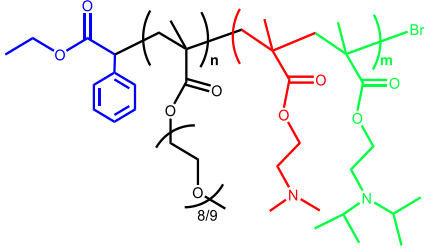
4.6. Preliminary tests for gene delivery applications

The results resented in this chapter were obtain at the Health Sciences Research Centre of the University of da Beira Interior (CICS-UBI), supervised by Professor Fani Sousa and kindly provided to be part of this thesis.

The most promising block copolymers synthesised (Table 15) were sent to the Health Sciences Research Centre of the University of Beira Interior to evaluate their cytotoxicity and gene complexation ability. This laboratory has a strong experience in gene therapy strategies, such as in the characterization of polyplexes involving small RNA and nanoparticles mediated delivery of pure p53 supercoiled plasmid DNA for gene therapy.[42, 68, 69] Due to time limitations, it was not possible to analyse all the block copolymer synthesized in this work. Therefore, as proof of concept, some block copolymers were selected for a preliminary evaluation.

Table 15. Block copolymers sent to the CICS-UBI – Health Sciences Research Centre.

Sample	Copolymer structure	Copolymer composition	M_n^{th} x10^{-3}	M_n^{SEC} x10^{-3}	Đ
FR 42		POEOMA$_{15}$-*b*-PDMAEMA$_{120}$	30.74	25.00	1.18
FR 61		POEOMA$_{16}$-*b*-PDMAEMA$_{78}$	25.58	29.94	1.2
FR 62		POEOMA$_{16}$-*b*-PDMAEMA$_{96}$	28.42	32.09	1.27

FR 65	POEOMA$_8$-b-PDMAEMA$_{30}$	12.80	24.25	1.13
FR 67	POEOMA$_{28}$-b-PDMAEMA$_{55}$	29.91	37.29	1.21
FR 10	PDMAEMA$_{70}$-co-PDPA$_{57}$	25.88	23.23	1.08
FR 64	POEOMA$_{16}$-b-(PDMAEMA$_{44}$-co-PDPA$_{37}$)	43.17	44.70	1.31
FR 68	POEOMA$_{15}$-b-(PDMAEMA$_{30}$-co-PDPA$_{27}$)	39.60	52.30	1.57

The p53 protein is an exclusive tumour suppressor, proficient in the selective induction of growth arrest and apoptosis in response to oncogenic or damage signalling, acting as a predominant guardian against malignant cell transformation. On the other hand, it is estimated that the p53 gene is mutated or deleted in approximately 50% of all human cancers and its omnipresent loss of function contributes as one of the fundamental events that trigger and sustain tumorigenesis. It becomes therefore rational that the reinstatement of the wild-type p53 expression and consequent reactivation of its downstream effector pathways has impact on cancer therapy, as recently reported.[42] However, an effective application of a p53 DNA-based cancer therapy has been hampered so far by issues associated with the transfection efficiency, intracellular delivery, and the purification of plasmid DNA (pDNA) expression vectors.

Purification of pharmaceutical-grade pDNA is a challenging process since the downstream processing must not be approached in an individual basis, but in an integrative standpoint that accounts for cell impurities and contaminants such as RNA, endotoxins and genomic DNA that derive from the upstream stages, causing toxic side effects if delivered to the host. Moreover, despite the fact that pDNA is a very stable biomolecule, during its production and recovery, it can suffer several types of stress that may disrupt its structural stability. [42]

As schematized in Figure 42, the development of an integrative method gathers the recent progresses concerning pDNA loading nanocarriers and transfection efficiency of plasmid biopharmaceuticals and the novel generation of gene delivery vehicles, efficiently covering the key issues that currently hamper the translation of non-viral gene therapy into clinical applications. [42]
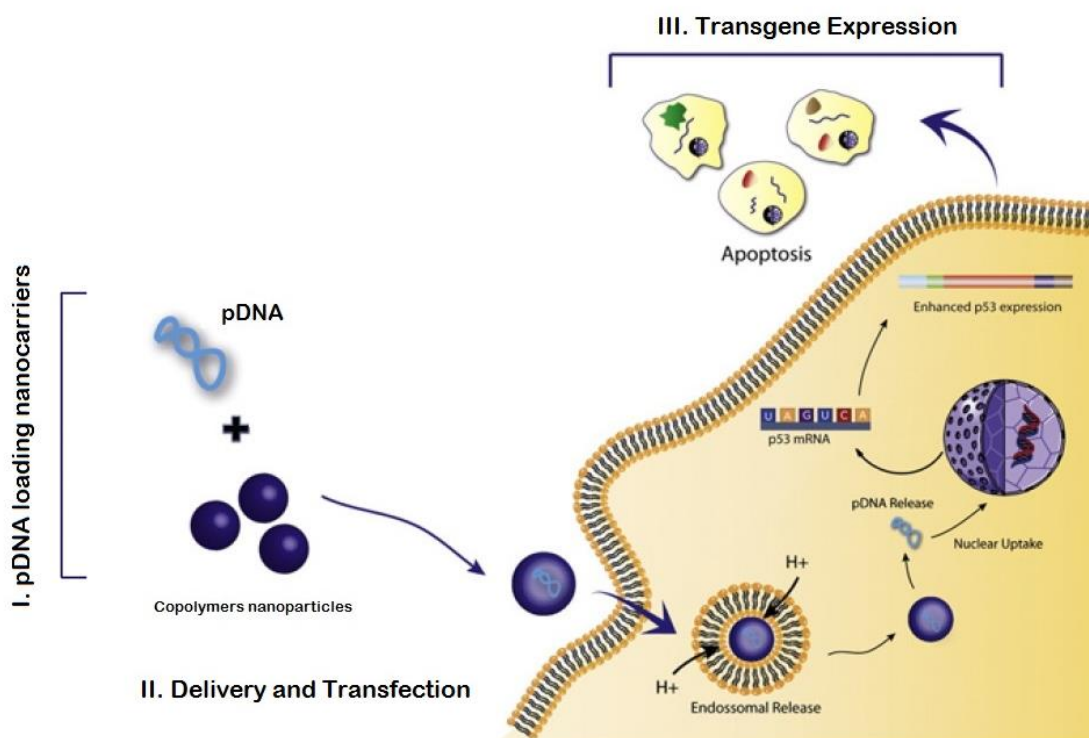
Figure 42. Schematics of an integrative approach for non-viral cancer gene therapy. (I.) pDNA loading nanocarriers; (II.) Nanoparticle mediated delivery and transfection; (III.) Expression of the p53 tumor suppressor. Adapted from ref.[42]

4.6.1. Characterization of pDNA loaded nanoparticles

pDNA loaded nanocarriers were prepared by the ionotropic gelation technique which is based on the electrostatic interactions that occur between the positively charged polymer backbone and pDNA. Different concentrations of copolymers (1.0 mg mL^{-1}; 0.1 mg mL^{-1}; 0.01 mg mL^{-1}) were tested to determine the highest pDNA encapsulation efficiency (EE). 20 µg mL^{-1} of pDNA were used in each assay. Relevant properties such as *ζ-potential*, and loading capacity were evaluated under controlled temperature conditions (25 °C) at a pH 8.0.

Table 16 presents the EE of the polyplex systems prepared with the different copolymer concentrations. The results showed that the encapsulation of pDNA for 0.1 mg mL^{-1} concentration of copolymer is significantly higher than that of 1.0 or 0.01 mg mL^{-1}.

Table 16. ζ-*potential* and EE of the polyplexes at different concentrations of the copolymer. Data is presented as the mean ± s.d.

Copolymers	[Copolymers]	ζ-*potential* (mV)	Encapsulation Efficiency (%)
PDMAEMA$_{70}$-*co*-PDPA$_{57}$	1 mg mL^{-1}		41.05 ± 1.94
	0.1 mg mL^{-1}	**-20.00 ± 0.99**	**91.47 ± 0.51**
	0.01 mg mL^{-1}		24.43 ± 4.48
POEOMA$_{16}$-*b*-PDMAEMA$_{78}$	1 mg mL^{-1}		32.36 ± 2.14
	0.1 mg mL^{-1}	**-10.09 ± 0.47**	**73.97 ± 5.33**
	0.01 mg mL^{-1}		25.94 ± 3.93
POEOMA$_{15}$-*b*-(PDMAEMA$_{30}$-*co*-PDPA$_{27}$)	1 mg mL^{-1}		31.05 ± 1.05
	0.1 mg mL^{-1}	**-23.40 ± 0.42**	**88.25 ± 7.82**
	0.01 mg mL^{-1}		21.66 ± 1.82
POEOMA$_{16}$-*b*-(PDMAEMA$_{44}$-*co*-PDPA$_{37}$)	1 mg mL^{-1}		16.98 ± 1.04
	0.1 mg mL^{-1}	**-18.07 ± 0 .84**	**85.74 ± 1.97**
	0.01 mg mL^{-1}		25.34 ± 1.33
POEOMA$_{16}$-*b*-PDMAEMA$_{96}$	1 mg mL^{-1}		49.49 ± 0.75
	0.1 mg mL^{-1}	**-14.63 ± 1.19**	**78.17 ± 2.25**
	0.01 mg mL^{-1}		28.43 ± 1.86
POEOMA$_{15}$-*b*-PDMAEMA$_{120}$	1 mg mL^{-1}		24.88 ± 0.44
	0.1 mg mL^{-1}	**-9.38 ± 0.22**	**78.70 ± 1.97**
	0.01 mg mL^{-1}		26.38 ± 0.70
POEOMA$_{8}$-*b*-PDMAEMA$_{30}$	1 mg mL^{-1}		22.40 ± 0.08
	0.1 mg mL^{-1}	**-7.61 ± 0.75**	**87.76 ± 1.98**
	0.01 mg mL^{-1}		26.64 ± 3.29
POEOMA$_{28}$-*b*-PDMAEMA$_{55}$	1 mg mL^{-1}		24.65 ± 1.33
	0.1 mg mL^{-1}	**-7.37 ± 0.60**	**87.66 ± 3.43**
	0.01 mg mL^{-1}		24.08 ± 0.24

It should also be pointed out that all the concentrations yielded particles comprised by a significant content of genetic material. For a 0.1 mg mL^{-1} concentration of copolymer the EE is 74–91% when compared to the concentration of 1 mg mL^{-1} (17–50%) and 0.01 mg mL^{-1} (22-28%), meaning that the delivery vehicle is formed by a considerable amount of the therapeutic transgene. The findings related with the process yield are more efficient compared to the content of chitosan-pDNA loaded nanoparticles (42–56%) synthesized by Gaspar and co-authors, and others reported in the literature.[42] These results are important for the overall formulation process and may be indicative that condensed pDNA at different concentrations of copolymers plays somehow an important role in positive/negative, polymer–DNA interactions. In fact, to further explore this possibility the surface charge of the pDNA biomolecules was determined for only a 0.1 mg mL^{-1} concentration of copolymers i.e., for the results with higher EE.

As shown in Table 16, the nanoparticles formulated with pDNA exhibit a negative charge on their surface, an important feature that not only influences particle–cell membrane interactions but also particle colloidal stability.[42] The results illustrate a distinct difference regarding the electrostatic characteristics of the various copolymers, which it has been explained due to the weight ratio of cationic copolymers/pDNA.[70] Cordeiro and co-authors have found that increasing the amount of cationic polymer with respect to a fixed amount of DNA resulted in an increase of the charge of the polyplexes due to the higher concentration of polymer on their surface.[53]

4.6.2. Agarose gel electrophoresis

The pK$_a$ values of PDMAEMA-*co*-PDPA, POEOMA-*b*-PDMAEMA, and POEOMA-*b*-(PDMAEMA-*co*-PDPA) were within the range 6.2–6.7. At pH 4.9, the copolymers and pDNA should be ionized to form polyelectrolyte complexes. The binding ability of copolymers with pDNA was also studied using an agarose gel electrophoresis retardation assay. At a copolymer concentration of 0.1 and 1.0 mg mL^{-1}, no free plasmid DNA bands were observed (Figure 43). This indicates that, under these conditions, DNA was fully associated with the copolymers. On the other hand, bands of DNA did appear

in the presence of a copolymer concentration of 0.01 mg mL^{-1}, demonstrated that the interaction between DNA and copolymers was inhibited.[70, 71]
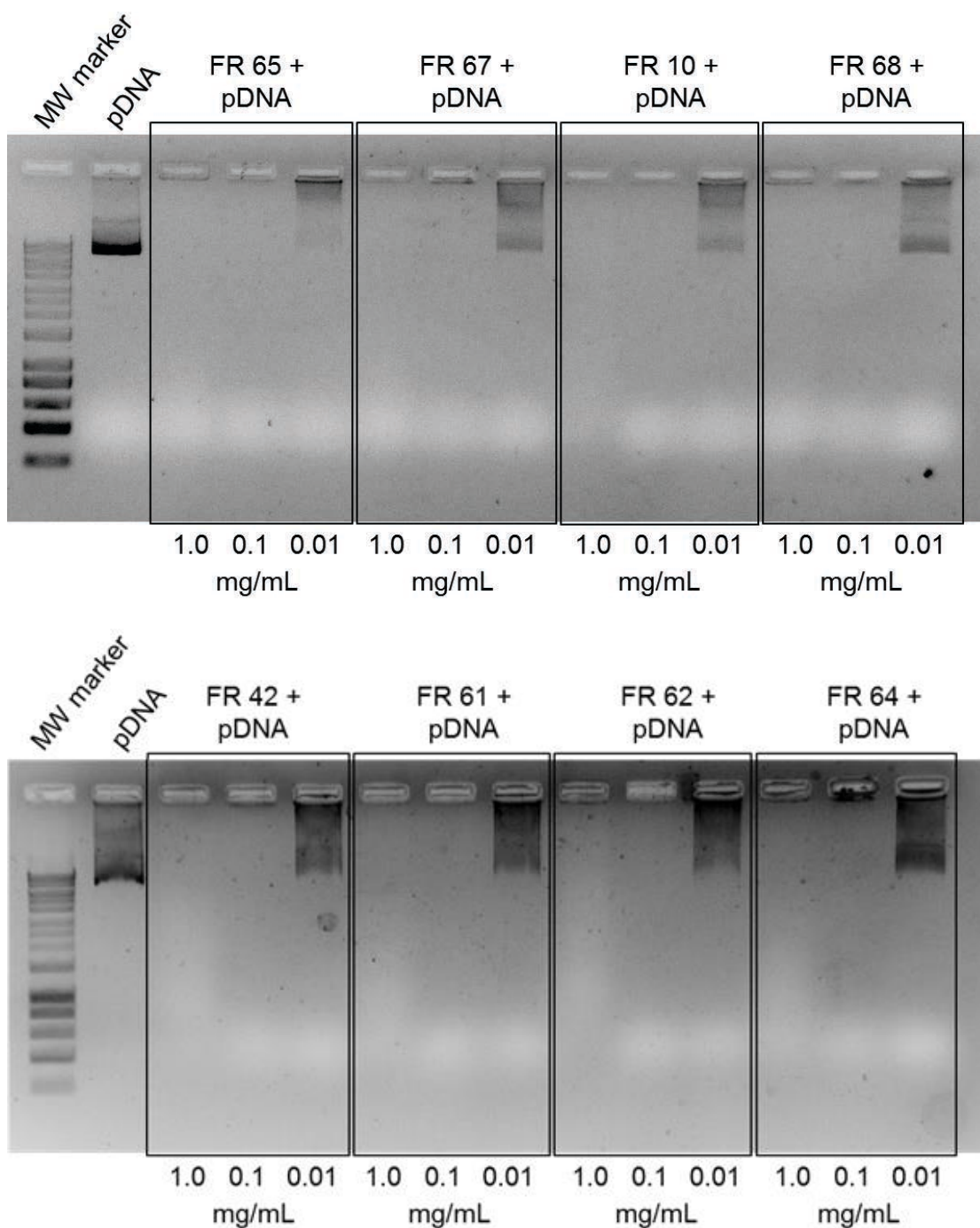
Figure 43. Agarose gel electrophoresis to test pDNA retention in different polyplexes with different copolymers concentrations. Naked pDNA and M_w marker were used as references. The polyplexes were prepared at pH 8.0 and complexed with pDNA at 20 µg/mL.

4.6.3. In vitro characterization of the cytotoxic profile of pDNA loaded nanoparticles

The cellular cytotoxicity profile of all copolymer/pDNA nanoparticles was characterized. The nanoparticle samples were exposed to different cells in culture and the viability of the populations was measured.[42] Human alveolar adenocarcinoma cell line (A549) is one of the human cell lines representing the airways that are used most often. They represent one important cell type, alveolar epithelial cells.

The results presented in Figure 44 show that the cell viability of copolymers was almost the same, reaching 91-109% and 92-115% for A549 and rat skin fibroblasts respectively, which indicates significantly higher cell viability compared to others reported in literature. For example, for the cytotoxicity of PDMAEMA and CSMA-modified PDMAEMA/pDNA polyplex synthesized by Lo and co-authors, the cell viability was only 40% and 90% respectively.[70, 71]
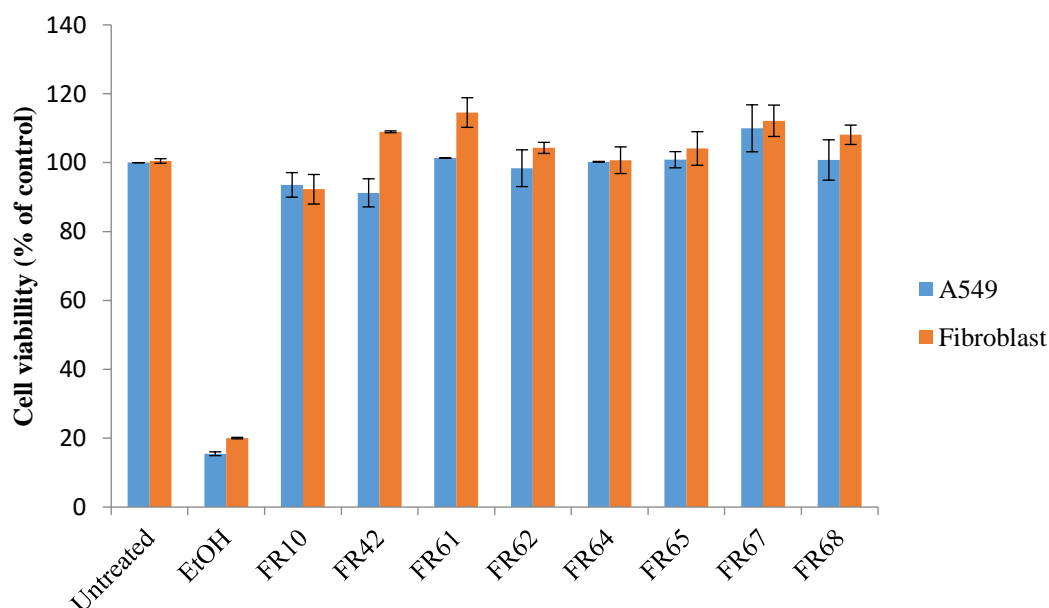
Figure 44. MTS cytotoxicity index of different nanoparticles formulated with the pDNA in: A549 (blue bars) and Rat skin fibroblasts (red bars), for a cell viability at 48h. Untreated cells were used as negative controls for cytotoxicity. Ethanol treated cells were used as positive control to induce toxicity.

Although preliminary, these tests show that the polymers are very promising and the tests in CICS-UBI will continue.

Conclusions and Future Work

Chapter 5

84

5. Conclusions and Future Work

Gene therapy is recognized as a major breakthrough of molecular medicine, by allowing disease treatment at a genetic level, changing today's therapeutic paradigm. Its main goal is to insert exogenous genetic material into specific cells or tissues of the patient in order to cure genetic diseases. In this context, the development of a safe and efficient gene delivery systems arises as the main challenge for its clinical application.[2] A new polymeric-based systems for gene delivery, composed by stimuli-responsive block copolymers was investigated. Well-defined block copolymers having different compositions and molecular weights were prepared by ATRP methodologies and were successfully used to prepare micelle structures in aqueous media. The type of nanostructures self-assembly were dependent on the preparation method and show differences when prepared using a titration method or a solvent exchange method.[43]

Well defined (co)polymers of a pH responsive monomer, DPA, were synthesized through SARA ATRP in the presence of the $Na_2S_2O_4$ and $Cu(II)Br_2$/ligand complex in a mixture of isopropanol and water [95/5 (v/v)]. The polymerization conditions of this eco-friendly and inexpensive SARA ATRP system were enhanced to prepare well-controlled polymers using relatively low copper catalyst concentrations. The living character of the synthesized polymers allow their chain-growth to obtain copolymeric structures.[24] The new catalytic system resulted in higher polymerization rates, higher monomer conversion, and significantly lower dispersity values at all conversions. The controlled molecular structure of the obtained polymers was confirmed by ^{1}H NMR analyses. The slow and continuous feeding of $Na_2S_2O_4$ solution into the reaction mixture improves the control over the polymerization. The use of TPMA as a ligand allowed the polymerization of DPA to be carried out in the presence of only 100 ppm of copper, reaching 82% of monomer conversion after 8h. The present method was also applied in the synthesis of well controlled poly(OEOMA-*b*-DPA), poly(OEOMA-*b*-DMAEMA) and poly(OEOMA-*b*-DMAEMA-*co*-DPA) block copolymers. Due to the reduced catalyst concentration, this is a promising method for the synthesis of pH/temperature responsive (co)polymers that could be used in the biomedical field.[18] POEOMA-*b*-PDPA and POEOMA-*b*-(PDMAEMA-*co*-PDPA) can self-assemble into uniform particles by the

hydrophilicity/hydrophobicity effect and electric interaction in aqueous solution at pH 7.4. Contrariwise, at a pH 5, both block copolymers present no aggregation suggesting that the copolymers were completely soluble, proving a conformational change in order a pH differences. Furthermore, all pure synthesized block copolymers reveal a very low remaining amount of Cu proving the safety of the final product in respect to copper contamination.[53]

The most promising block copolymers synthesized were sent to the Health Sciences Research Centre of the University of Beira Interior to evaluate their cytotoxicity and gene complexation ability. It was proved that the block copolymers were able to efficiently encapsulate the genetic material with no cytotoxicity effect to cells. The results are very promising and the tests in CICS-UBI will continue.

Since it possesses highly desirable properties of enhanced tumor accumulation and retention, improved cell uptake and controllable drug release behavior, the pH-sensitive nanocarriers constructed from POEOMA-*b*-PDPA and POEOMA-*b*-(PDMAEMA-*co*-PDPA) are highly promising for efficient tumor therapy.[31]

In addition, there is interest in the development of new shell-forming materials, which might elicit an appropriate response to a biological trigger. Perhaps the introduction of targeting moieties to the hydrophilic shell-forming blocks will become more important and prevalent as researchers continue to strive for ''smart'' delivery systems that might be capable of targeting specific receptors or cell types exclusively. In order to achieve that, there is a possible development of a folic acid functionalized ATRP initiator that allows the direct synthesis of polymers with a target moiety.[2] The use of ABCs for delivery purposes will likely increase as scientists are confronted with more and more challenging compounds and biologicals.[2]

References

Chapter 6

6. References

1. Park, T.G., J.H. Jeong, and S.W. Kim, *Current status of polymeric gene delivery systems.* Advanced Drug Delivery Reviews, 2006. **58**(4): p. 467-486.

2. Adams, M.L., A. Lavasanifar, and G.S. Kwon, *Amphiphilic block copolymers for drug delivery.* Journal of Pharmaceutical Sciences. **92**(7): p. 1343-1355.

3. Matyjaszewski, K., *Atom Transfer Radical Polymerization: From Mechanisms to Applications.* Israel Journal of Chemistry, 2012. **52**(3-4): p. 206-220.

4. Ibraheem, D., A. Elaissari, and H. Fessi, *Gene therapy and DNA delivery systems.* International Journal of Pharmaceutics, 2014. **459**(1–2): p. 70-83.

5. Murali Ramamoorth, A.N., *Non Viral Vectors in Gene Therapy- An Overview.* Journal of Clinical and Diagnostic Research, 2015.

6. Sons, J.W.a., The Journal of Gene Medicine, 2016.

7. Mintzer, M.A. and E.E. Simanek, *Nonviral Vectors for Gene Delivery.* Chemical Reviews, 2009. **109**(2): p. 259-302.

8. Nouri Nayerossadat, T.M., and Palizban Abas Ali, *Viral and nonviral delivery systems for gene delivery.* Advanced Biomedical Research, 2016.

9. Kakizawa, Y. and K. Kataoka, *Block copolymer micelles for delivery of gene and related compounds.* Advanced Drug Delivery Reviews, 2002. **54**(2): p. 203-222.

10. Rafati, A.B.a.S., *Non-Viral Delivery Systems in Gene Therapy and Vaccine Development.* InTech, 2011.

11. He, X., et al., *pH-sensitive drug-delivery systems for tumor targeting.* Therapeutic Delivery, 2013. **4**(12): p. 1499-1510.

12. Kim, W., J. Xiao, and E.L. Chaikof, *Recombinant Amphiphilic Protein Micelles for Drug Delivery.* Langmuir, 2011. **27**(23): p. 14329-14334.

13. Dayananda, K., et al., *Synthesis and characterization of MPEG-b-PDPA amphiphilic block copolymer via atom transfer radical polymerization and its pH-dependent micellar behavior.* Macromolecular Research, 2007. **15**(4): p. 385-391.

14. Iwasaki, Y. and K. Akiyoshi, *Design of Biodegradable Amphiphilic Polymers: Well-Defined Amphiphilic Polyphosphates with Hydrophilic Graft Chains via ATRP.* Macromolecules, 2004. **37**(20): p. 7637-7642.

15. Mendonca, P.V., et al., *Synthesis of cationic poly((3-acrylamidopropyl)trimethylammonium chloride) by SARA ATRP in ecofriendly solvent mixtures.* Polymer Chemistry, 2014. **5**(19): p. 5829-5836.

16. Konkolewicz, D., et al., *Aqueous RDRP in the Presence of Cu0: The Exceptional Activity of CuI Confirms the SARA ATRP Mechanism.* Macromolecules, 2014. **47**(2): p. 560-570.

17. Matyjaszewski, K., *Atom Transfer Radical Polymerization (ATRP): Current Status and Future Perspectives.* Macromolecules, 2012. **45**(10): p. 4015-4039.

18. Gois, J.R., et al., *Improvement of the control over SARA ATRP of 2-(diisopropylamino)ethyl methacrylate by slow and continuous addition of sodium dithionite.* Polymer Chemistry, 2014. **5**(16): p. 4617-4626.

19. Grajales, S., *Controlled Radical Polymerization Guide.* Aldrich Materials Science, 2012.

20. Boyer, C., et al., *Copper-Mediated Living Radical Polymerization (Atom Transfer Radical Polymerization and Copper(0) Mediated Polymerization): From Fundamentals to Bioapplications.* Chemical Reviews, 2016. **116**(4): p. 1803-1949.

21. Treat, N.J., et al., *Metal-Free Atom Transfer Radical Polymerization.* Journal of the American Chemical Society, 2014. **136**(45): p. 16096-16101.

22.   Cordeiro, R.A., et al., *Synthesis of well-defined poly(2-(dimethylamino)ethyl methacrylate) under mild conditions and its co-polymers with cholesterol and PEG using Fe(0)/Cu(ii) based SARA ATRP.* Polymer Chemistry, 2013. **4**(10): p. 3088-3097.

23.   Visnevskij, C. and R. Makuska, *SARA ATRP in Aqueous Solutions Containing Supplemental Redox Intermediate: Controlled Polymerization of [2-(Methacryloyloxy)ethyl] trimethylammonium Chloride.* Macromolecules, 2013. **46**(12): p. 4764-4771.

24.   Gois, J.R., et al., *Synthesis of well-defined functionalized poly(2-(diisopropylamino)ethyl methacrylate) using ATRP with sodium dithionite as a SARA agent.* Polymer Chemistry, 2014. **5**(12): p. 3919-3928.

25.   Simona Mura, J.N.a.P.C., *Stimuli-responsive nanocarriers for drug delivery.* Nature Materials, 2013. p. 991–1003

26.   Karimi, M., et al., *Smart External Stimulus-Responsive Nanocarriers for Drug and Gene Delivery*. 2015, Morgan & Claypool Publishers.

27.   Alarcon, C.d.l.H., S. Pennadam, and C. Alexander, *Stimuli responsive polymers for biomedical applications.* Chemical Society Reviews, 2005. **34**(3): p. 276-285.

28.   Matyjaszewski, K. and J. Spanswick, *Controlled/living radical polymerization.* Materials Today, 2005. **8**(3): p. 26-33.

29.   Tianyu Zhao, B., MA, *Controlled/living Radical Polymerization of Multi-vinyl Monomer towards Hyperbranched Polymers for Biomedical Applications.* 2015.

30.   York, A.W., S.E. Kirkland, and C.L. McCormick, *Advances in the synthesis of amphiphilic block copolymers via RAFT polymerization: Stimuli-responsive drug and gene delivery.* Advanced Drug Delivery Reviews, 2008. **60**(9): p. 1018-1036.

31.   Wu, W., et al., *Tumor-targeted aggregation of pH-sensitive nanocarriers for enhanced retention and rapid intracellular drug release.* Polymer Chemistry, 2014. **5**(19): p. 5668-5679.

32.   Yu, H., et al., *Intracellular pH-activated PEG-b-PDPA wormlike micelles for hydrophobic drug delivery.* Polymer Chemistry, 2013. **4**(19): p. 5052-5055.

33.   Fernando C. Giacomelli, P.S.a., Cristiano Giacomelli, Vanessa Schmidt, Eliezer Jager, and A.J.a.K. Ulbrichb, *pH-triggered block copolymer micelles based on a pH-responsive PDPA (poly-[2-(diisopropylamino)ethyl methacrylate]) inner core and a PEO (poly-(ethylene oxide)) outer shell as a potential tool for the cancer therapy.* Soft Matter, 2011.

34.   Bougard, F., et al., *Influence of the Macromolecular Architecture on the Self-Assembly of Amphiphilic Copolymers Based on Poly(N,N-dimethylamino-2-ethyl methacrylate) and Poly(ε-caprolactone).* Langmuir, 2008. **24**(15): p. 8272-8279.

35.   Chen, D., J.P. Kennedy, and A.J. Allen, *Amphiphilic Networks. I. Network Synthesis by Copolymerization of Methacryloyl-Capped Polyisobutylene with 2-(Dimethylamino) Ethyl Methacrylate and Characterization of The Networks.* Journal of Macromolecular Science: Part A - Chemistry, 1988. **25**(4): p. 389-401.

36.   Lin, S., et al., *An Acid-Labile Block Copolymer of PDMAEMA and PEG as Potential Carrier for Intelligent Gene Delivery Systems.* Biomacromolecules, 2008. **9**(1): p. 109-115.

37.   van Steenis, J.H., et al., *Preparation and characterization of folate-targeted pEG-coated pDMAEMA-based polyplexes.* Journal of Controlled Release, 2003. **87**(1–3): p. 167-176.

38.   Weihang Ji, D.P., R. Noelle Palumbo, Rupei Tang, and Chun Wang, *Poly(2-aminoethyl methacrylate) with Well-Defined Chain Length for DNA Vaccine Delivery to Dendritic Cells.* BioMacromolecules, 2011.

39.   Daniel J. Siegwart, J.K.O., Haifeng Gao, Sidi A. Bencherif, Fabien Perineau, Andrew K. Bohaty, Jeffrey O. Hollinger, Krzysztof Matyjaszewski, *Biotin-, Pyrene-, and GRGDS-Functionalized Polymers and Nanogels via ATRP and End Group Modification.* Macromolecular Chemistry and Physics, 2008.

40. Oh, J.K., S.A. Bencherif, and K. Matyjaszewski, *Atom transfer radical polymerization in inverse miniemulsion: A versatile route toward preparation and functionalization of microgels/nanogels for targeted drug delivery applications.* Polymer, 2009. **50**(19): p. 4407-4423.

41. Ibarra-Montaño, E.L., et al., *Determination of pKa Values for Acrylic, Methacrylic and Itaconic Acids by 1H and 13C NMR in Deuterated Water.* Journal of Applied Solution Chemistry and Modeling, 2015. **4**(1): p. 7.

42. Gaspar, V.M., et al., *Nanoparticle mediated delivery of pure P53 supercoiled plasmid DNA for gene therapy.* Journal of Controlled Release, 2011. **156**(2): p. 212-222.

43. Rocha, N., et al., *Poly(ethylene glycol)-block-poly(4-vinyl pyridine) as a versatile block copolymer to prepare nanoaggregates of superparamagnetic iron oxide nanoparticles.* Journal of Materials Chemistry B, 2014. **2**(11): p. 1565-1575.

44. Guo, S., et al., *Poly(Ɛ-caprolactone)-graft-poly(2-(N, N-dimethylamino) ethyl methacrylate) nanoparticles: pH dependent thermo-sensitive multifunctional carriers for gene and drug delivery.* Journal of Materials Chemistry, 2010. **20**(33): p. 6935-6941.

45. Ji, W., et al., *Poly(2-aminoethyl methacrylate) with Well-Defined Chain Length for DNA Vaccine Delivery to Dendritic Cells.* Biomacromolecules, 2011. **12**(12): p. 4373-4385.

46. Abreu, C.M.R., et al., *Ambient temperature rapid SARA ATRP of acrylates and methacrylates in alcohol-water solutions mediated by a mixed sulfite/Cu(ii)Br2 catalytic system.* Polymer Chemistry, 2013. **4**(23): p. 5629-5636.

47. Cheng-Liang, P., et al., *Development of pH sensitive 2-(diisopropylamino)ethyl methacrylate based nanoparticles for photodynamic therapy.* Nanotechnology, 2010. **21**(15): p. 155103.

48. *HIGH RESOLUTION NMR OF MACROMOLECULES.* Analytical Chemistry, 1972. **44**(9): p. 44A-44A.

49. Jiang, X., et al., *Thermoregulated phase transfer catalysis in aqueous/organic biphasic system: facile and highly efficient ATRP catalyst separation and recycling in situ using typical alkyl halide as initiator.* Polymer Chemistry, 2015. **6**(35): p. 6394-6401.

50. Qianqian You, H.C., Qipeng Guo, Yudong Zhang, Puyu Zhang, *Polystyrene-b-poly(oligo(ethylene oxide) Monomethyl Ether Methacrylate)-bpolystyrene Triblock Copolymers as Potential Carriers for Hydrophobic Drugs.* Bull. Korean Chem. Soc., 2013. **34**.

51. Qian, J. and C. Berkland, *pH-sensitive triblock copolymers for efficient siRNA encapsulation and delivery.* Polymer Chemistry, 2015. **6**(18): p. 3472-3479.

52. Mendonça, P.V., et al., *Straightforward ARGET ATRP for the Synthesis of Primary Amine Polymethacrylate with Improved Chain-End Functionality under Mild Reaction Conditions.* Macromolecules, 2014. **47**(14): p. 4615-4621.

53. Cordeiro, R.A., et al., *Novel Cationic Triblock Copolymer of Poly[2-(dimethylamino)ethyl methacrylate]-block-poly(β-amino ester)-block-poly[2-(dimethylamino)ethyl methacrylate]: A Promising Non-Viral Gene Delivery System.* Macromolecular Bioscience, 2015. **15**(2): p. 215-228.

54. Curtright, R., et al., *Facilitating student understanding of buffering by an integration of mathematics and chemical concepts.* Biochemistry and Molecular Biology Education, 2004. **32**(2): p. 71-77.

55. Emma Lilia Ibarra-Montaño, N.R.-L., Aníbal Sánchez-Hernández and Alberto Rojas-Hernández, *Determination of pKa Values for Acrylic, Methacrylic and Itaconic Acids by ^{1}H and ^{13}C NMR in Deuterated Water.* Journal of Applied Solution Chemistry and Modeling, 2016: p. 7-18.

56. Lomas, H., et al., *Biomimetic pH Sensitive Polymersomes for Efficient DNA Encapsulation and Delivery.* Advanced Materials, 2007. **19**(23): p. 4238-4243.

57. Pearson, R.T., et al., *Effect of pH and Temperature on PMPC–PDPA Copolymer Self-Assembly.* Macromolecules, 2013. **46**(4): p. 1400-1407.

58. McCormick, R.M. and B.L. Karger, *Role of organic modifier sorption on retention phenomena in reversed-phase liquid chromatography.* Journal of Chromatography A, 1980. **199**: p. 259-273.

59. Zeng, F. and S.C. Zimmerman, *Dendrimers in Supramolecular Chemistry: From Molecular Recognition to Self-Assembly.* Chemical Reviews, 1997. **97**(5): p. 1681-1712.

60. Colin, H., N. Ward, and G. Guiochon, *Third International Symposium on Column Liquid ChromatographyComparison of some packings for reversed-phase high-performance liquid-solid chromatography.* Journal of Chromatography A, 1978. **149**: p. 169-197.

61. Dawber, J.G., J. Ward, and R.A. Williams, *A study in preferential solvation using a solvatochromic pyridinium betaine and its relationship with reaction rates in mixed solvents.* Journal of the Chemical Society, Faraday Transactions 1: Physical Chemistry in Condensed Phases, 1988. **84**(3): p. 713-727.

62. Park, S.-J., T.A. Taton, and C.A. Mirkin, *Array-Based Electrical Detection of DNA with Nanoparticle Probes.* Science, 2002. **295**(5559): p. 1503-1506.

63. Cao, Y.C., R. Jin, and C.A. Mirkin, *Nanoparticles with Raman Spectroscopic Fingerprints for DNA and RNA Detection.* Science, 2002. **297**(5586): p. 1536-1540.

64. Xiong, Z., et al., *Dual-stimuli responsive behaviors of diblock polyampholyte PDMAEMA-b-PAA in aqueous solution.* Journal of Colloid and Interface Science, 2011. **356**(2): p. 557-565.

65. Lee, M., et al., *Repression of GAD Autoantigen Expression in Pancreas [beta]-Cells by Delivery of Antisense Plasmid/PEG-g-PLL Complex.* Mol Ther, 2001. **4**(4): p. 339-346.

66. Kwoh, D.Y., et al., *Stabilization of poly-l-lysine/DNA polyplexes for in vivo gene delivery to the liver.* Biochimica et Biophysica Acta (BBA) - Gene Structure and Expression, 1999. **1444**(2): p. 171-190.

67. Sabelle Ydens, S.M., François Botteman, Philippe Degée, Philippe Dubois, *Removal of copper-based catalyst in atom transfer radical polymerization using different extraction techniques.* e-Polymers, 2004: p. 414-420.

68. Pereira, P., et al., *Characterization of polyplexes involving small RNA.* Journal of Colloid and Interface Science, 2012. **387**(1): p. 84-94.

69. Pereira, P.A., et al., *Recombinant pre-miR-29b for Alzheimer´s disease therapeutics.* Scientific Reports, 2016. **6**: p. 19946.

70. Lo, Y.-L., Y.-S. Wang, and L.-F. Wang, *The Copolymer of Poly(2-dimethylaminoethyl methacrylate) and Methacrylated Chondroitin Sulfate with Low Cytotoxicity for Gene Delivery.* Advanced Healthcare Materials, 2013. **2**(11): p. 1458-1468.

71. Iwai, R., et al., *Enhanced Transfection Efficiency of Poly(N,N-dimethylaminoethyl methacrylate)-Based Deposition Transfection by Combination with Tris(hydroxymethyl)aminomethane.* Bioconjugate Chemistry, 2013. **24**(2): p. 159-166.

Attachments

Chapter 7

94

7. Attachments
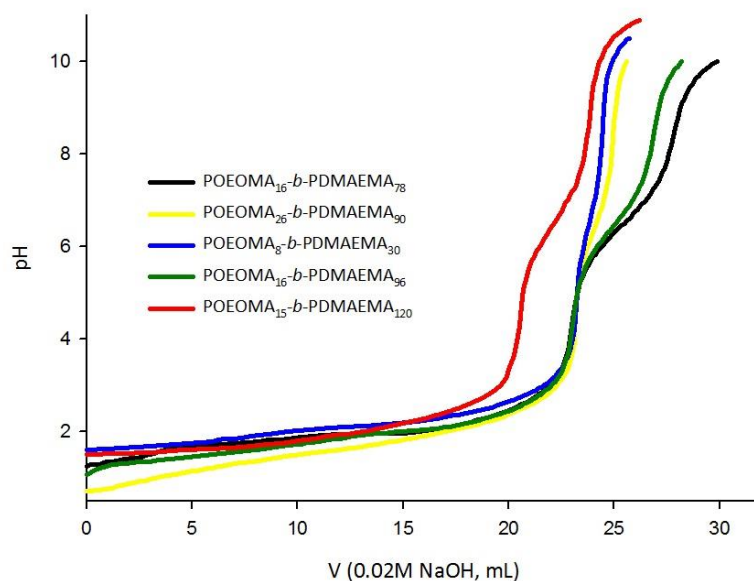
Figure 45. Potentiometric titration curves at 37°C of block copolymers of POEOMA-b-PDMAEMA in milli-Q water. The initial copolymer solutions were prepared to contain a fixed amount of mass (10 mg) in a total initial volume of 5mL of 0.1M HCl. The solution was the titrated with 100μL aliquots of 0.02M NaOH. The x-axis label of the plot, V_{NaOH} denotes the total volume of added NaOH. Measurements were taken using a Jenway 3510 pH meter (Stone, Staffs, UK).
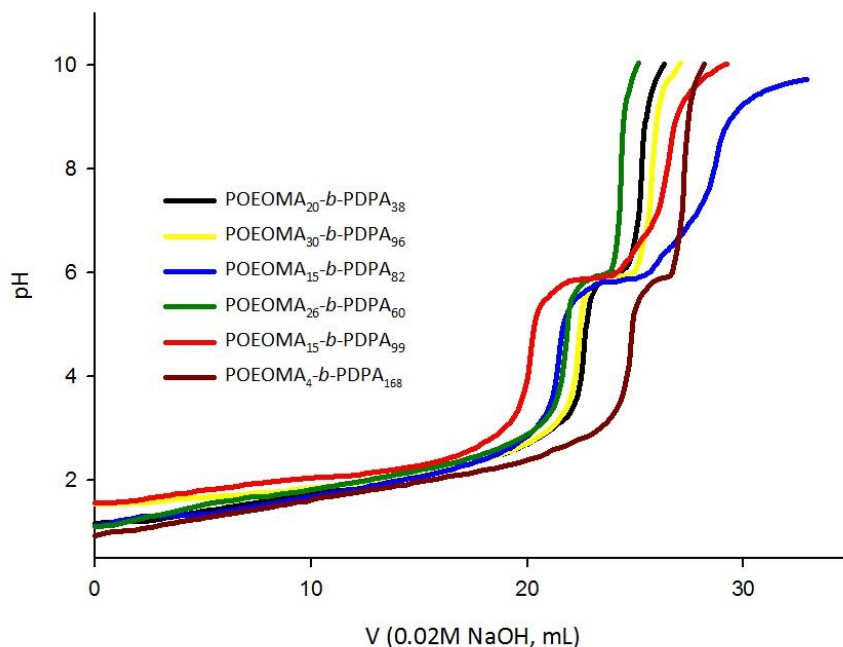
Figure 46. Potentiometric titration curves at 37°C of block copolymers of POEOMA-b-PDPA in milli-Q water. The initial copolymer solutions were prepared to contain a fixed amount of mass (10 mg) in a total initial volume of 5mL of 0.1M HCl. The solution was the titrated with 100μL aliquots of 0.02M NaOH. The x-axis label of the plot, V_{NaOH} denotes the total volume of added NaOH. Measurements were taken using a Jenway 3510 pH meter (Stone, Staffs, UK).
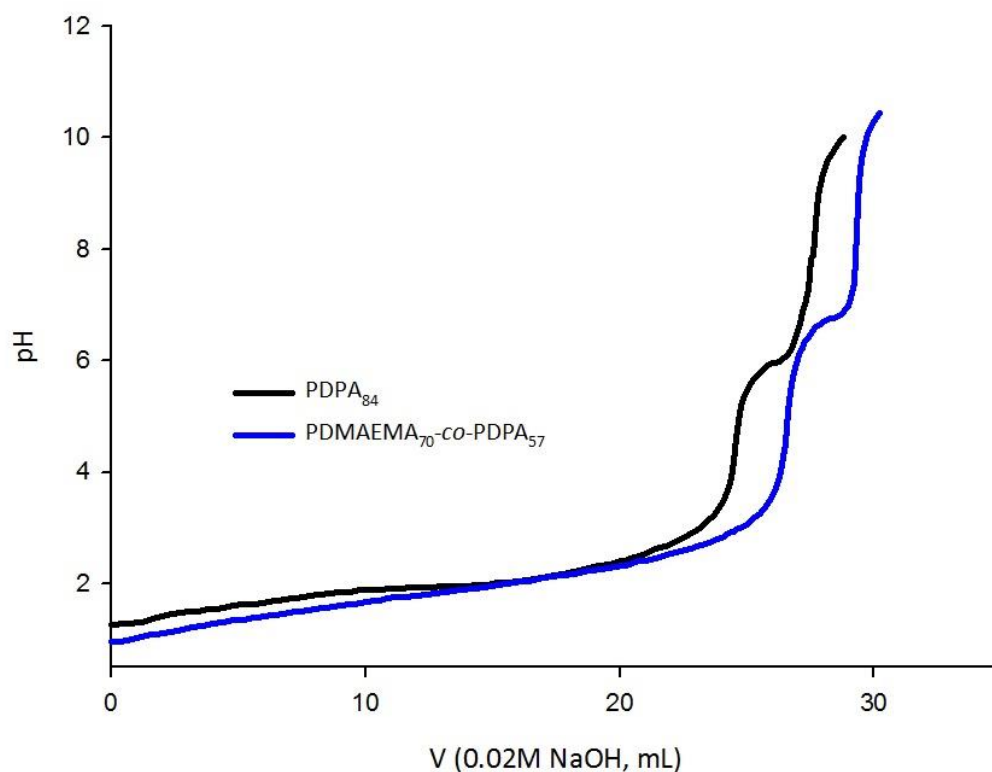
Figure 47. Potentiometric titration curves at 37°C of homopolymers/copolymers in milli-Q water. The initial copolymer solutions were prepared to contain a fixed amount of mass (10 mg) in a total initial volume of 5mL of 0.1M HCl. The solution was the titrated with 100μL aliquots of 0.02M NaOH. The x-axis label of the plot, V_{NaOH} denotes the total volume of added NaOH. Measurements were taken using a Jenway 3510 pH meter (Stone, Staffs, UK).

Table 17. Determination the residual content of Cu in the final purified polymer.

Elemental Analysis						
Sample Code	Atomic Absorption (mg Cu/l)	Volume of water (ml)	Amount of polymer (mg)	m(Cu) (mg)	m(Cu)/m(cop)	ppm (Cu)
FR13	0.055	10	50	0.00055	0.000011	11
FR58	0.032	10	50	0.00032	0.0000064	6.4
FR01	0.059	10	50	0.00059	0.0000118	11.8
FR43	0.109	10	50	0.00109	0.0000218	21.8
FR64	0.13	10	50	0.0013	0.000026	26
FR65	0.056	10	50	0.00056	0.0000112	11.2

Table 18. All macroinitiators/homopolymers/copolymers results reactions.

	Legend			---------	good results														
				---------	bad results														
				---------	usable copolymers/homopolymers														
	EXPERIMENT																Pure polymer	
	Monomer	target DP	Initiator	Catalyst		Ligand	ratio	ppm (Cu)	Solvent		sol./mon.	T (°C)	time (h)	conv. (%)	Mn^{th}x10^{-3}	Mn^{SEC}x10^{-3}	D	Mn^{SEC}x10^{-3}	D
FR 01	DPA	100	EBPA	$Na_2S_2O_4$	$CuBr_2$	TPMA	100:1:0.2:0.01:0.02	99.50	IPA (0.95)	H_2O (0.05)	1:1	40	21.08	84.31	15.871	24.840	1.08	23.199	1.10
FR 02	DPA	100	PgBIB	$Na_2S_2O_4$	$CuBr_2$	TPMA	100:1:0.2:0.01:0.02	98.10	IPA (0.95)	H_2O (0.05)	1:1	40	17.08	84.7	18.645	40.460	1.60	--	--
FR03	DPA	100	EBPA	$Na_2S_2O_4$	$CuBr_2$	TPMA	99.91:1:0.2:0.01:0.02	99.70	IPA (0.95)	H_2O (0.05)	2:2	40	24	62.62	13.589	---	---	--	--
FR04	DPA	100	EBPA	$Na_2S_2O_4$	$CuBr_2$	TPMA	100.17:1:0.51:0.01:0.02	99.80	IPA (0.95)	H_2O (0.05)	2:2	40	24	91.45	19.783	38.580	1.23	--	--
FR05	DPA	50	EBPA	$Na_2S_2O_4$	$CuBr_2$	TPMA	50.28:1:0.51:0.01:0.02	198.42	IPA (0.95)	H_2O (0.05)	2:2	40	20	94.12	10.339	17.895	1.19	--	--
FR06	DPA	50	EBPA	$Na_2S_2O_4$	$CuBr_2$	TPMA	50.43:1:0.51:0.01:0.02	197.83	IPA (0.95)	H_2O (0.05)	2:2	40	24	94.8	10.442	19.052	1.19	--	--
FR07	DPA	50	EBPA	$Na_2S_2O_4$	$CuBr_2$	TPMA	50.08:1:0.51:0.01:0.02	199.22	IPA (0.95)	H_2O (0.05)	2:2	40	17	82.05	9.009	30.660	1.30	--	--
FR08	DPA	100	EBPA	$Na_2S_2O_4$	$CuBr_2$	TPMA	100.86:1:0.52:0.01:0.02	99.11	IPA (0.95)	H_2O (0.05)	2:2	40	24	77.31	16.878	33.390	1.33	--	--
FR09	DPA-co-DMAEMA	50-50	EBPA	$Na_2S_2O_4$	$CuBr_2$	TPMA	50.36:1:0.21:0.00:0.01	0	IPA (0.95)	H_2O (0.05)	2:2	40	---	---	---	---	---	---	---
FR10	DPA-co-DMAEMA	50-100	EBPA	$Na_2S_2O_4$	$CuBr_2$	TPMA	70.68:1:0.20:0.01:0.01	84.28	IPA (0.95)	H_2O (0.05)	2:2	40	24	95.83	6.347	22.350	1.08	23.234	1.08
FR11	OEOMA$_{500}$	50	EBPA	$Na_2S_2O_4$	$CuBr_2$	TPMA	50.22:1:0.25:0.01:0.02	193.24	IPA (0.95)	H_2O (0.05)	mon. 29%	40	24	7.01	2.003	6.560	1.19	7.580	1.18
FR12	OEOMA$_{300}$	50	EBPA	$Na_2S_2O_4$	$CuBr_2$	TPMA	50.05:1:0.26:0.01:0.02	196.87	IPA (0.95)	H_2O (0.05)	mon. 29%	40	5	1.81	0.515	---	---	--	--
FR13	OEOMA$_{500}$	50	EBPA	$Na_2S_2O_4$	$CuBr_2$	TPMA	50.32:1:0.26:0.01:0.02	192.86	IPA (0.95)	H_2O (0.05)	mon. 29%	40	5	37.50	9.678	15.000	1.17	13.000	1.12
FR14	OEOMA$_{500}$	50	EBPA	$Na_2S_2O_4$	$CuBr_2$	TPMA	50.29:1:0.26:0.01:0.02	192.89	IPA (0.95)	H_2O (0.05)	mon. 29%	40	6	52.08	13.337	33.000	1.07	26.000	1.19
FR15	OEOMA$_{500}$	50	EBPA	$Na_2S_2O_4$	$CuBr_2$	TPMA	50.15:1:0.26:0.01:0.02	193.50	IPA (0.95)	H_2O (0.05)	mon. 29%	40	5	5.96	1.737	6.780	1.13	--	--
FR16	OEOMA$_{300}$	50	EBPA	$Na_2S_2O_4$	$CuBr_2$	TPMA	50.07:1:0.26:0.01:0.02	196.74	IPA (0.95)	H_2O (0.05)	mon. 29%	40	5	0	0	---	---	--	--
FR 17	OEOMA$_{500}$	100	EBPA	$Na_2S_2O_4$	$CuBr_2$	TPMA	100.59:1:0.26:0.01:0.02	100.19	IPA (0.95)	H_2O (0.05)	mon. 38%	40	5	22.28	11.449	14.557	1.22	--	--
FR 18	OEOMA$_{500}$	80	EBPA	$Na_2S_2O_4$	$CuBr_2$	TPMA	80.35:1:0.26:0.01:0.02	123.75	IPA (0.95)	H_2O (0.05)	mon. 38%	40	5.25	6.78	2.968	---	---	--	--
FR 19	POEOMA-b-DPA	200	POEOMA	$Na_2S_2O_4$	$CuBr_2$	TPMA	202.03:1:0.28:0.05:0.08	245.87	IPA (0.95)	H_2O (0.05)	3	40	24	84.13	42.756	55.064	1.37	54.953	1.36
FR 20	OEOMA$_{500}$	50	EBPA	$Na_2S_2O_4$	$CuBr_2$	TPMA	50.15:1:0.26:0.01:0.02	199.45	IPA (0.95)	H_2O (0.05)	mon. 29%	40	22	39.39	10.122	17.000	1.09	--	--
FR 21	POEOMA-b-DPA	150	POEOMA	$Na_2S_2O_4$	$CuBr_2$	TPMA	150.07:1:0.26:0.05:0.08	332.92	IPA (0.95)	H_2O (0.05)	3	40	24	55.16	32.657	39.500	1.23	39.100	1.23
FR 22	POEOMA-b-DPA	150	POEOMA	$Na_2S_2O_4$	$CuBr_2$	TPMA	151.88:1:0.27:0.05:0.08	330.16	IPA (0.95)	H_2O (0.05)	3	40	24	63.83	50.682	37.529	2.02		
FR 23	POEOMA-b-DMAEMA	200	POEOMA	$Na_2S_2O_4$	$CuBr_2$	TPMA	200.99:1:0.27:0.05:0.08	245.30	IPA (0.95)	H_2O (0.05)	3	40	24	86.20	57.256	28.281	1.48	--	--
FR 24	OEOMA$_{500}$	50	EBPA	$Na_2S_2O_4$	$CuBr_2$	TPMA	50.04:1:0.26:0.01:0.02	201.34	IPA (0.95)	H_2O (0.05)	mon. 54%	40	5	60.20	15.304	22.500	1.20	24.373	1.20
FR 25	OEOMA$_{500}$	50	EBPA	$Na_2S_2O_4$	$CuBr_2$	TPMA	44.26:1:0.23:0.01:0.02	199.72	IPA (0.95)	H_2O (0.05)	mon. 54%	40	4	29.72	6.820	11.960	1.17	13.257	1.11
FR 26	OEOMA$_{500}$	50	EBPA	$Na_2S_2O_4$	$CuBr_2$	TPMA	50:1:0.26:0.01:0.02	201.48	IPA (0.95)	H_2O (0.05)	mon. 54%	40	5	59.15	15.030	22.850	1.15	23.880	1.18
FR 27	OEOMA$_{500}$	50	EBPA	$Na_2S_2O_4$	$CuBr_2$	TPMA	50.15:1:0.26:0.01:0.02	200.87	IPA (0.95)	H_2O (0.05)	mon. 54%	40	5	53.11	13.561	20.250	1.14	20.991	1.09
FR 28	OEOMA$_{500}$	50	EBPA	$Na_2S_2O_4$	$CuBr_2$	TPMA	50.12:1:0.26:0.01:0.02	201.01	IPA (0.95)	H_2O (0.05)	mon. 54%	40	4,5	58.98	15.023	23.090	1.17	25.175	1.14
FR 29	OEOMA$_{500}$	50	EBPA	$Na_2S_2O_4$	$CuBr_2$	TPMA	50.07:1:0.26:0.01:0.02	201.21	IPA (0.95)	H_2O (0.05)	mon. 54%	40	4	26.82	6.958	11.250	1.16	17.298	1.04
FR 30	OEOMA$_{500}$	50	EBPA	$Na_2S_2O_4$	$CuBr_2$	TPMA	50.04:1:0.26:0.01:0.02	201.34	IPA (0.95)	H_2O (0.05)	mon. 54%	40	4	40.24	10.310	18.842	1.13	23.483	1.18
FR 31	OEOMA$_{500}$	50	EBPA	$Na_2S_2O_4$	$CuBr_2$	TPMA	50.10:1:0.26:0.01:0.02	201.08	IPA (0.95)	H_2O (0.05)	mon. 54%	40	4	38.78	9.957	16.007	1.15	16.147	1.20
FR 32	POEOMA-b-DPA	200	POEOMA	$Na_2S_2O_4$	$CuBr_2$	TPMA	200.17:1:0.28:0.05:0.08	251.29	IPA (0.95)	H_2O (0.05)	3	40	42	---	---	52.757	1.90	--	--
FR 33	POEOMA-b-DPA	100	POEOMA	$Na_2S_2O_4$	$CuBr_2$	TPMA	99.80:1:0.27:0.05:0.08	501.47	IPA (0.95)	H_2O (0.05)	3	40	17.5	64.04	37.198	38.650	1.44	--	--
FR 34	POEOMA-b-DMAEMA	100	POEOMA	$Na_2S_2O_4$	$CuBr_2$	TPMA	100.40:1:0.27:0.05:0.08	498.11	IPA (0.95)	H_2O (0.05)	3	40	17.5	86.73	36.199	34.771	1.70	--	--
NOTA	From here we tripled the volume of IPA to lower the polidespersividade of copolymers																	--	--
FR 35	POEOMA-b-DPA	150	POEOMA	$Na_2S_2O_4$	$CuBr_2$	TPMA	150.5:1:0.35:0.05:0.08	333.17	IPA (0.95)	H_2O (0.05)	9	40	----	----	----	----	84.887	1.47	--	--
FR 36	POEOMA-b-DMAEMA	150	POEOMA	$Na_2S_2O_4$	$CuBr_2$	TPMA	150.5:1:0.26:0.05:0.08	332.29	IPA (0.95)	H_2O (0.05)	9	40	----	----	----	----	27.572	1.89	--	--

	Monomer	target DP	Initiator	Catalyst	Ligand	ratio	ppm (Cu)	Solvent		sol./mon.	T (°C)	time (h)	conv. (%)	$Mn^{th} \times 10^{-3}$	$Mn^{SEC} \times 10^{-3}$	D	Pure polymer $Mn^{SEC} \times 10^{-3}$	D
NOTA	From here started making feeding for all copolymers, but not in macroiniciadores																--	--
FR 37	POEOMA-b-DPA	120	POEOMA	$Na_2S_2O_4$	$CuBr_2$	TPMA	120:1:0.26:0.05:0.08	415.47	IPA(0.95)	H_2O (0.05)	9	40	12	55.36	34.421	31.831	1.31	30.903	1.30
FR 38	POEOMA-b-DMAEMA	120	POEOMA	$Na_2S_2O_4$	$CuBr_2$	TPMA	120:1:0.26:0.05:0.08	415.58	IPA(0.95)	H_2O (0.05)	9	40	12	75.39	34.482	25.896	1.19	25.913	1.19
FR 39	POEOMA-b-DPA	200	POEOMA	$Na_2S_2O_4$	$CuBr_2$	TPMA	200.57:1:0.26:0.05:0.08	250.34	IPA(0.95)	H_2O (0.05)	9	40	12	48.72	43.935	33.049	1.29	31.005	1.29
FR 40	POEOMA-b-(DMAEMA-co-DPA)	200-200	POEOMA	$Na_2S_2O_4$	$CuBr_2$	TPMA	200:1:0.26:0.05:0.08	251.34	IPA(0.95)	H_2O (0.05)	9	40	12	52.04	39.463	28.441	1.20	26.715	1.22
FR 41	POEOMA-b-DPA	150	POEOMA	$Na_2S_2O_4$	$CuBr_2$	TPMA	150.3:1:0.26:0.05:0.08	333.62	IPA(0.95)	H_2O (0.05)	9	40	12	65.64	33.005	35.639	1.32	34.911	1.32
FR 42	POEOMA-b-DMAEMA	150	POEOMA	$Na_2S_2O_4$	$CuBr_2$	TPMA	150:1:0.26:0.05:0.08	333.31	IPA(0.95)	H_2O (0.05)	9	40	12	79.59	30.742	25.001	1.18	23.745	1.18
FR 43	POEOMA-b-DPA	100	POEOMA	$Na_2S_2O_4$	$CuBr_2$	TPMA	100.28:1:0.26:0.05:0.08	499.47	IPA(0.95)	H_2O (0.05)	9	40	12	82.23	28.842	38.373	1.36	36.043	1.35
FR 44	POEOMA-b-DMAEMA	100	POEOMA	$Na_2S_2O_4$	$CuBr_2$	TPMA	100:1:0.26:0.05:0.08	501.11	IPA(0.95)	H_2O (0.05)	9	40	12	90.98	25.563	30.717	1.25	29.808	1.28
FR 45	POEOMA-b-DPA	50	POEOMA	$Na_2S_2O_4$	$CuBr_2$	TPMA	50:1:0.26:0.05:0.08	1001.31	IPA(0.95)	H_2O (0.05)	9	40	12	85.66	32.620	28.778	1.55	--	--
FR 46	POEOMA-b-DPA	50	POEOMA	$Na_2S_2O_4$	$CuBr_2$	TPMA	49.88:1:0.26:0.05:0.08	1002.14	IPA(0.95)	H_2O (0.05)	9	40	12	76.01	24.235	26.352	1.21	25.618	1.22
FR 47	$OEOMA_{500}$	30	EBPA	$Na_2S_2O_4$	$CuBr_2$	TPMA	30.03:1:0.26:0.01:0.02	333.22	IPA(0.95)	H_2O (0.05)	mon. 38%	40	24	43.54	---	---	---	---	---
FR 48	$OEOMA_{500}$	30	EBPA	$Na_2S_2O_4$	$CuBr_2$	TPMA	30:1:0.31:0.01:0.02	334.12	IPA(0.95)	H_2O (0.05)	mon. 69%	40	6.75	53.69	8.296	13.650	1.51	---	---
FR 49	$OEOMA_{500}$	30	EBPA	$Na_2S_2O_4$	$CuBr_2$	TPMA	30:1:0.31:0.01:0.02	333.21	IPA(0.95)	H_2O (0.05)	mon. 38%	40	---	---	---	---	---	---	---
FR 50	$OEOMA_{500}$	30	EBPA	$Na_2S_2O_4$	$CuBr_2$	TPMA	30:1:0.31:0.01:0.02	333.59	IPA(0.95)	H_2O (0.05)	mon. 69%	40	9	8.91	1.580	0.146	1.70	---	---
FR 51	$OEOMA_{500}$	30	EBPA	$Na_2S_2O_4$	$CuBr_2$	TPMA	30:1:0.31:0.01:0.02	333.45	IPA(0.95)	H_2O (0.05)	mon. 69%	40	15.42	55.95	8.638	13.344	1.27	13.526	1.23
FR 52	$OEOMA_{500}$	30	EBPA	$Na_2S_2O_4$	$CuBr_2$	TPMA	30.04:1:0.31:0.01:0.02	333.07	IPA(0.95)	H_2O (0.05)	mon. 69%	40	13.5	28.38	4.507	7.967	1.21	7.569	1.20
FR 53	$OEOMA_{500}$	30	EBPA	$Na_2S_2O_4$	$CuBr_2$	Me_6TREN	30.03:1:0.31:0.01:0.02	3330.00	IPA(0.95)	H_2O (0.05)	mon. 22%	40	22	28.89	4.581	7.743	1.29	---	---
FR 54	$OEOMA_{500}$	30	EBPA	$Na_2S_2O_4$	$CuBr_2$	Me_6TREN	30.02:1:0.51:0.01:0.02	3331.63	IPA(0.95)	H_2O (0.05)	mon. 22%	40	12	94.00	14.350	21.984	1.25	21.291	1.10
FR 55	$OEOMA_{500}$	50	EBPA	$Na_2S_2O_4$	$CuBr_2$	TPMA	50.01:1:0.26:0.01:0.02	199.96	IPA(0.95)	H_2O (0.05)	mon. 58%	40	4	4.59	1.390	0	0	---	---
FR 56	$OEOMA_{500}$	40	EBPA	$Na_2S_2O_4$	$CuBr_2$	TPMA	40.07:1:0.26:0.01:0.02	249.57	IPA(0.95)	H_2O (0.05)	mon. 58%	40	4	6.25	1.495	0	0	--	--
FR 57	$OEOMA_{500}$	50	EBPA	$Na_2S_2O_4$	$CuBr_2$	TPMA	50.10:1:0.26:0.01:0.02	199.59	IPA(0.95)	H_2O (0.05)	mon. 58%	40	6	63.14	16.060	27.655	1.17	27.721	1.25
FR 58	$OEOMA_{500}$	40	EBPA	$Na_2S_2O_4$	$CuBr_2$	TPMA	40.03:1:0.26:0.01:0.02	249.80	IPA(0.95)	H_2O (0.05)	mon. 58%	40	6	74.34	15.121	19.856	1.15	19.011	1.17
FR 59	$OEOMA_{500}$	50	EBPA	$Na_2S_2O_4$	$CuBr_2$	TPMA	50.07:1:0.26:0.01:0.02	199.72	IPA(0.95)	H_2O (0.05)	mon. 54%	40	5	30.85	7.966	12.324	1.17	11.851	1.12
FR 60	$OEOMA_{500}$	50	EBPA	$Na_2S_2O_4$	$CuBr_2$	TPMA	50.08:1:0.26:0.01:0.02	199.65	IPA(0.95)	H_2O (0.05)	mon. 54%	40	4	18.51	4.879	8.495	1.38	--	--
FR 61	POEOMA-b-DMAEMA	90	POEOMA	$Na_2S_2O_4$	$CuBr_2$	TPMA	90.36:1:0.26:0.05:0.08	553.39	IPA(0.95)	H_2O (0.05)	9	40	12	86.05	25.576	29.942	1.20	28.697	1.22
FR 62	POEOMA-b-DMAEMA	110	POEOMA	$Na_2S_2O_4$	$CuBr_2$	TPMA	110.20:1:0.26:0.05:0.08	454.20	IPA(0.95)	H_2O (0.05)	9	40	12	86.96	28.420	32.092	1.27	30.332	1.29
FR 63	POEOMA-b-DPA	150	POEOMA	$Na_2S_2O_4$	$CuBr_2$	TPMA	150.90:1:0.26:0.05:0.08	332.29	IPA(0.95)	H_2O (0.05)	9	40	12	51.57	29.943	44.197	1.57	--	--
FR 64	POEOMA-b-(DMAEMA-co-DPA)	200-200	POEOMA	$Na_2S_2O_4$	$CuBr_2$	TPMA	200.40:1:0.26:0.05:0.08	249.22	IPA(0.95)	H_2O (0.05)	9	40	8	46.81	28.101	44.870	1.29	44.700	1.31
FR 65	POEOMA-b-DMAEMA	34	POEOMA	$Na_2S_2O_4$	$CuBr_2$	TPMA	34.10:1:0.26:0.05:0.08	1466.92	IPA(0.95)	H_2O (0.05)	9	40	12	90.14	12.802	24.251	1.13	23.610	1.14
FR 66	POEOMA-b-DPA	55	POEOMA	$Na_2S_2O_4$	$CuBr_2$	TPMA	55.16:1:0.26:0.05:0.08	906.11	IPA(0.95)	H_2O (0.05)	9	40	12	63.90	15.485	29.158	1.20	27.367	1.17
FR 67	POEOMA-b-DMAEMA	68	POEOMA	$Na_2S_2O_4$	$CuBr_2$	TPMA	68.39:1:0.26:0.05:0.08	730.38	IPA(0.95)	H_2O (0.05)	9	40	12	80.07	29.906	37.294	1.21	36.530	1.21
FR 68	POEOMA-b-(DMAEMA-co-DPA)	100-100	POEOMA	$Na_2S_2O_4$	$CuBr_2$	TPMA	100.65:1:0.26:0.05:0.08	496.75	IPA(0.95)	H_2O (0.05)	9	40	12	46.67	19.713	55.895	1.57	52.298	1.65
FR 69	POEOMA-b-DMAEMA-b-DPA	200	POEOMA	$Na_2S_2O_4$	$CuBr_2$	TPMA	199.38:1:0.26:0.05:0.08	251.50	IPA(0.95)	H_2O (0.05)	9	40	12	20.63	34.776	31.599	1.41	--	--
FR 70	$OEOMA_{500}$	50	EBPA	$Na_2S_2O_4$	$CuBr_2$	TPMA	50.04:1:0.26:0.01:0.02	201.34	IPA(0.95)	H_2O (0.05)	mon. 54%	40	24	53.20	13.570	20.987	1.20	--	--